Supplementary Information

Identification of the Bacterial Maytansinoid Gene Cluster *asc* Provides Insights into the Post-PKS Modifications of Ansacarbamitocin Biosynthesis

Xiaoman Li[†], Xingkang Wu[†], and Yuemao Shen[*,†]

[†]Key Laboratory of Chemical Biology (Ministry of Education), School of Pharmaceutical Sciences, Shandong University, No. 44 West Wenhua Road, Jinan, Shandong 250012, P. R. China

Table of Contents

1, Materials and Methods

1.1 Bioinformatic analysis (Table S1)

Genome sequence of *Amycolatopsis alba* DSM 44262 was analyzed by antiSMASH bacterial version 3.0.5 (https://antismash.secondarymetabolites.org/). The *asc* gene cluster annotation was performed by BLASTp webserver (http://www.ncbi.nih.gov/BLAST) and listed in Table S1.

Table S1. Deduced functions of ORFs in the *asc* biosynthetic gene cluster

gene	aa	proposed function	identity/ similarity (%)	protein homologue in *asm* or genbank
ascL4	479	MFS transporter	91/95	OOC07982
ascL3	311	Alpha/beta hydrolase	99/90	OOC08316
ascL2	151	Unknown	98/99	OOC07984
ascL1	271	Class I SAM-dependent methyltransferase	88/92	OOC07985
asc9	262	Amide synthase	60/70	AAM54087, Asm9
ascA	4330	Polyketide synthase	57/66	AAM54075, AsmA
loading		ADE-ACP		
module 1		KS-AT-DH-ER-KR-ACP		
module 2		KS-AT-DH-KR-ACP		
asc47	334	aDHQ synthase	69/76	AAC14006, Asm47
orf1	397	Unknown	82/86	ANN16105
asc45	218	Phosphatase	69/78	AAC14004, Asm45
asc44	346	Oxidoreductase	54/66	AAC14003, Asm44
asc43	384	AHBA synthase	72/83	AAC13997, Asm43
asc23	142	aDHQ dehydratase	75/88	AAM54101, Asm23
orf2	214	Unknown	90/91	ANN16099
asc20	120	Unknown	69/81	AAM54098, Asm20
asc11	472	Epoxidase	67/75	AAM54089, Asm11
asc12	441	Halogenase	66/77	AAM54090, Asm12
asc13	307	3-hydroxyacyl-CoA dehydrogenase	65/72	AAM54091, Asm13
asc14	82	Acyl carrier protein	71/79	AAM54092, Asm14
asc15	369	Acyl-CoA dehydrogenase	66/76	AAM54093, Asm15
asc16	355	Unknown	65/75	AAM54094, Asm16
asc17	239	*O*-methyltransferase	63/75	AAM54095, Asm17
asc3	71	Unknown	46/63	AAM54081, Asm3
asc4	749	ABC transporter	50/65	AAM54082, Asm4
asc18	881	Transcriptional activator	72/83	AAM54096, Asm18
asc25	387	Glycosyltransferase	52/61	AAM54103, Asm25
asc21a	665	*O*-carbamyltransferase	58/71	AAM54099, Asm21
asc21b	657	*O*-carbamyltransferase	58/71	AAM54099, Asm21
orf3	250	ABC transporter ATP-binding protein	91/94	ANN16089
orf4	581	Peptide ABC transporter ATPase	88/91	ANN16088
orf5	319	Peptide ABC transporter permease	94/96	ANN16087
orf6	542	ABC transporter substrate-binding protein	86/91	ANN16086
asc8	837	Transcriptional regulator	47/55	AAM54086, Asm8
ascC	1530	Polyketide synthase	57/66	AAM54077, AsmC
module 5		KS-AT-KR-ACP		
ascD		Polyketide synthase		

module 6	3237	KS-AT-DH-KR-ACP	59/68	AAM54078, AsmD
module 7		KS-AT-DH*-KR-ACP		
ascB	2721	Polyketide synthase	58/66	AAM54076, AsmB
module 3		KS-AT-DH-KR-ACP		
module 4		KS-AT-ACP		
orf7	82	Unknown	93/94	ANN21707
orf8	114	Unknown	80/83	ANN16111
asc22	283	Kinase	43/56	AAM54100, Asm22
orf9	285	FkbM family methyltransferase	82/87	WP_052675174
ascR1	131	Unknown	85/92	OXM50191
ascR2	259	Ribonuclease	95/96	OXM50192
ascR3	110	Unknown	42/51	WP_020639457
ascR4	168	GNAT family *N*-acetyltransferase	87/91	AUI58232

*Inactive domain.

1.2 Strains, plasmids and primers (Table S2)

For ansacarbamitocin analogs production, the strain *Amy. alba* 44262 and its mutants were cultivated on Waksman solid medium (3% glycerin, 0.5‰ KCl, 1‰ $K_2HPO_4 \cdot 3H_2O$, 2‰ $NaNO_3$, 0.5‰ $MgSO_4 \cdot 7H_2O$, 0.01‰ $FeSO_4 \cdot 7H_2O$, pH 7.2), and the mutants of HGF052+pJTU824-*asm18* on YMG solid medium (0.4 % yeast extract, 1 % malt extract, 0.4 % glucose, pH 7.2). *Escherichia coli* XL-1 blue strain and ET12567/pUZ8002 strain were used as the general cloning host and the donor in intergeneric conjugations, respectively. Conjugation between *E. coli* and *Actinosynnema pretiosum* was performed on YMG solid medium supplemented with 10mM $MgCl_2$ as described in Ref. 20. *E. coli* strains were grown in Luria-Bertani (LB) medium. Apramycin or kanamycin was added into media as an antibiotic at a final concentration of 50 μg/mL for all strains in this study.

Suicide vector pOJ260 (1) was used throughout the study for in-frame gene inactivation. The integrating vector pSBT11 was used for gene expression in HGF052+pJTU824-*asm18* strain.

E. coli strains and plasmids used in this study are listed in Table S2.

Table S2. *E. coli* strains and plasmids used in this study

strains or plasmids	description	source
E.coli		
XL1-Blue	Host strain for general clone	Stratagene
ET12567/pUZ8002	Host strain for conjugation between *E.coli* and *Actinosynnema*	(2)
BL21 (DE3)	Host strain for protein production	Novagen
Plasmids		
pOJ260	*aac(3)IV oriT* rep^{PUC} *lacZ*	(1)
pSET152	*aac(3)IV oriT*(RK2) *ori*(pUC18) *int*(*φC31*), *attP*(*φC31*) *lacZα*	(1)
pSET152ER	pSET152 carrying *PermE**	This study
pSBT11	Replacement of *φC31 attP-int* fragment of pSET152ER with *φBT1 attP-int* fragment	This study
pET-28a-MBP	Modified pET-28a with an N-terminal MBP fusion tag	(3)
pET-28a-SUMO	Modified pET-28a with an N-terminal SUMO fusion tag	(4)

1.3 DNA manipulation (Table S3)

Gene inactivation. The knockout plasmids for specific genes were generated as the following steps. The ~2.5-kb upstream and downstream homologous arms of the target genes were amplified by PCR of the genomic DNA, respectively. Purified PCR fragments were inserted into the linearized pOJ260 by Gibson assembly (5), which was then transformed into 100 μL XL-1 Blue competent cells. Positive clones were identified by restriction enzyme digestion and DNA sequencing. The knockout vectors were propagated in XL-1 Blue, and transformed into *Amy. alba* 44262 competent cells by electroporation as described by Ding *et al*. (6). The apramycin-resistant recombinants resulting from the homologous recombination between the knockout vector and genomic DNA of the receptor strain were selected, transferred to YMG agar for several rounds of nonselective growth. Apramycin-sensitive recombinants derived from a second crossover event were screened and verified by PCR.

Reverse transcription PCR (RT-PCR). The mycelia of the strains *Amy. alba* 44262, *Δasc21a* and *Δasc21b* were collected after being cultured on Waksman solid medium for 72 h, then quickly frozen in liquid nitrogen and ground into fine white powder. Total RNA was isolated using the Trizol reagent (Invitrogen) according to the manufacturer's Instructions. The genomic DNA was eliminated using the gDNA Eraser reagent (TaKaRa, Dalian China). Purified RNA were used to generate complementary DNA (cDNA) using the PrimeScript RT reagent Kit (TaKaRa, Dalian China). The resulting cDNA was amplified by PrimeSTAR Max DNA Polymerase (TaKaRa, Dalian China) using the corresponding primers (Table S3). The RNA polymerase principal sigma factor gene *hrdB* was used as an internal control.

Heterologous expression in HGF052+pJTU824-*asm18*. The integrating vector pSBT11 was used for gene expression in HGF052+pJTU824-*asm18* strain. Synthesized *ermE** promoter fragment (7) was digested with *Spe*I and *Xba*I, and inserted into *Xba*I-pretreated pSET152 vector (1) to yield pSET152ER. The *φ*C31 *attP-int* sequence in pSET152ER was then replaced with the *φ*BT1 *attP-int*-containing fragment as described previously (8) to yield pSBT11. The *asc21a* and *asc21b* genes were amplified by PCR using the genomic DNA of *Amy. alba* 44262 as a template, respectively. The *Nde*I/*Eco*RI PCR fragments were inserted into the downstream of *ermE** promoter in pSBT11, respectively. The resultant plasmids pSBT11-*asc21a* and pSBT11-*asc21b* were transformed into *E. coli* ET12567/pUZ8002, respectively, and then introduced into HGF052+pJTU824-*asm18* strain by conjunction.

Heterologous expression in *E. coli* BL21(DE3). The genes encoding full-length Asc21b and Asc25 were amplified by PCR, and cloned into the *Bam*HI and *Xho*I sites of pET-28a-MBP vector and pET-28a-SUMO, respectively.

Primers used in this study are listed in Table S3.

Table S3. Primers used in this study

Gene disruption	
asc9	asc9-UP-F: TTGGGCTGCAGGTCGACTCTAGAAGACCCTGTGCGTGCCG asc9-UP-R: GTTCGCTATCACCGCCAGCCCGCCGCCGTCGTCGGGAAAC asc9-DOWN-F: ACGACGGCGGCGGGCTGGCGGTGATAGCGAACACCACCAT asc9-DOWN-R: GATTACGAATTCGATATCCAGTCTCGGTACCGCGTGTGCC
ascL1	ascL1-UP-F: ACGGCCAGTGCCAAGCTTGTCCTTCCGGAAATGCTCGACC ascL1-UP-R: TCGCCGAGGATCGAGCGGGGCAG ascL1-DOWN-F: CCGCTCGATCCTCGGCGACGACGACCCACGCGACCCCGAG ascL1-DOWN-R: TGACATGATTACGAATTCCTGGGTGCCCGCACGGGTCGAT
asc22	asc22-UP-F: CCAGTGCCAAGCTTGGATCCGTCGAGTTGCTGACCGAGCC asc22-UP-R: CGTTCTTCGACACGCACGCCCGCCCGTACGACGTCCGAGG asc22-DOWN-F: TACGGGCGGGCGTGCGTGTCGAAGAACGATCACTTGCCTG asc22-DOWN-R: ATGATTACGAATTCACAAAGCTTGCCTGGGCGGGCAAGGC
orf9	orf9-UP-F: CCAGTGCCAAGCTTGAGCCCACGTCTCCGACCACAACGCG orf9-UP-R: TCCGCTCGTTCGACCACGAGTCCGATATGGGCTCCCACGT orf9-DOWN-F:ATATCGGACTCGTGGTCGAACGAGCGGAACTGGAAGTGCT orf9-DOWN-R: ATGATTACGAATTCCGGCTCCCGGTGGTCTCGAACGTGAC
ascR1	ascR1-UP-F: CCAGTGCCAAGCTTGCCGACAAAGCGCACGTCGCGTTCGG ascR1-UP-R: GCCATCGGTCTGCCGCGAAGTCGTTCAAGGTCAGCTCGGT ascR1-DOWN-F: GACCTTGAACGACTTCGCGGCAGACCGATGGCTGAAGAAT ascR1-DOWN-R: ATGATTACGAATTCTCGACTTCATCGACAACGAACTCGGC
asc21a	asc21a-UP-F: GCCAGTGCCAAGCTTGGCCGACTGCGTTCGGTCCTACTCG asc21a-UP-R: TCGGGTTTGCGGGTCTTGTCGTCGGGCAGGTCCCAGTCCA asc21a-DOWN-F: GCCCGACGACAAGACCCGCAAACCCGACTGGCGAAGTCG asc21a-DOWN-R: ATGATTACGAATTCAAGCTGGATCTGACGATCCTGTTCAT
asc21b	asc21b -UP-F: AGTGCCAAGCTTGGGCTGCAGACCGTCCAGCTGTTCGTCA asc21b -UP-R: TGATCCAAGAGCTCCTCGTAGTTCCCCTTCTCCTGCAACG asc21b-DOWN-F: GGGGAACTACGAGGAGCTCTTGGATCAAAGTGGAACAGC asc21b-DOWN-R: CGGCCGCGCTGGGGCCAGGGGTGGCGATCGTGCTGGCGG
asc25	asc25-UP-F: GCCAGTGCCAAGCTTACGGCGAGGTGATGCGCGAGCTGGA asc25-UP-R: GCCAGTCGTCGCGCCTCCCGCGCGTGAGAGCGAGCTCCCG asc25-DOWN-F: CTCACGCGCGGGAGGCGCGACGACTGGCGCTCCTCGCCTC asc25-DOWN-R: ATGATTACGAATTCTCACCGGCCAATCGGGGTGAGGGTGA
Verification of gene disruption	
asc9	asc9-VER-F: GCAAGGAACCCGCGTACT asc9-VER-R: ACGATCGACCCGGACATC

asmL1	ascL1-VER-F: CGAGTGGGACGGTTTCACC ascL1-VER-R: AGGACGAGATGCTGCGGTGG
asc22	asc22-VER-F: GCAAGACAGCCAGGCTGATC asc22-VER-R: GCAAGCGATGTCCCCGTCTG
orf9	orf9-VER-F: TGCCTGTCAAGGAAAACC orf9-VER-R: GGGTGAACTCGGGCATCT
ascR1	ascR1-VER-F: ATCGCCGTCTGCACAGCCAC ascR1-VER-R: TCTCCTTGAGACAGCGGAAG
asc21a	asc21a -VER-F: TGGAGTTCTTCTGCCACGATT asc21a -VER-R: GGATCTCGCTTCCCGTAAC
asc21b	asc21b-VER-F: ATGCTGGTGCTCGGACTGAACG asc21b-VER-R: TCCGTCCCGAGGATCGGCTGATC
asc25	asc25-VER-F: CAGGCGGAGGACGAGGTTT asc25-VER-R: GTTGAGGACCATGTCCATGTGA
RT-PCR	
asc21a	asc21a-F:CCGACGACATCGTCGAGCGGGCAG asc21a-R:CCTGCGGACCGGATCTCACGAGCC
asc21b	asc21b-F:GGACGACATCGTCGAGCGGGCAGC asc21b-R:TGTCACCGCAGGGGTCCGGTGCTC
hrdB	hrdB-F: CCAAGCGCATCGAGGCCGGGCTCT hrdB-R:GCAGCACCGACTGGAGCTGGTCCT
Gene expression and verification	
asc21a	asc21a-pSBT11-F: GGAGGCGGACATATGCTCGTACTCGGTTTGAACGGGAAC asc21a-pSBT11-R: CATGATTACGAATTCTCACCGGCCAATCGGGGTGAGGGTG
asc21b	asc21b-pSBT11-F: AAAGGAGGCGGACATATGCTGGTGCTCGGACTGAACGGC asc21b-pSBT11-R: ATGATTACGAATTCTCAGGCCGGAGTGAGGGTGAAGAAG
pSBT11	SBT-F: CGCCCGATGCTAGTCGCGGTTGA SBT-R: AGCGGATAACAATTTCACACA
Protein production	
asc21b	asc21b-MBP-F:GGGGCCCCTGGGATCCATGCTGGTGCTCGGACTGAACGGC asc21b-MBP-R:TTTGTTAGCAGCCGGATCTCAGGCCGGAGTGAGGGTGAAG
asc25	asc25-SUMO-F:ACAGATTGGTGGATCCGTGCGGCGAATATTGTGCACGGTG asc25-SUMO-R:GGTGGTGGTGCTCGAGTTACCTTGCAGAGGCGAGGAGCGC

1.4 Detection and analysis of the metabolites in mutants

For ansamitocins production, *Amy. alba* 44262 and its mutants were inoculated on Waksman medium (100 mL) in petri dishes and cultivated for 10 days at 28 °C. The culture was diced and extracted overnight with EtOAc/MeOH (4:1, v/v) at room temperature. The concentrated crude extract was then dissolved in 1 mL

MeOH, and analyzed by high-pressure liquid chromatography (HPLC; CAPCELL PAK ADME 4.6×250 mm, 5 μm). Chromatographic conditions were as follows: solvents: A) water, and B) CH_3CN; Samples were eluted with a linear gradient from 20 to 35% B in the first 5 min, increased to 55% B at 19 min, to 65% B at 20 min, to 100% B at 23 min, followed by 4 min with 100% B; flow rate: 1 mL/min, and UV detection at 254 nm. The metabolites of each *Act. pretiosum* strain was extracted and analyzed according to Li *et al*'s method in Ref. 20.

1.5 Fermentation and isolation of ansamitocin derivatives

The fermentation and extraction of each mutant strain of *Amy. alba* 44262 was performed as the procedure described in Ref. 8. In general, after the removal of glycerin in the crude extract, the MeOH extract was fractionated by MPLC over RP-18 silica gel with 30, 50, 70 and 100% MeOH, to obtain 4 fractions Fr. A–D. Target compounds were identified by HPLC as described above, and the corresponding fractions were further purified by semipreparative reversed-phase HPLC (CAPCELL PAK ADME 10 × 250 mm, 5 μm, flow rate: 4 ml/min, UV detection at 254 nm) to afford the main products of each mutant. Specifically, Fr. C (45.6 mg) of *Δorf9* was purified by HPLC (CH_3CN-H_2O (28:72, v/v)) to afford **3** (t_R 17.5 min, 3.1 mg), **4** (t_R 22.5 min, 5.8 mg) and **5** (t_R 25.0 min, 7.6 mg); Fr. C (280.0 mg) of *Δasc25* was purified by HPLC (CH_3CN-H_2O (40:60, v/v)) to afford **6** (t_R 4.5 min, 30.0 mg) and **7** (t_R 9.5 min, 8.3 mg); Fr. B (91.0 mg) of *Δasc21a* was purified by HPLC (CH_3CN-H_2O (30:70, v/v)) to afford **8** (t_R 16.1 min, 3.2 mg), **9** (t_R 17.3 min, 5.1 mg) and **10** (t_R 19.7 min, 7.3 mg); Fr. B (46.0 mg) of *Δasc21b* was purified by HPLC (CH_3CN-H_2O (32:68, v/v)) to afford **8** (t_R 13.5 min, 8.0 mg), **9** (t_R 15.0 min, 9.7 mg) and **10** (t_R 19.0 min, 10.6 mg).

The strain HGF052+pJTU824-*asm18*+pSBT11-*asc21b* was cultured on YMG agar medium (15L) for 10 days at 28 °C. The culture was chopped into small pieces and extracted four times with EtOAc/MeOH (4:1, v/v) to give a crude extract. The extract was subjected to medium pressure liquid chromatograph (MPLC) over RP-18 silica gel eluted with H_2O, 30, 70 and 100 % MeOH to obtain 4 fractions Fr. A–D. Fr. C (2.2 g) was further subjected to column chromatograph (CC) over Sephadex LH-20 eluted with methanol to give 5 subfractions (Fr. C1−C5). Fr. C3 (954.9 mg) was further purified by semipreparative reversed-phase HPLC (ZORBAX Eclipse XDB-C18 column 9.4 × 250 mm, 5 μm, 36% CH_3CN, flow rate: 4 ml/min, UV detection at 254 nm) to afford **11** (t_R 19.8 min, 3.7 mg), **12** (t_R 18.0 min, 10.7 mg), **13** (t_R 15.2 min, 5.7 mg), and **14** (t_R 8.5 min, 4.5 mg).

1.6 Protein production, purification and enzymatic assays

Protein production vectors were transformed into *E. coli* BL21 (DE3) cells for protein production. The transformed cells were grown in LB medium supplemented with 50 μg/ml kanamycin at 37°C to an OD_{600} of 0.4–0.6. Then protein production was induced by 0.1 mM isopropyl-β-D-1-thiogalactopyranoside at 16°C overnight for MBP-Amb21b or 25°C for 8 h for SUMO-Asc25. The following procedures were carried out at 4°C. Cells were harvested at 4,000 rpm for 30 min, and resuspended in 20 mM Tris–HCl (pH 8.0) buffer containing 100 mM NaCl. After lysed by high pressure, the supernatant was obtained by centrifugation at 10,000 rpm for 40 min, and loaded onto Ni–NTA affinity resin (Qiagen) for affinity chromatography of the N-terminal His_6-tagged protein. Unspecific bound proteins were washed out with wash buffer A (20 mM Tris-HCl, pH 8.0, 100 mM NaCl, 20 mM imidazole) and wash buffer B (20 mM Tris-HCl, pH 8.0, 100 mM NaCl, 50 mM imidazole), respectively. The target proteins were eluted with buffer C (20 mM Tris-HCl, pH 8.0, 100 mM NaCl, and 250 mM imidazole). Protein concentrations were determined by the modified Bradford method (Sangon

Biotech) with bovine serum albumin as standard.

The *in vitro N*-glycosyltransferase activity of Asc25 was assayed with mixture containing 25 mM Tris-HCl (pH 8.0), 200 mM NaCl, 10 mM $MgCl_2$, 1 mM DTT, 10% glycerol, 0.4 mM UDP-Glucose, 0.2 mM **6**, and purified SUMO-Asm21 (32 μM) in a total volume of 100 μL. The mixtures were incubated at 37 °C for 4 and 24 h, and then quenched by addition of 200 μL *n*-butanol. The samples were dissolved in methanol after the evaporation of the organic solvent, and analyzed by HPLC (YMC Pack-Pro C18, 250 x 4.6mm, 5 μm, 63% methanol with formic acid (0.1%), flow rate: 1 ml/min, UV detection at 254 nm). The electrospray ionization mass spectrometry (ESIMS) was carried out on a LTQ VELOS PRO ORBITRAP instrument (Thermo Fisher) equipped with an YMC Pack-Pro C18 (250 x 4.6mm, 5 μm) column in positive mode.

The *in vitro* 3-*O*-carbamyltransferase activity of Asc21b was assayed with mixture containing 20 mM Tris-HCl (pH 8.0), 100 mM NaCl, 10 mM $MgCl_2$, 2 mM DTT, 10% glycerol, 2 mM ATP, 0.2 mM carbamyl phosphate disodium, 0.1 mM **12**, and purified MBP-Asm21 (1 mM) in a total volume of 300 μL. After incubated at 30 °C overnight, the reaction was quenched by addition of 300 μL ethyl acetate, and then extracted twice with ethyl acetate. The samples were dissolved in methanol after the evaporation of the organic solvent, and analyzed by HPLC (YMC Pack-Pro C18, 250 x 4.6mm, 5 μm, 35% acetonitrile with formic acid (0.1%), flow rate: 1 ml/min, UV detection at 254 nm). The electrospray ionization mass spectrometry (ESIMS) was carried out on a LTQ ORBITRAP XL instrument (Thermo Fisher) equipped with an YMC Pack-Pro C18 (250 x 4.6mm, 5 μm) column in positive mode.

1.7 Cell proliferation inhibition assay

Cancer cells were seeded in 96-well plates at the density of 3,000 cells/well/100 μL. After 24 h of cultivation, cells were treated with various concentrations of compounds and incubated at 37 °C and 5 % CO_2 for 72 h. The sulforhodamine B (SRB) assay was used to measure the inhibition of cell proliferation (9). Briefly, the cell culture medium was removed, and cold 10% (w/v) trichloroacetic acid (TCA) was gently added into each well. After fix at 4°C for at least 1 h, the cells were rinsed five times with slow-running tap water, and stained in 0.4% (w/v) SRB solution for 15 min at room temperature. Cells were then immediately washed five times with 1% (v/v) acetic acid and air-dried. The protein-bound dye SRB was then extracted in 10 mM Tris base solution (pH 10.5), and the microplates were assayed at 570 nm by a microplate reader (Bio-Rad 680, USA). All experiments were carried out in parallel triplicate. The cell inhibitory rate at a certain concentration of the compound was calculated using the following formula:

$$\text{Cell viability (\%)} = \frac{\text{OD}_{\text{Sample}} - \text{OD}_{\text{Blank}}}{\text{OD}_{\text{Control}} - \text{OD}_{\text{Blank}}} \times 100$$

The cytotoxicities of compounds were expressed as IC_{50} that was defined as compound concentration required inhibiting growth by 50% relative to controls.

2, NMR data of compounds 3–14

Table S4. NMR (600 MHz) spectroscopic data for **3** in CD_3OD (δ in ppm, J in Hz)

No.	^{1}H (mult., J in Hz)	^{13}C mult.	HMBC (H→C)	COSY (H↔H)
1		173.2s		
2a	2.16 (d, 13.6)	34.7t	C-1	H-2b, H-3
2b	2.51-2.47 (m)		C-1, C-3	H-2a, H-3
3	4.33-4.31 (m)	79.3d		H-2a, H-2b
4		62.0s		
5	2.86 (d, 8.3)	69.2d	C-3, C-6, C-6-Me	H-6
6	1.52 (br s)	39.5d	C-5	H-5, H-6-Me, H-7
7	4.28-4.24 (m)	76.1d		H-6
8a	1.46-1.42 (m)	37.4t	C-7	H-7, H-8b
8b	1.69 (d, 11.9)		C-9	H-8a
9		81.9s		
10	3.57-3.53 (m)[a]	90.3d	C-9, C-10-OMe, C-12	H-11
11	5.58-5.54 (m)	129.0d	C-13	H-10, H-12
12	6.60-6.55 (m)	134.5d	C-10	H-11, H-13
13	6.29 (d, 10.7)	125.4d	C-11, C-12, C-14-Me, C-15	H-12
14		141.5s		
15a	3.13 (d, 11.5)	46.9t	C-16, C-17, C-21	H-15b
15b	3.57-3.53 (m)[a]		C-14-Me, C-16, C-17, C-21	H-15a
16		141.0s		
17	7.08 s	125.6d	C-15, C-18, C-19, C-21	
18		137.0s		
19		121.6s		
20		155.3s		
21	6.97 s	119.1d	C-15, C-17, C-19, C-20	
1’	5.80 (d, 9.0)	84.1d	C-1,C-18, C-3’	H-2’
2’	3.19-3.15 (m)[a]	72.0d	C-1’, C-3’	H-1’, H-3’
3’	3.64 (br s)	76.7d	C-4’	H-2’, H-4’
4’	4.36-4.35 (m)	72.9d	C-3’, C-4’-carbam, C-6’	H-3’, H-5’
5’	3.70 (br s)	75.3d		H-4’, H-6’a
6’a	4.01-4.00 (m)	64.1t		H-5’, H-6’b
6’b	4.14 (d, 12.9)			H-5’, H-6’a
3-carbam		158.1s		
4-Me	0.76 (s)	11.7q	C-3, C-4, C-5	
6-Me	1.22 (br s)	14.7q	C-5, C-6, C-7	H-6
7-carbam		155.4s		
10-OMe	3.35 (s)	56.9q	C-10	
14-Me	1.74 (s)	15.9q	C-13, C-14, C-15	
4’-carbam		158.9s		
6’-Ac C=O		172.6s		
6’-Ac	2.00 (s)	20.7q		

[a]Overlapped signals.

Table S5. NMR (600 MHz) spectroscopic data for **4** in CD_3OD (δ in ppm, J in Hz)

No.	^{1}H (mult., J in Hz)	^{13}C mult.	HMBC (H→C)	COSY (H↔H)
1		173.2s		
2a	2.14 (d, 13.1)	34.7t	C-1,	H-2a, H-3
2b	2.45 (t, 12.4)		C-1, C-3, C-4	H-2b, H-3
3	4.38-4.35 (m)[a]	79.3d	C-2, C-5	H-2a, H-2b
4		61.9s		
5	2.88 (d, 9.4)	69.1d	C-3, C-6, C-6-Me	H-6
6	1.55-1.48 (m)	39.4d	C-5, C-7	H-5, H-6-Me, H-7
7	4.23 (t, 10.9)	76.2d		H-8a, H-8b
8a	1.40 (t,12.9)	37.4t		H-7, H-8b
8b	1.63 (d,13.6)		C-9	H-8a
9		81.8s		
10	3.52 (d, 8.3)	90.2d	C-9, C-10-OMe, C-12	H-11
11	5.48-5.44 (m)	128.8d	C-13	H-10, H-12
12	6.55 (t, 12.8)	134.5d	C-10, C-13, C-14	H-11, H-13
13	6.32 (d, 10.7)	125.3d	C-11, C-12, C-14-Me, C-15	H-12
14		141.6s		
15a	3.12 (d, 12.2)	46.8t	C-14-Me, C-16, C-17, C-21	H-15b
15b	3.56 (d, 10.6)		C-14-Me, C-16, C-17, C-21	H-15a
16		141.0s		
17	7.05 (s)	125.5d	C-15, C-18, C-19, C-21	
18		136.9s		
19		121.6s		
20		155.3s		
21	6.97 (s)	119.1d	C-15, C-17, C-19, C-20	
1’	5.79 (d, 8.9)	84.0d	C-1,C-18, C-3’	H-2’
2’	3.16 (t, 8.6)	72.0d	C-1’, C-3’	H-1’, H-3’
3’	3.68-3.62 (m)[a]	76.7d	C-4’	H-2’, H-4’
4’	4.38-4.35 (m)[a]	72.9d	C-3’, C-4’-carbam	H-3’
5’	3.72-3.66 (m)[a]	75.3d		H-4’, H-6’a, H-
6’a	4.03-3.98 (m)	64.1t		H-5’, H-6’b
6’b	4.14 (d, 11.9)		C-4’	H-5’, H-6’a
3-carbam		157.8s		
NMe	2.76 (s)	27.9q	C-3-carbam	
4-Me	0.76 (s)	11.7d	C-3, C-4, C-5	
6-Me	1.22 (br s)	14.8d	C-5, C-6, C-7	H-6
7-carbam		155.5s		
10-OMe	3.35 (s)	56.9q	C-10	
14-Me	1.73 (s)	15.9d	C-13, C-14, C-15	
4’-carbam		158.9s		
6’-Ac C=O		172.6s		
6’-Ac	2.00 (s)	20.7q		

[a]Overlapped signals.

Table S6. NMR (600 MHz) spectroscopic data for **5** in CD_3OD (δ in ppm, J in Hz)

No.	^{1}H (mult., J in Hz)	^{13}C mult.	HMBC (H→C)	COSY (H↔H)
1		173.3s		
2	2.29-2.23 (m, 2H)[a]	38.7t	C-1, C-3	H-3
3	5.29 (d, 9.8)	75.8d	C-2, C-5	H-2
4		136.5s		
5	5.17 (d, 7.1)	129.0d	C-3, C-6-Me	H-6
6	2.51 (br s)	38.0d	C-5, C-7	H-5, H-6-Me, H-7
7	4.10-4.03 (m)	78.8d		H-6, H-8a
8a	1.36-1.22 (m)[a]	36.1t		H-7, H-8b
8b	1.54 (d, 12.5)		C-9	H-8a
9		82.1s		
10	3.54 (d, 8.9)	89.3d	C-9, C-10-OMe, C-12	H-11
11	5.41-5.35 (m)	127.9d	C-13	H-10, H-12
12	6.51 (t, 13.1)	134.1d	C-10, C-13, C-14	H-11, H-13
13	6.00 (d, 9.8)	125.5d	C-11, C-12, C-14-Me, C-15	H-12
14		141.5s		
15a	3.19 (d, 13.2)	46.4t	C-14-Me, C-16, C-17, C-21	H-15b
15b	3.43 (d, 12.5)		C-14-Me, C-16, C-17, C-21	H-15a
16		141.3s		
17	7.00 (s)	124.8d	C-15, C-18, C-19	
18		136.7s		
19		121.9s		
20		155.5s		
21	6.95 (s)	118.8d	C-15, C-19, C-20	
1’	5.74 (d, 8.9)	84.4d	C-1,C-18, C-2’	H-2’
2’	3.20-3.14 (m)[a]	71.8d	C-1’, C-3’	H-1’, H-3’
3’	3.61-3.58 (m)[a]	76.9d	C-4’	H-2’, H-4’
4’	4.34 (t, 8.2)	72.8d	C-3’, C-4’-carbam, C-6’	H-3’, H-5’
5’	3.70-3.66 (m)[a]	75.2d		H-4’, H-6’a
6’a	4.02-3.97 (m)	64.1t		H-5’, H-6’b
6’b	4.13 (d, 12.0)		C-4’, C-5’	H-5’, H-6’a
3-carbam		158.4s		
NMe	2.71 (s)	27.6q	C-3-carbam	
4-Me	1.30 (s)	13.7q	C-3, C-4, C-5	
6-Me	1.07 (br s)	17.0q	C-5, C-6, C-7	H-6
7-carbam		155.9s		
10-OMe	3.35 (s)	57.1q	C-10	
14-Me	1.85 (s)	16.9q	C-13, C-14, C-15	
4’-carbam		158.9s		
6’-Ac C=O		172.6s		
6’-Ac	1.99 (s)	20.7q		

[a]Overlapped signals.

Table S7. NMR (400 MHz) spectroscopic data for **6** in $(CD_3)_2SO$ (δ in ppm, J in Hz)

No.	^{1}H (mult., J in Hz)	^{13}C mult.	HMBC (H→C)	COSY (H↔H)
1		169.9s		
2a	1.92 (br s)	32.0t		H-2b
2b	2.59-2.52 (m)			H-2a, H-3
3	4.36 (br s)	76.3d		H-2b
4		60.9s		
5	2.86 (d, 9.6)	66.7d	C-3, C-4, C-6, C-6-Me	H-6
6	1.47-1.40 (m)[a]	37.8d		H-5, H-6-Me
7	4.11 (m)	73.8d		H-6
8	1.47-1.40 (m, 2H)[a]	35.9t		H-7
9		80.1s		
10	3.47 (d, 8.4)	88.4d	C-9, C-10-OMe, C-12	H-11
11	5.35 (dd,14.8, 8.9)	128.3d	C-13	H-10, H-12
12	6.53 (dd, 14.8, 11.1)	132.2d	C-10, C-13, C-14	H-11
13	6.45 (br s)	125.6d		
14		138.3s		
15a	3.02 (d, 10.2)	44.9t		H-15b
15b	3.56 (br s)			H-15a
16		139.5s		
17	6.83 (s)	121.0d		
18		136.4s		
19		115.4s		
20		153.3s		
21	6.80 (s)	116.1d		
3-carbam		155.3s		
NH	6.12 (br s)			H-NMe
NMe	2.62 d (4.5)	27.3q	C-3-carbam	H-NH
4-Me	0.87 (s)	11.4q		
6-Me	1.09 (d, 5.4)	14.5q	C-5, C-6, C-7	H-6
7-carbam		151.4s		
10-OMe	3.23 (s)	56.2q	C-10	
14-Me	1.59 (s)	15.4q	C-13, C-14, C-15	
18-NH	9.39 (s)		C-1, C-2, C-17, C-18, C-19, C-20	

[a]Overlapped signals.

Table S8. NMR (400 MHz) spectroscopic data for **7** in $(CD_3)_2SO$ (δ in ppm, J in Hz)

No.	^{1}H (mult., J in Hz)	^{13}C mult.	HMBC (H→C)	COSY (H↔H)
1		167.5s[c]		
2a	2.87 (br s)	37.8t		H-3
2b	nd[a]			
3	5.20-5.10 (m)[b]	72.5d	C-1, C-2, C-4, C-4-Me, C-5	H-2a
4		135.9s		
5	5.20-5.10 (m)[b]	123.1d	C-3, C-4, C-6, C-6-Me	H-6
6	2.58-2.52 (m)[b]	36.8d		H-5, H-6-Me, H-7
7	4.17 (br s)	76.8d		H-6, H-8a
8a	1.29-1.24 (m)	34.4t		H-7, H-8b
8b	1.76-1.65 (m)[b]			H-8a
9		80.5s		
10	3.51 (d, 8.5)	86.6d	C-9, C-10-OMe, C-12	H-11
11	5.41 (br s)	127.0d		H-10, H-12
12	6.59-6.53 (m)[b]	131.7d	C-10	H-11, H-13
13	5.97-5.78 (m)	127.0d		H-12
14		137.7s		
15a	3.10 (d, 15.0)	44.1t	C-13, C-14-Me, C-16, C-21	H-15b
15b	3.27 (d, 15.0)			H-15a
16		138.8s		
17	6.94 (s)	117.7d		
18		nd[a]		
19		nd[a]		
20		151.8s		
21	6.59 (s)	112.6d[d]		
3-carbam		156.0s		
NH	7.31 (br s)			H-NMe
NMe	2.55 (d, 4.4)	27.0q	C-3-carbam	H-NH
4-Me	1.61 (s)	14.8q		
6-Me	0.96 (d, 6.4)	17.8q	C-5, C-6, C-7	H-6
7-carbam		153.0s		
9-NH	8.98 (s)			
10-OMe	3.22 (s)	55.9q	C-10	
14-Me	1.69 (s)	17.1q	C-13, C-14, C-15	
18-NH	10.1 (s)			

[a]nd: not observed and/or not defined.
[b]Overlapped signals.
[c]Estimated from HMBC correlations.
[d]Estimated from HMQC correlations.

Table S9. NMR (400 MHz) spectroscopic data for **8** in CD_3COCD_3 (δ in ppm, J in Hz)

No.	^{1}H (mult., J in Hz)	^{13}C mult.	HMBC (H→C)	COSY (H↔H)
1		nd[b]		
2	2.88-2.80 (m, 2H)	43.1t[c]		H-3
3	4.30 (dd, 3.4, 6.3)	72.3d	C-4, C-5	H-2
4		138.3s		
5	5.46 (d, 10.1)	126.8d	C-3 , C-4-Me, C-6	H-6
6	2.54-2.48 (m)	39.6d		H-5, H-6-Me
7	3.70-3.67 (m)	74.3d		H-6, H-8a, H-8b
8a	2.56 (dd, 8.8, 15.5)	44.0t	C-7, C-9	H-7, H-8b
8b	3.13 (br d, 15.3)			H-7, H-8a
9		198.2s		
10		152.2s		
11	6.80 (d, 10.6)	129.7d	C-9, C-10, C-13	H-12
12	6.49 (dd, 10.7, 15.6)	120.8d	C-10, C-11, C-14	H-11, H-13
13	6.23 (d, 15.5)	148.8d	C-11, C-14, C-14-Me	H-12
14		73.1s		
15	2.77 (d, 1.8)	51.3t	C-13, C-14, C-14-Me, C-16, C-17, C-21	
16		138.0s		
17	7.43 (s)	117.7d[c]		
18		135.7s		
19		112.6s		
20		153.6s		
21	6.72 (s)	114.1d		
4-Me	1.66 (s)	16.2q	C-3, C-4, C-5	
6-Me	1.01 (d, 6.6)	17.6q	C-5, C-6, C-7	H-6
10-OMe	3.57 (s)	59.9q	C-10	
14-Me	1.35 (s)	27.8q	C-13, C-14, C-15	

[a]Overlapped signals.
[b]nd: not observed and/or not defined.
[c]Estimated from HMQC correlations.

Table S10. NMR (400 MHz) spectroscopic data for **9** in CD_3COCD_3 (δ in ppm, J in Hz)

No.	^{1}H (mult., J in Hz)	^{13}C mult.	HMBC (H→C)	COSY (H↔H)
1		170.7s		
2	2.95-2.83 (m, 2H)[a]	43.6t		H-3
3	4.35-4.32 (m)	72.1d		H-2
4		137.8s		
5	5.47 (d, 9.8)	127.1d	C-3 , C-4-Me	H-6
6	2.48-2.41 (m)[a]	39.3d	C-4, C-5	H-5, H-6-Me, H-7
7	3.73-3.67 (m)	73.3d		H-6, H-8a, H-8b
8a	2.48-2.41 (m)[a]	44.6t	C-7, C-9	H-7, H-8b
8b	3.13 (dd, 16.2, 1.8)		C-9	H-7, H-8a
9		198.1s		
10		151.7s		
11	6.71 (d, 11.1)	129.3d	C-9, C-10, C-12, C-13	H-12
12	6.48 (dd, 15.4, 10.8)	120.8d	C-10, C-11, C-14	H-11, H-13
13	6.18 (d, 15.4)	148.9d	C-12, C-11, C-14	H-12
14		73.5s		
15	2.77 (s, 2H)	51.0t	C-13, C-14, C-14-Me, C-16, C-17, C-21	
16		138.2s		
17	7.44 (s)	117.6d		
18		135.9s		
19		109.4s[b]		
20		153.3s		
21	6.70 (s)[a]	114.5d	C-15, C-17, C-19	
4-Me	1.72 (s)	16.1q	C-3, C-4, C-5	
6-Me	1.00 (d, 6.6)	17.0q	C-5, C-6, C-7	H-6
10-OMe	3.55 (s)	59.9q	C-10	
14-Me	1.36 (s)	28.5q	C-13, C-14, C-15	

[a]Overlapped signals.
[b]Estimated from HMBC correlations.

Table S11. NMR (400 MHz) spectroscopic data for **10** in CD_3OD (δ in ppm, J in Hz)

No.	^{1}H (mult., J in Hz)	^{13}C mult.	HMBC (H→C)	COSY (H↔H)
1		171.3s		
2a	2.71-2.64 (m)	43.3t		H-3
2b	2.83-2.79 (m)[a]			H-3
3	4.38 (br s)	75.0d		H-2a
4		136.6s		
5	5.36 (d, 9.8)	129.7d		H-6
6	2.46-2.37 (m)[a]	38.8d	C-4, C-5	H-5, H-6-Me, H-7
7	4.04 (br s)	72.4d		H-6, H-8a, H-8b
8a	2.46-2.37 (m)[a]	45.3t		H-7, H-8b
8b	2.83-2.79 (m)[a]			H-7, H-8a
9		nd[b]		
10	4.47 (d, 6.9)	89.0d		
11	5.42 (dd, 14.8, 8.1)	126.2d		H-10, H-12
12	6.80-6.77 (m)	134.2d		H-11, H-13
13	5.98 (d, 9.6)	128.0d		H-12
14		140.3s		
15a	3.20 (d, 14.6)	46.1t	C-13, C-14, C-14-Me, C-21	
15b	3.34-3.29 (m)[a]		C-13, C-14, C-14-Me, C-21	
16		137.6s		
17	7.02 (s)	116.5d		
18		137.6s		
19		nd[b]		
20		nd[b]		
21	6.63 (s)	115.0d		
4-Me	1.66 (s)	12.9q	C-4	
6-Me	0.82 (br d, 4.6)	16.0q	C-5, C-6, C-7	H-6
10-OMe	3.33 (s)	56.9q	C-10	
14-Me	1.75 (s)	16.9q	C-13, C-14, C-15	

[a]Overlapped signals.
[b]nd: not observed and/or not defined.

Table S12. NMR (400 MHz) spectroscopic data for **11** in CD_3COCD_3 (δ in ppm, J in Hz)

No.	^{1}H (mult., J in Hz)	^{13}C mult.	HMBC (H→C)	COSY (H↔H)
1		171.0s		
2a	1.87 (dd, 1.1, 12.8)	35.9t	C-1, C-3	H-2b, H-3
2b	2.31 (td, 1.2,12.1)			H-2a, H-3
3	3.52-3.48 (m)[a]	76.6d	C-1, C-2, C-4, C-4-Me	H-2a, H-2b
4		63.9s		
5	2.58 (d, 9.8)	67.1d	C-3, C-6, C-6-Me	H-6
6	1.53-1.45 (m)	39.1d		H-5, H-6-Me, H-7
7	4.21 (td, 1.6, 11.2)	75.7d		H-8a, H-8b
8a	1.36 (dt, 11.9, 13.0)	35.9t	C-6, C-7, C-10	H-8b
8b	2.12-2.08 (m)[a]		C-9	H-8a, H-7
9		81.6s		
10	3.61 (d, 9.2)	89.6d	C-9, C-10-OMe, C-12	H-11
11	5.48 (dd, 9.2, 15.3)	128.3d	C-13	H-10, H-12
12	6.65 (dd, 11.0, 15.4)	134.0d	C-10, C-13, C-14	H-11, H-13
13	6.17 (d, 10.8)	126.1d	C-11, C-12, C-14-Me, C-15	H-12
14		139.3s		
15a	3.24 (d, 13.2)	47.1t	C-14, C-14-Me, C-16, C-17, C-21	H-15b
15b	3.52-3.48 (m)[a]			H-15a
16		141.4s		
17	7.13 (d, 1.4)	124.8d	C-15, C-18, C-19, C-21	
18		143.4s		
19		118.9s		
20		156.4s		
21	7.15 (d, 1.4)	113.9d	C-15, C-16, C-17, C-19, C-20	
4-Me	0.89 (s)	11.5q	C-3, C-4, C-5	
6-Me	1.18 (d, 6.4)	14.9q	C-5, C-6, C-7	H-6
7-carbam		152.0s		
10-OMe	3.32 (s)	56.6q	C-10	
14-Me	1.73 (s)	15.7q	C-13, C-14, C-15	
18-NMe	3.12 (s)	35.6q	C-1, C-18	
20-OMe	3.98 (s)	56.8q	C-20	

[a]Overlapped signals.

Table S13. NMR (400 MHz) spectroscopic data for **12** in $CDCl_3$ (δ in ppm, J in Hz)

No.	^{1}H (mult., J in Hz)	^{13}C mult.	HMBC (H→C)	COSY (H↔H)
1		169.5s		
2	2.99-2.83 (m, 2H)	38.5t		H-3
3	4.36-4.19 (m)[a]	71.7d		H-2
4		135.2s		
5	5.63-5.44 (m)	124.1d		H-6
6	2.54 (br s)	37.3d		H-5, H-6-Me, H-7
7	4.36-4.19 (m)[a]	78.2d		H-6, H-8a
8a	1.27-1.20 (m)	34.5t		H-8b, H-7
8b	2.00-1.90 (m)[a]			H-8a
9		81.5s		
10	3.46 (d, 8.6)[a]	87.9d	C-9, C-10-OMe, C-12	H-11
11	5.63-5.44 (m)	125.2d		H-10, H-12
12	6.51-6.47 (m)	134.3d		H-11, H-13
13	6.13 (d, 8.5)	126.5d		H-12
14		139.4s		
15a	3.09 (d, 13.5)	46.3t		H-15b
15b	3.43 (m)[a]		C-14, C-14-Me	H-15a
16		139.9s		
17	7.91 (s)	112.0d		
18		136.2s		
19		121.0s		
20		153.1s		
21	6.54 (s)	108.3d		
4-Me	1.62 (s)	14.5q	C-3	
6-Me	1.14 (d, 6.3)	17.6q	C-5, C-6, C-7	H-6
7-carbam		151.6s		
10-OMe	3.32 (s)	55.9q	C-10	
14-Me	1.67 (s)	16.6q	C-13, C-14, C-15	
20-OMe	3.89 (s)	56.3q	C-20	

[a]Overlapped signals.

Table S14. NMR (400 MHz) spectroscopic data for **13** in $CDCl_3$ (δ in ppm, J in Hz)

No.	^{1}H (mult., J in Hz)	^{13}C mult.	HMBC (H→C)	COSY (H↔H)
1		nd[b]		
2	2.85 (br s, 2H)	39.8t		H-3
3	5.20 (br s)	73.9d		H-2
4		133.2s		
5	5.35 (d, 7.7)	125.1d		H-6
6	2.62-2.56 (m)	37.7d	C-7	H-5, H-6-Me, H-7
7	4.39-4.34 (m)	78.0d		H-6, H-8a
8a	1.31-1.25 (m)	34.3t		H-7, H-8b
8b	2.02 (d, 9.8)			H-8a
9		81.4s		
10	3.48 (d, 9.1)	87.2d	C-9, C-10-OMe, C-12	H-11
11	5.53 (dd, 14.6, 9.4)	125.1d		H-10, H-12
12	6.56-6.50 (m)[a]	133.3d	C-10	H-11, H-13
13	6.01 (d, 10.4)	126.9d		H-12
14		138.8s		
15a	3.15 (d, 14.4)	45.4t	C-13, C-14-Me, C-16, C-17, C-21	H-15b
15b	3.38 (d, 14.9)		C-13, C-14-Me, C-16, C-17, C-21	H-15a
16		139.9s		
17	7.91 (s)	112.5d		
18		139.6s		
19		nd[b]		
20		154.6s		
21	6.53 (s)	108.2d	C-15, C-17	
3-carbam		156.2s		
4-Me	1.65 (s)	15.2q	C-3, C-4, C-5	
6-Me	1.12 d (6.5)	17.8q	C-5, C-6, C-7	H-6
7-carbam		152.9s		
10-OMe	3.32 (s)	56.0q	C-10	
14-Me	1.74 (s)	17.3q	C-13, C-14, C-15	
20-OMe	3.88 (s)	56.3q	C-20	

[a]Overlapped signals.
[b]nd: not observed and/or not defined.

Table S15. NMR (400 MHz) spectroscopic data for **14** in CD_3OD (δ in ppm, J in Hz)

No.	^{1}H (mult., J in Hz)	^{13}C mult.[a]	HMBC (H→C)	COSY (H↔H)
1		173.4s		
2a	2.24-2.07 (m)	33.5t		H-2b
2b	2.66 (dd, 13.4, 11.2)		C-3	H-2a
3	4.57 (d, 10.5)	78.4d		H-2b
4		62.4s		
5	2.90 (d, 9.6)	68.2d	C-4, C-4-Me, C-6, C-7, C-7	H-6
6	1.65-1.48 (m)[b]	39.4d		H-5, H-6-Me
7	4.34-4.29 (m)	76.3d		H-6, H-8a
8a	1.65-1.48 (m)[b]	37.3t		H-7, H-8b
8b	1.80 (d, 13.9)			H-8a
9		81.9s		
10	3.63-3.59 (m)[b]	89.9d	C-9, C-10-OMe, C-12	H-11
11	5.59 (dd, 8.9, 15.3)	129.7d	C-13	H-10, H-12
12	6.62 (dd, 11.0, 15.3)	134.0d	C-10, C-13, C-14	H-11, H-13
13	6.32 (br d, 8.1)	126.5d		H-12
14		141.0s		
15a	3.25 (d, 13.4)	47.1t	C-13, C-14-Me, C-16, C-17, C-21	H-15b
15b	3.63-3.59 (m)[b]			H-15a
16		141.8s		
17	7.02 (s)[b]	123.4d		
18		137.4s		
19		nd[c]		
20		157.0s		
21	7.02 (s)[b]	113.9d	C-15, C-17	
3-carbam		157.8s		
4-Me	1.01 (s)	12.7q		
6-Me	1.23 (d, 6.5)	14.8q	C-5, C-6, C-7	H-6
7-carbam		155.4s		
10-OMe	3.37 (s)	57.0q	C-10	
14-Me	1.74 (s)	16.1q	C-13, C-14, C-15	
20-OMe	3.95 (s)	57.0q	C-20	

[a] ^{13}C NMR spectra were obtained at 150MHz
[b] Overlapped signals.
[c] nd: not observed and/or not defined.

3, Supplementary figures

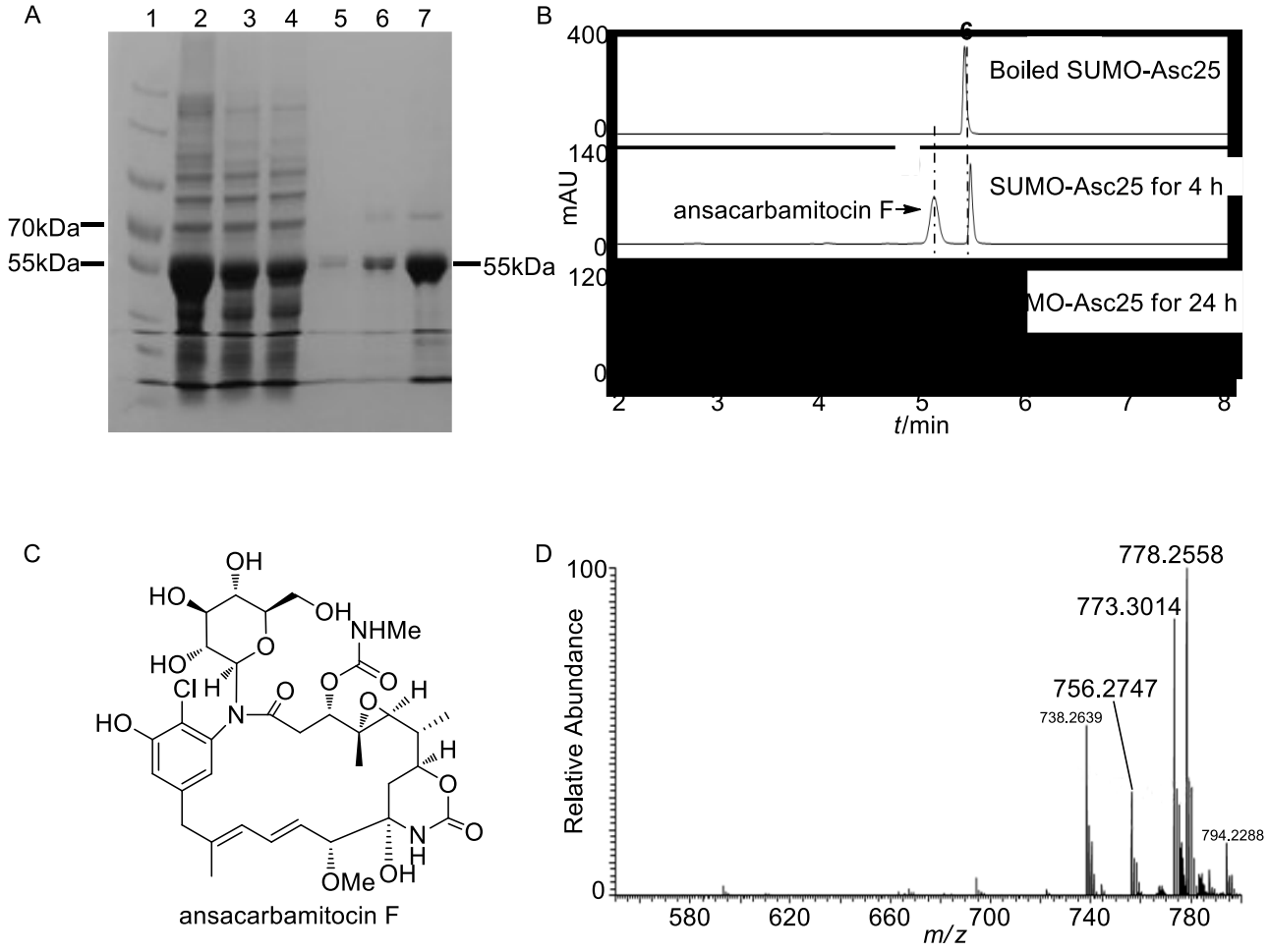

Figure S1. Production of SUMO-Asc25 and enzymatic assays.

(A) Analysis of SUMO-Asc25 protein purified from *E. coli* BL21 (DE3) by 10 % SDS-PAGE. Lane 1, protein ladder (Thermo Fisher, 26616); lane 2, cell lysate of *E. coli* BL21 (DE3) harbouring protein production vector pET-28a-SUMO-*asc25*; lane 3, supernatant of cell lysate of *E. coli* BL21 (DE3) harbouring protein production vector pET-28a-SUMO-*asc25*; lane 4, the flow-through fractions; lane 5, the elution fractions of wash buffer A; lane 6, the elution fractions of wash buffer B; lane 7, purified SUMO-Asc25. (B) HPLC analysis of enzymatic assays with **6** as substrate. (C) The structure of the presumed reaction product of SUMO-Asc25. (D) LC-MS analysis of the reaction product of SUMO-Asc25.

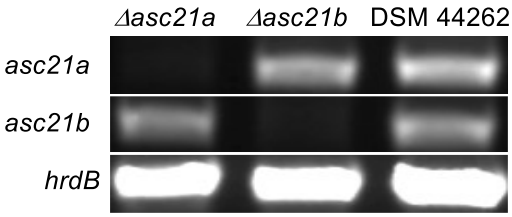

Figure S2. RT-PCR of carbamyltransferase genes.

These results suggested the inactivation of *asc21a* had no polarity effect on the transcription of *asc21b* and *vice versa*. RNA polymerase principal sigma factor gene *hrdB* was used as a reference.

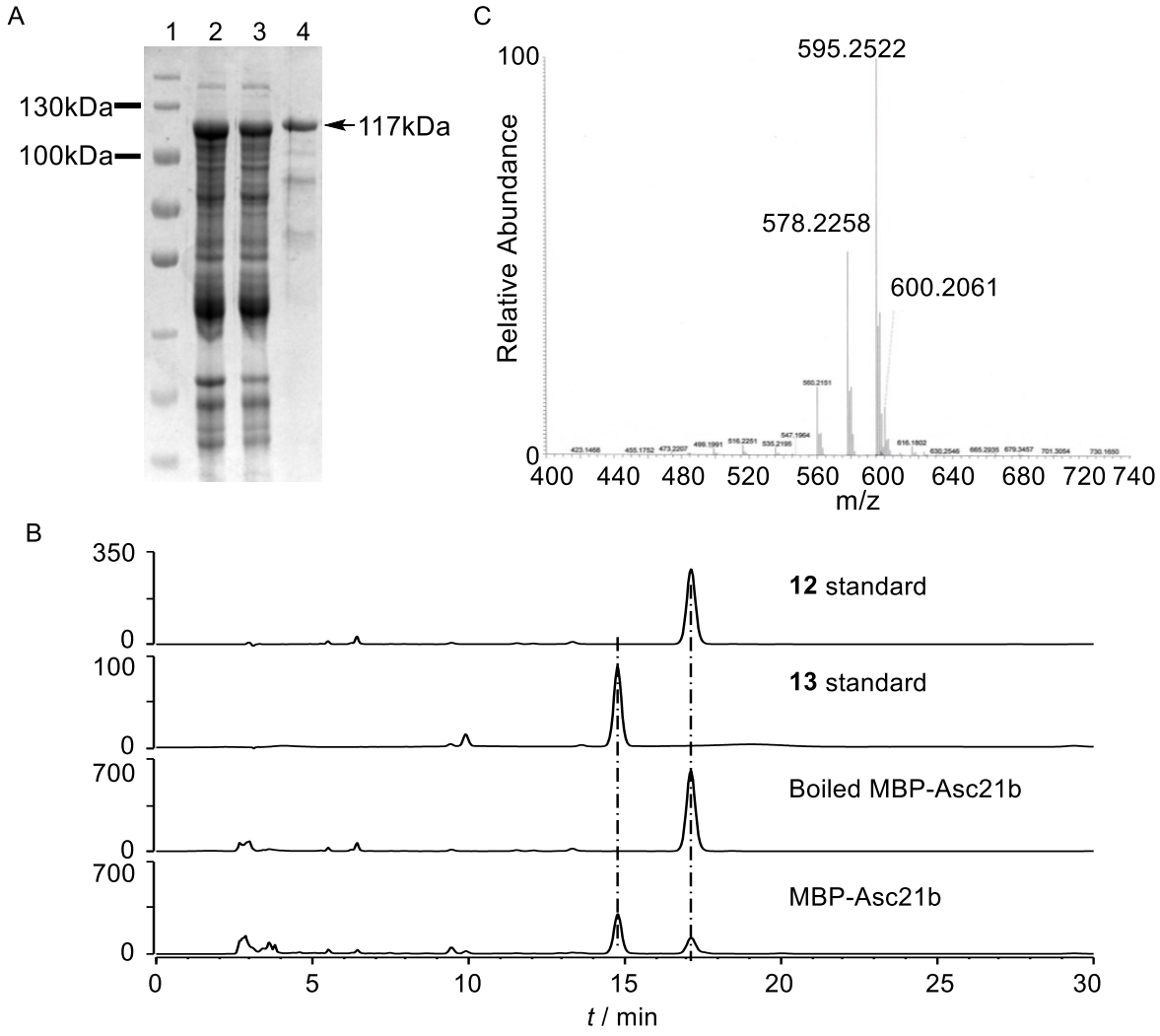

Figure S3. Production of MBP-Asc21b and enzymatic assays.

(A) Analysis of MBP-Asc21b protein purified from *E. coli* BL21 (DE3) by 10 % SDS-PAGE. Lane 1, protein ladder (Thermo Fisher, 26616); lane 2, cell lysate of *E. coli* BL21 (DE3) harbouring protein production vector pET-28a-MBP-*asc21b*; lane 3, supernatant of cell lysate of *E. coli* BL21 (DE3) harbouring protein production vector pET-28a-MBP-*asc21b*; lane 4, purified MBP-Asc21b. (B) HPLC analysis of enzymatic assays with **12** as substrate. (C) LC-MS analysis of the reaction product of MBP-Asc21b.

Figure S4-S81. NMR and HRESIMS spectra of compounds **3-14.**

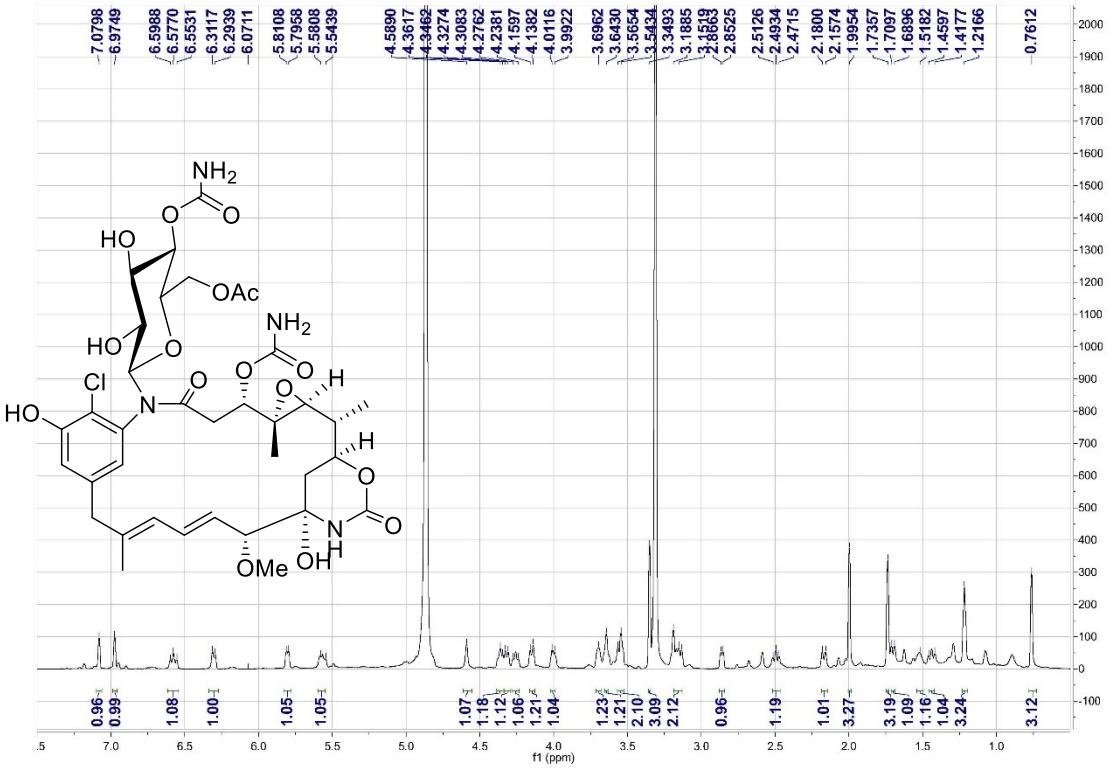

Figure S4. The ^{1}H NMR spectrum of **3** in CD_3OD.

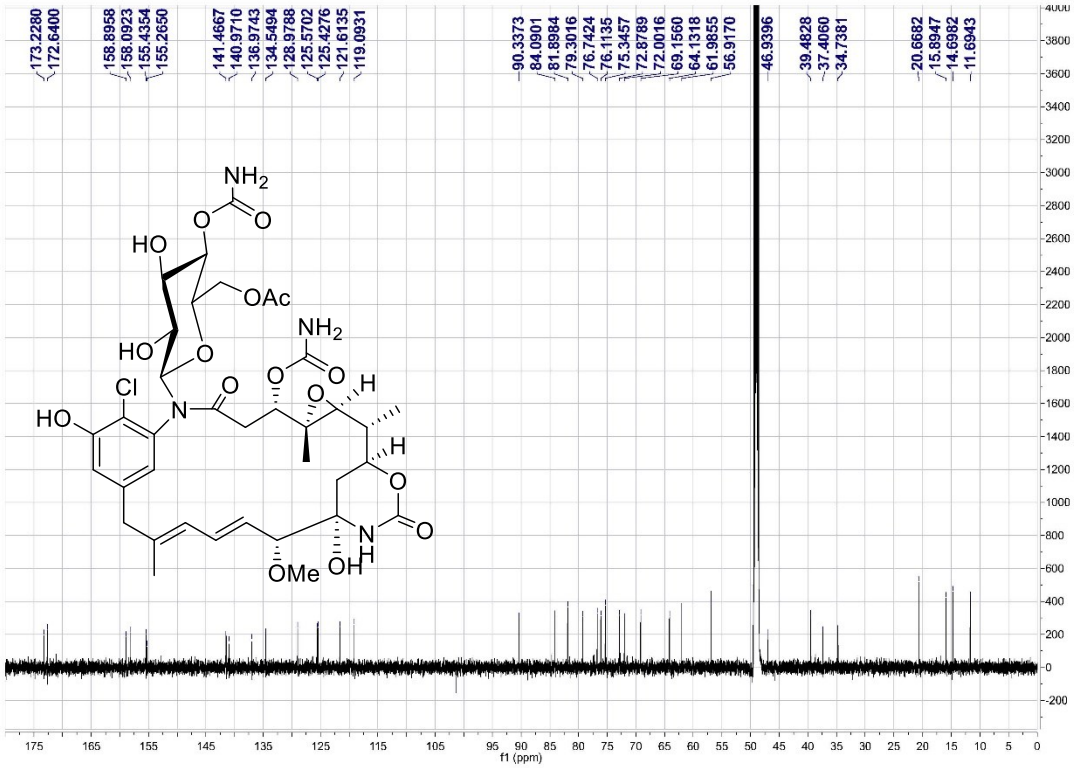

Figure S5. The ^{13}C NMR spectrum of **3** in CD_3OD.

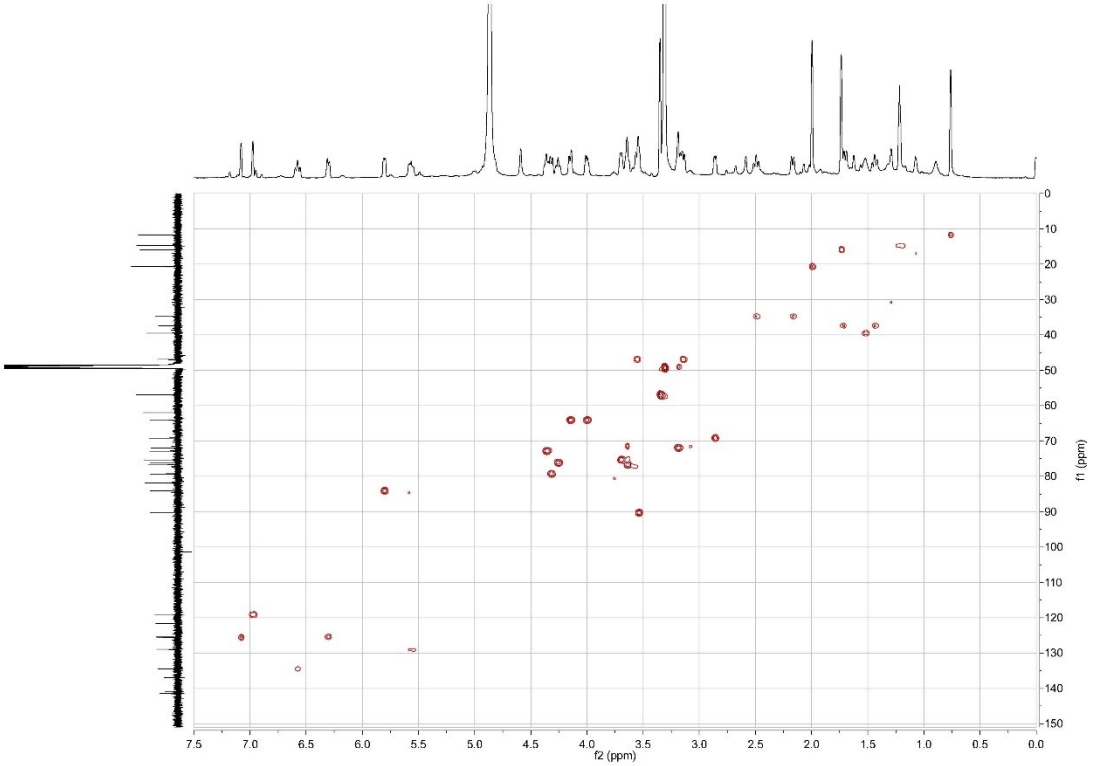

Figure S6. The HMQC spectrum of **3** in CD_3OD.

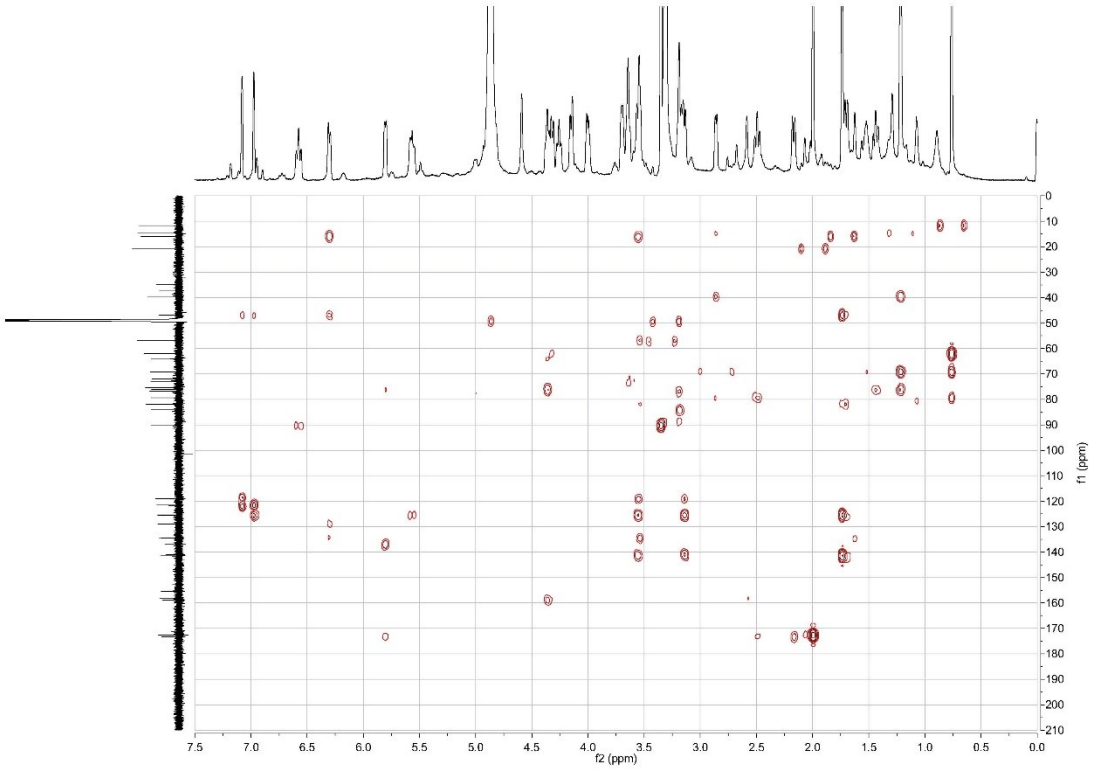

Figure S7. The HMBC NMR spectrum of **3** in CD_3OD.

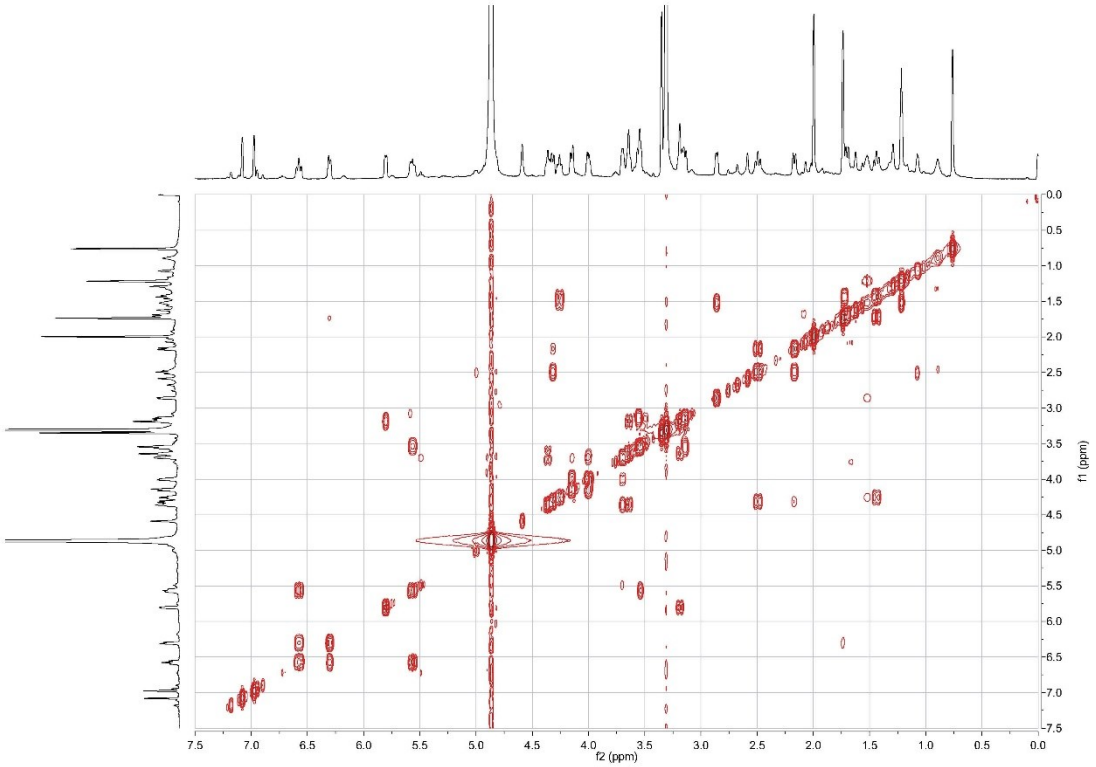

Figure S8. The ^{1}H-^{1}H COSY spectrum of **3** in CD_3OD.

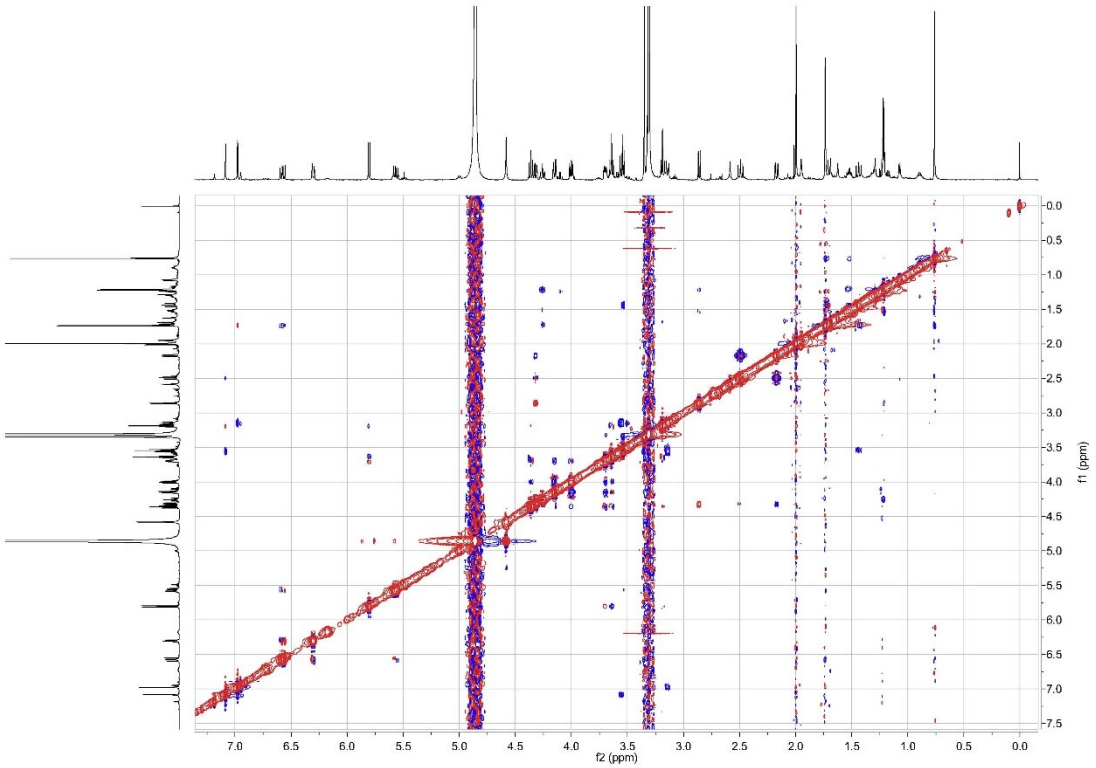

Figure S9. The NOESY spectrum of **3** in CD_3OD.

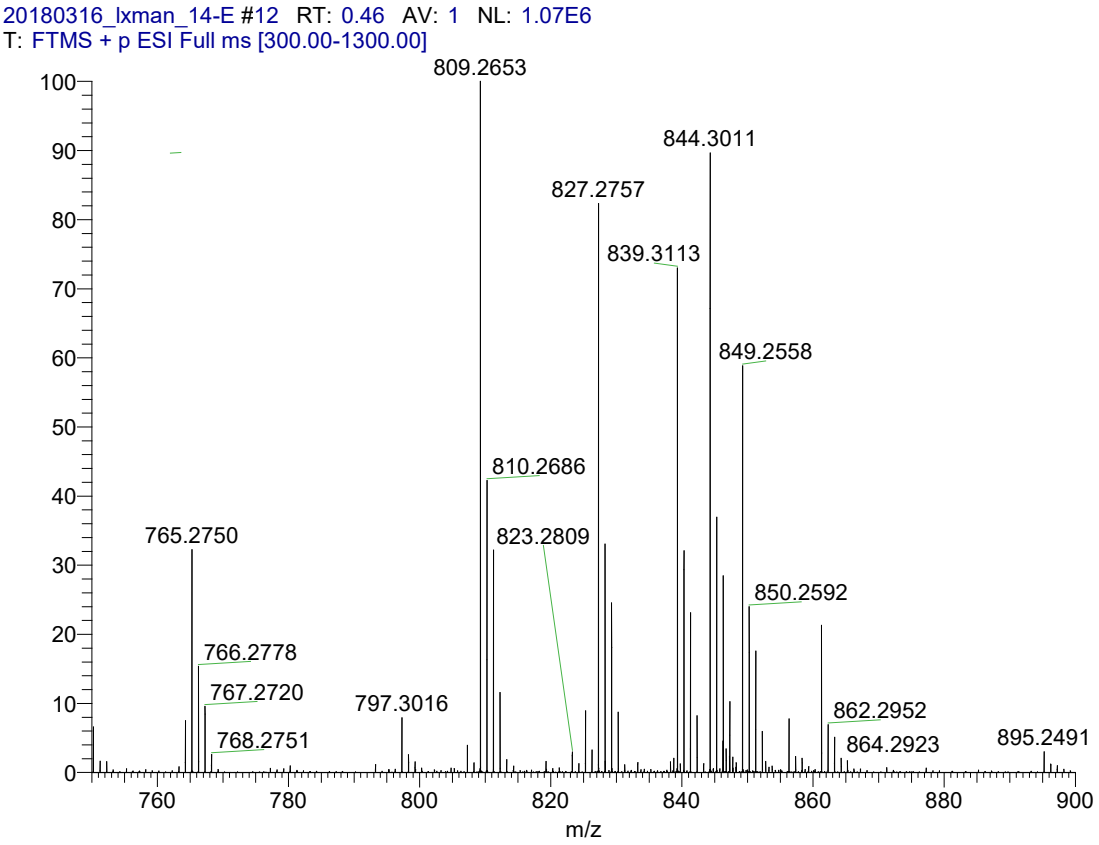

Figure S10. The HRESI mass spectrum of **3**.

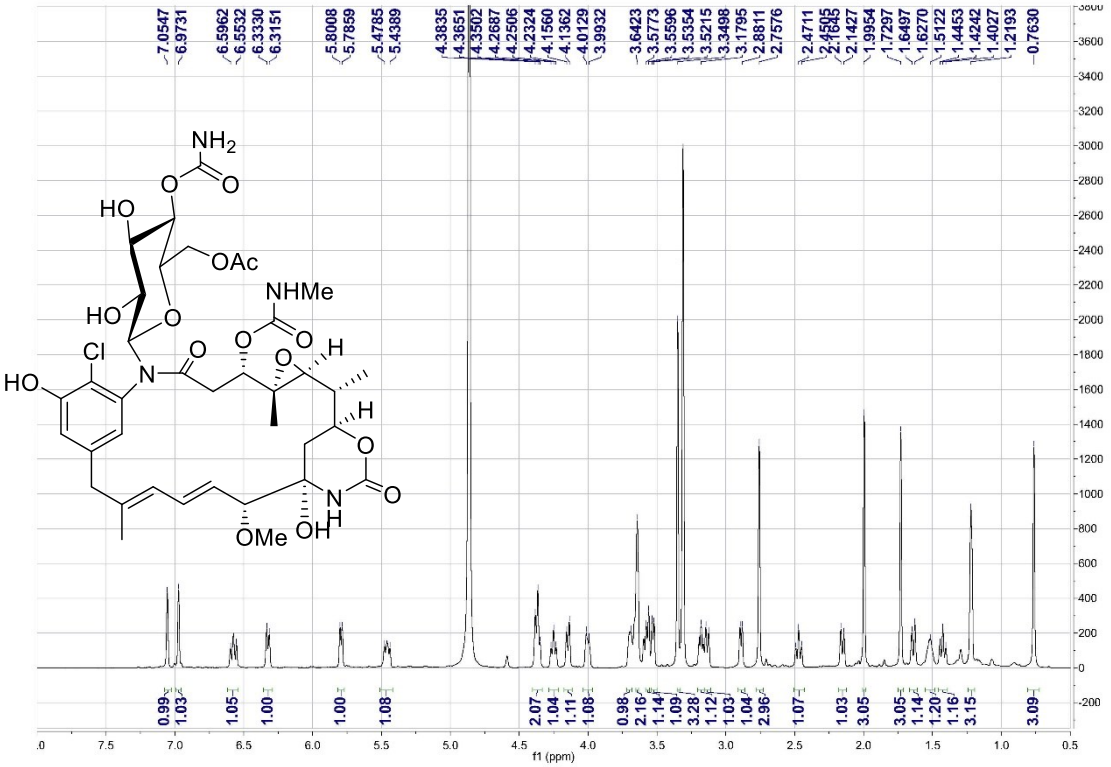

Figure S11. The ^{1}H NMR spectrum of **4** in CD_3OD.

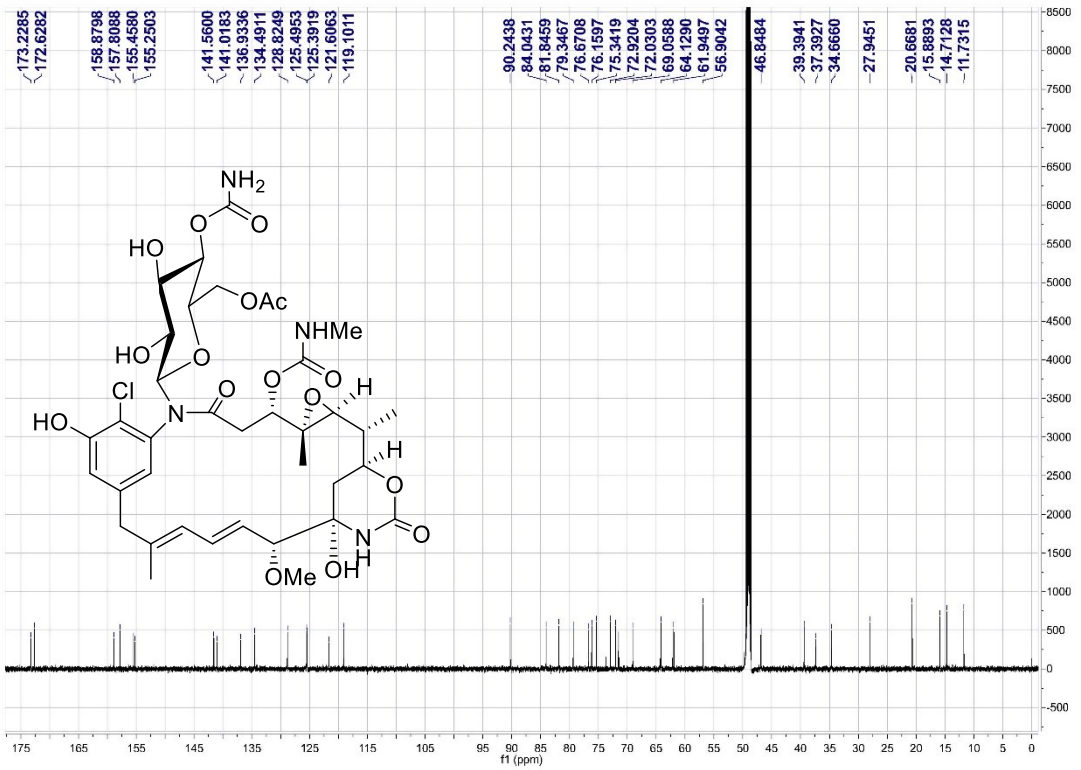

Figure S12. The ^{13}C NMR spectrum of **4** in CD_3OD.

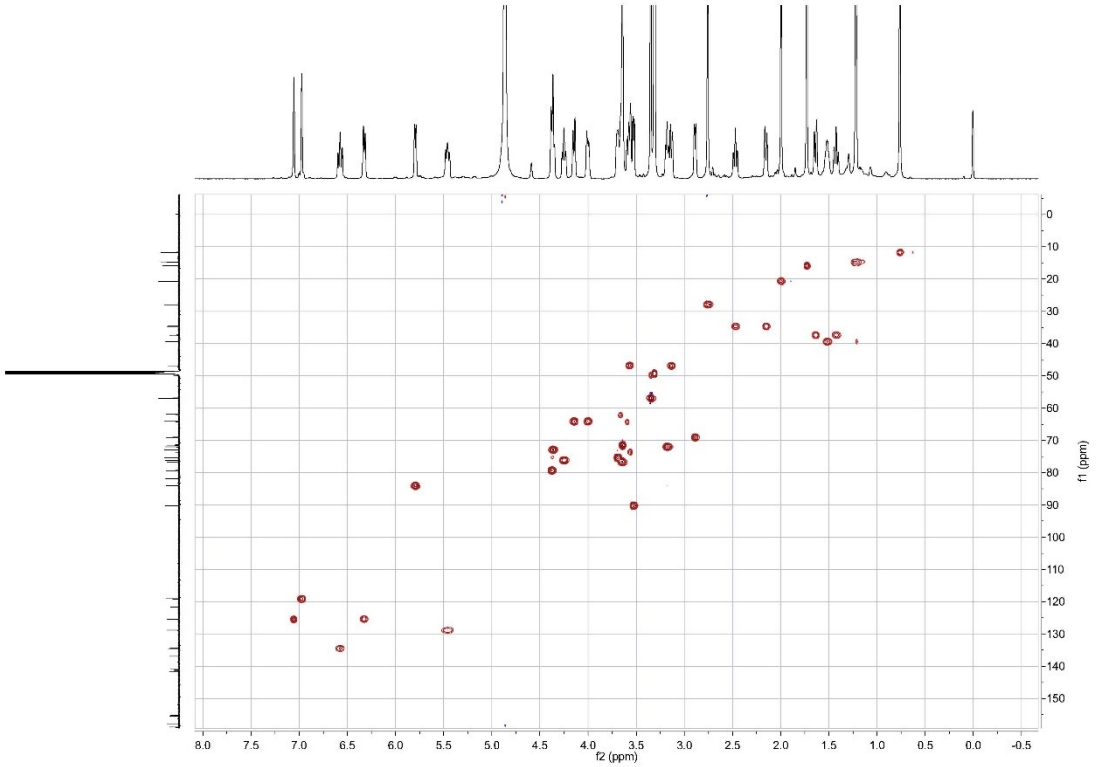

Figure S13. The HMQC spectrum of **4** in CD_3OD.

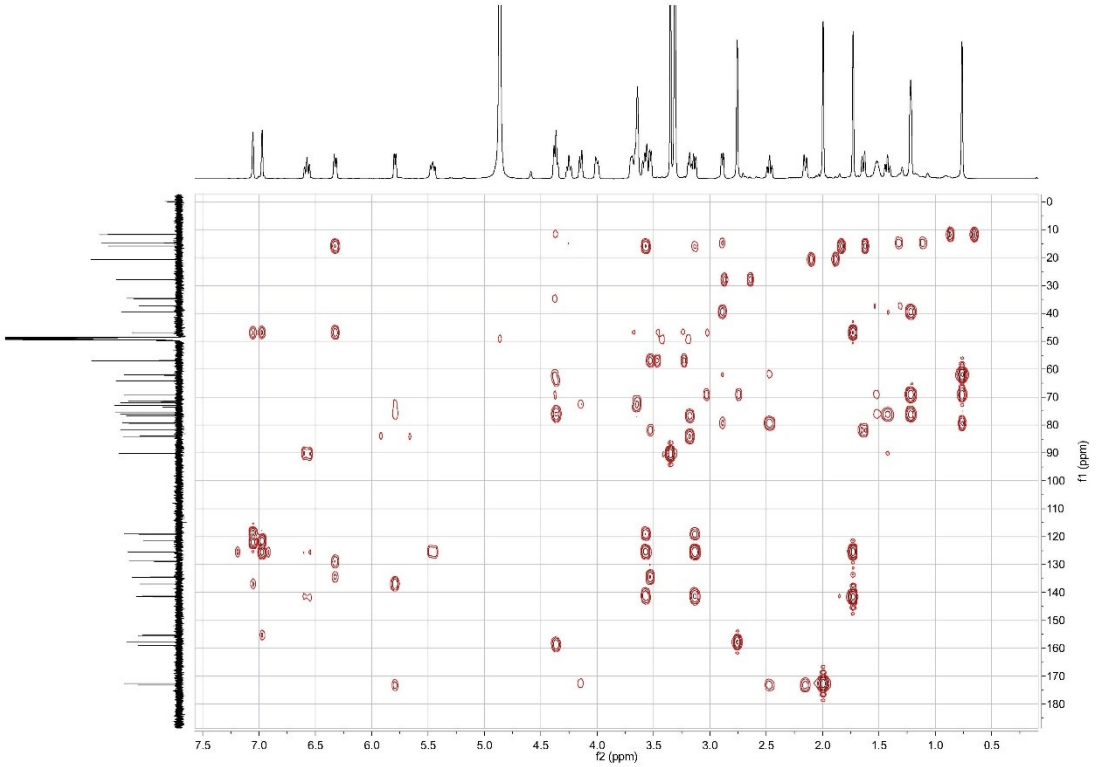

Figure S14. The HMBC NMR spectrum of **4** in CD_3OD.

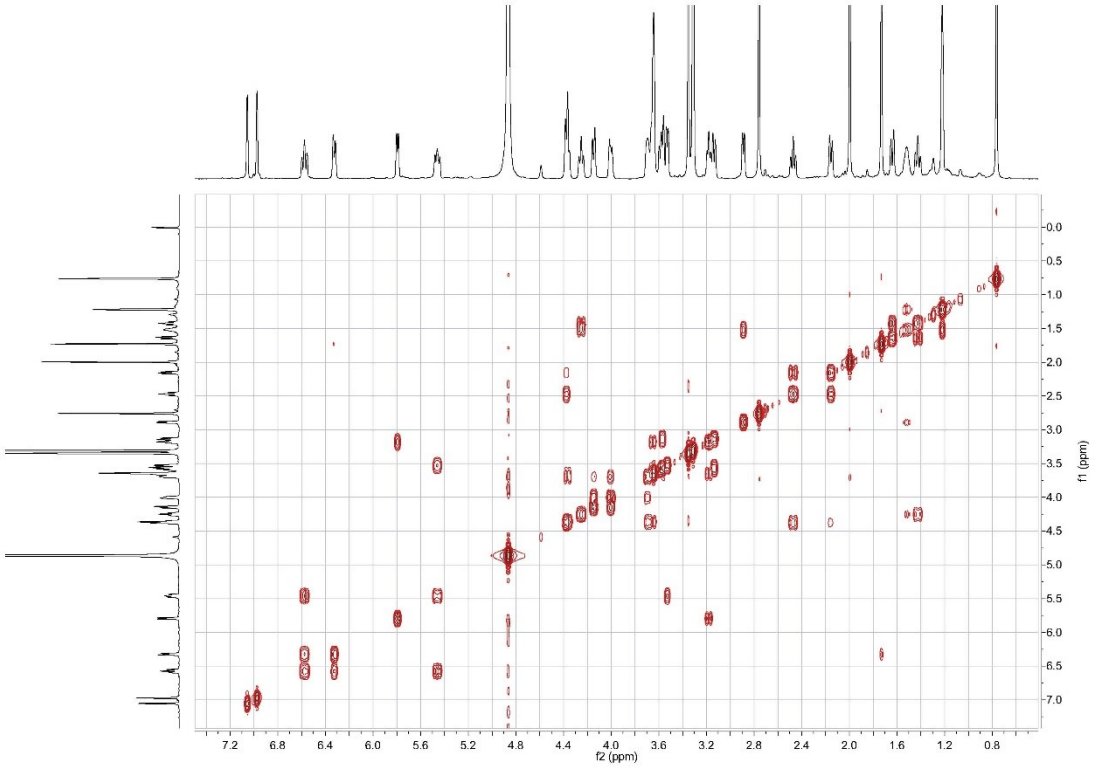

Figure S15. The ^{1}H-^{1}H COSY spectrum of **4** in CD_3OD.

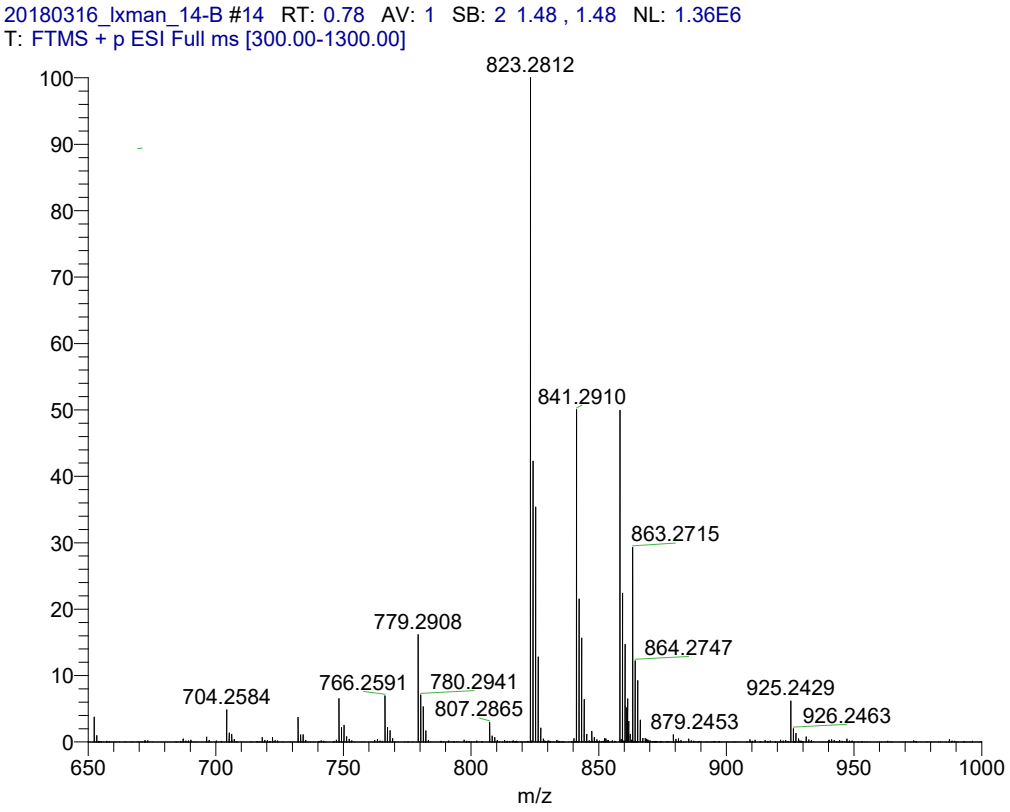

Figure S16. The HRESI mass spectrum of **4**.

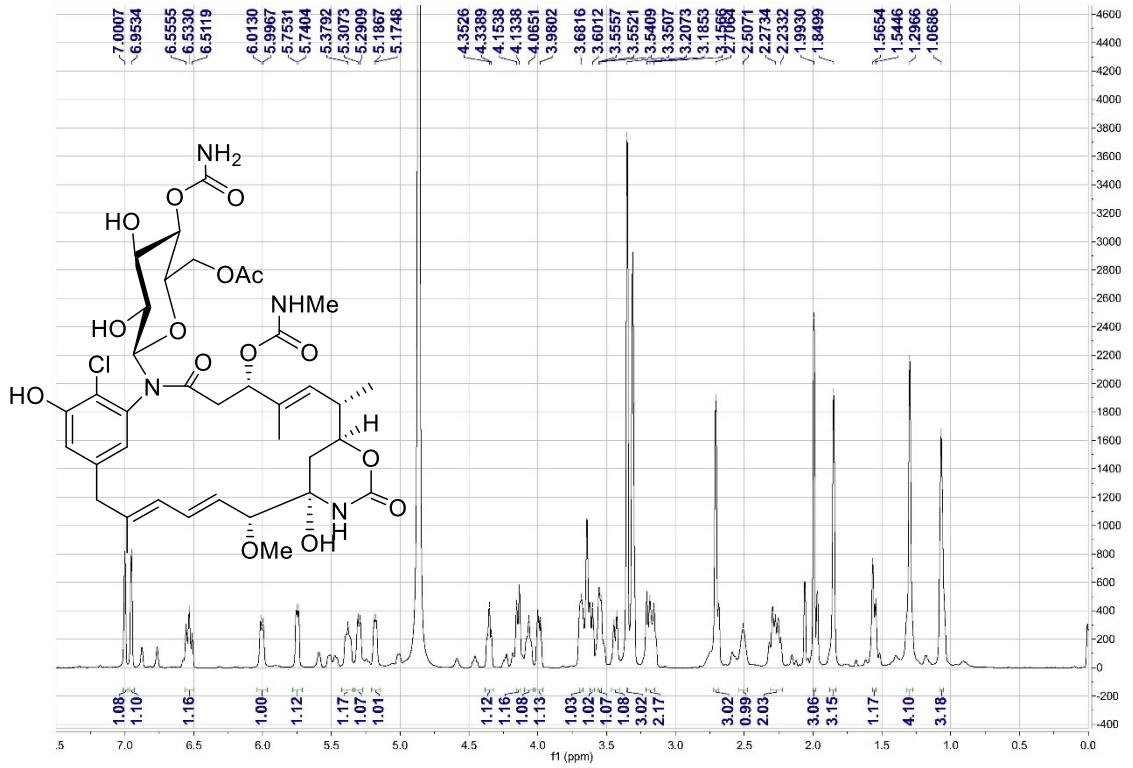

Figure S17. The ^{1}H NMR spectrum of **5** in CD_3OD.

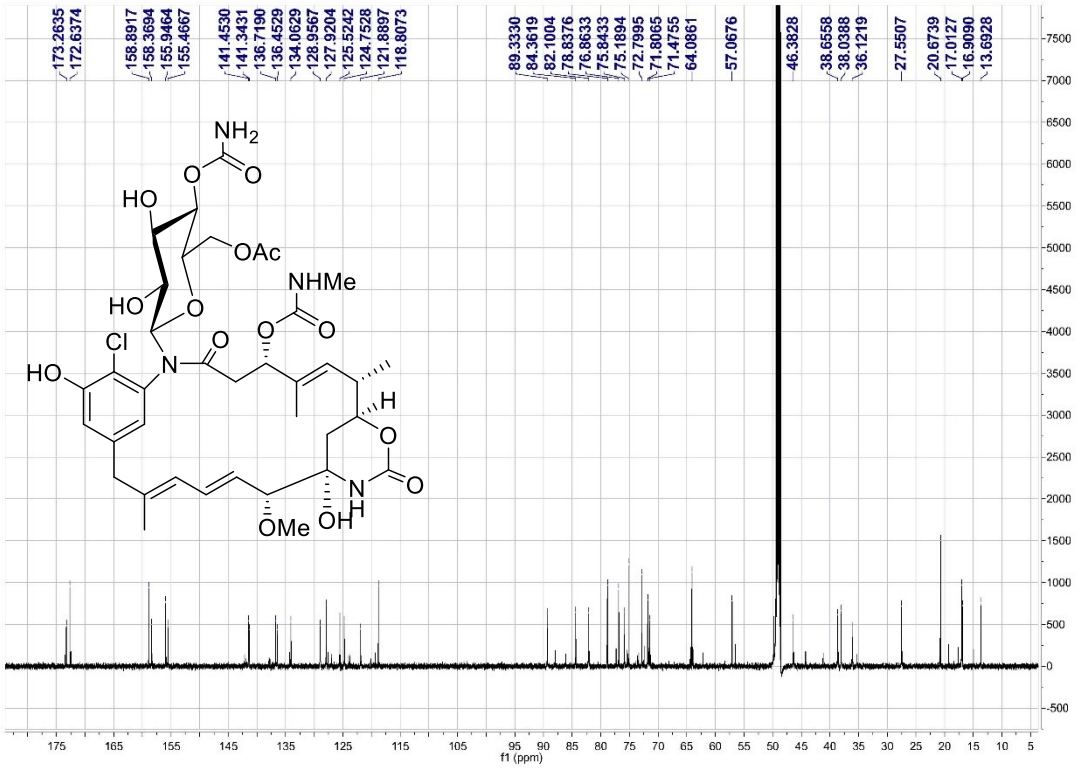

Figure S18. The ^{13}C NMR spectrum of **5** in CD_3OD.

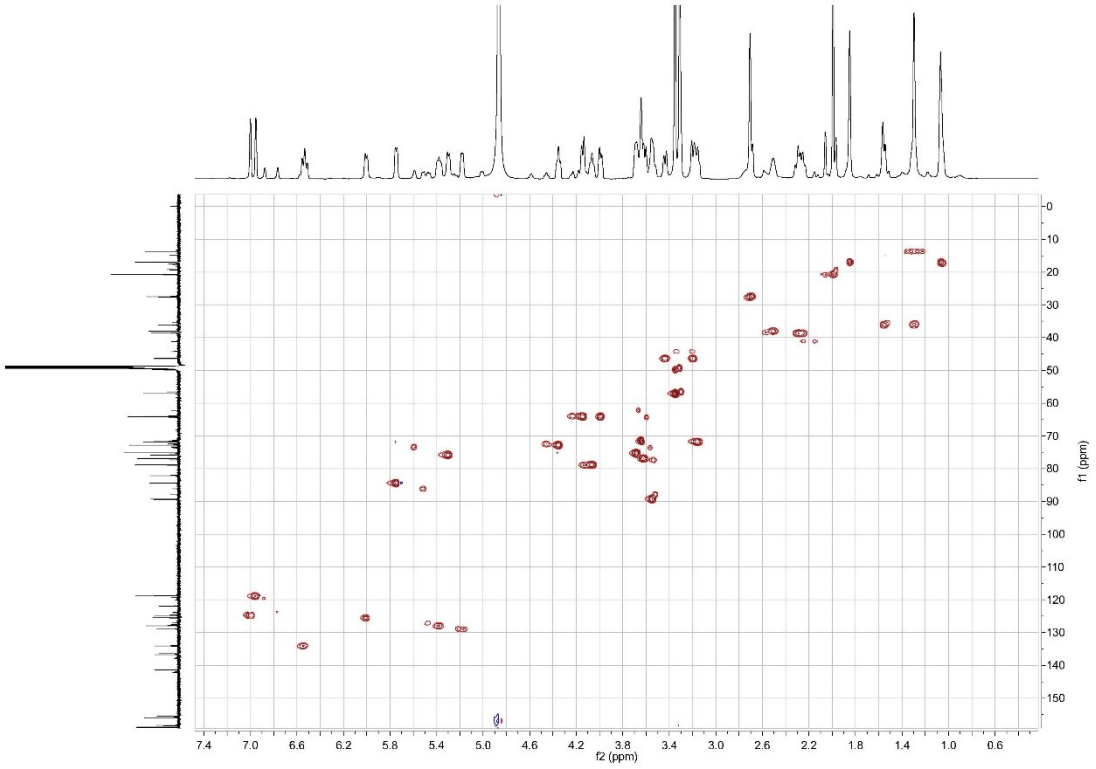

Figure S19. The HMQC spectrum of **5** in CD_3OD.

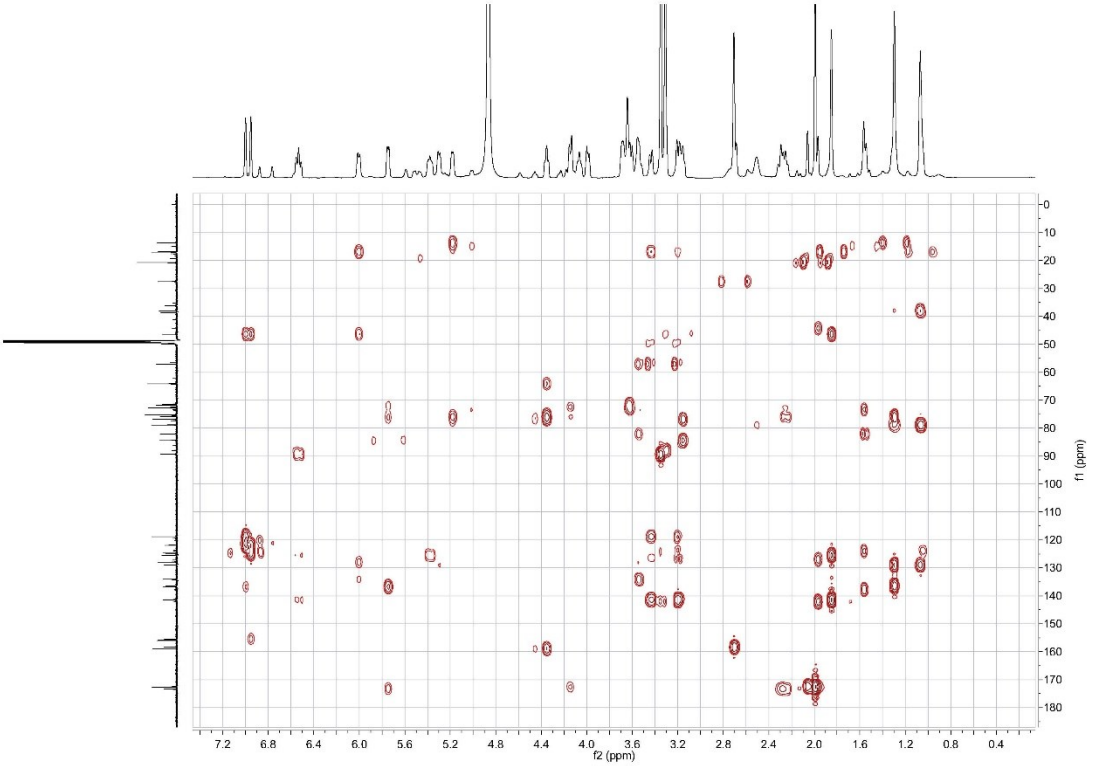

Figure S20. The HMBC NMR spectrum of **5** in CD_3OD.

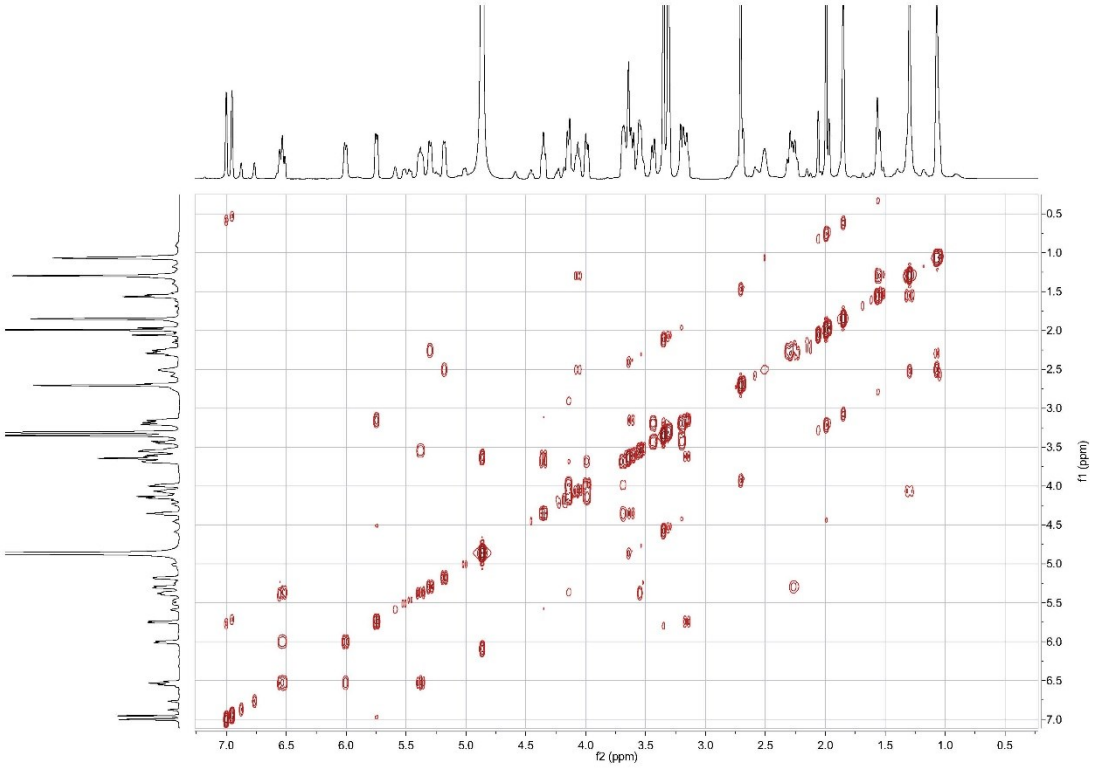

Figure S21. The ^{1}H-^{1}H COSY spectrum of **5** in CD_3OD.

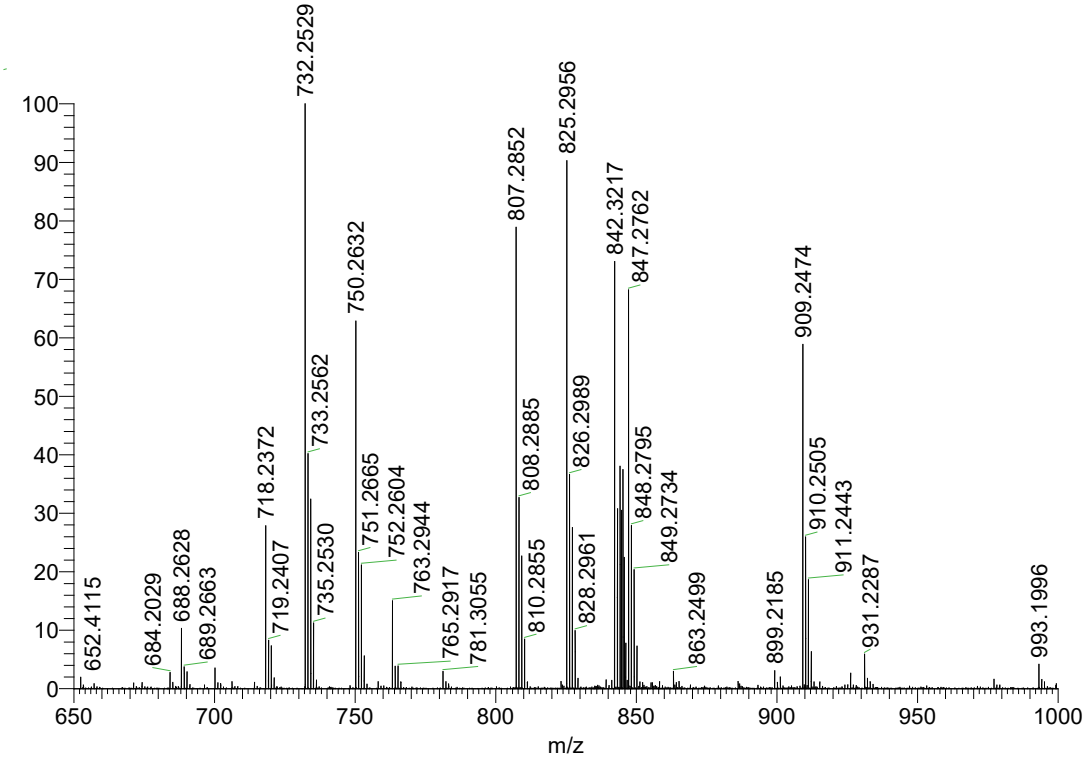

Figure S22. The HRESI mass spectrum of **5**.

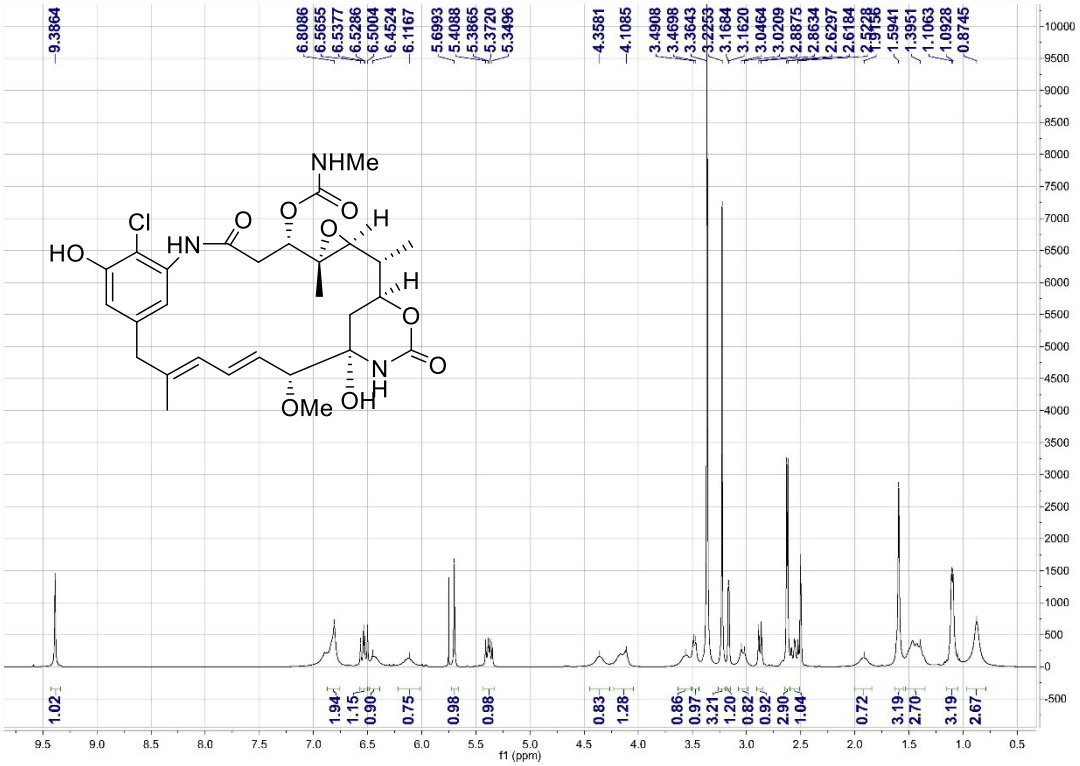

Figure S23. The ^{1}H NMR spectrum of **6** in $(CD_3)_2SO$.

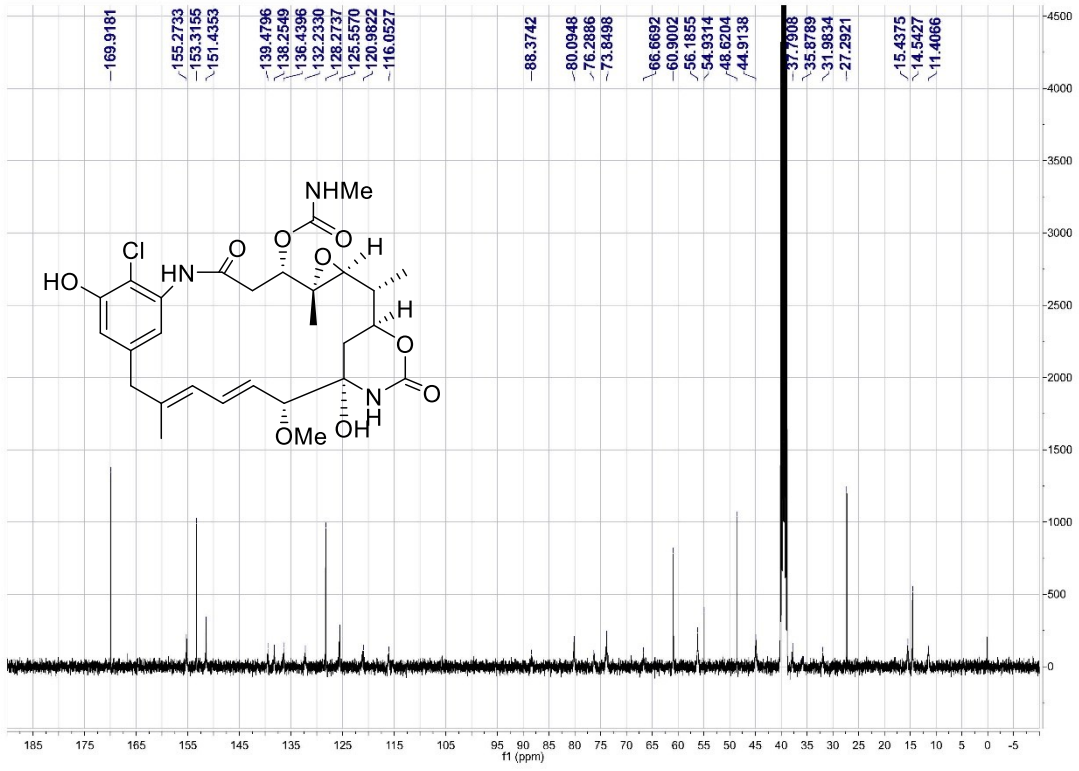

Figure S24. The ^{13}C NMR spectrum of **6** in $(CD_3)_2SO$.

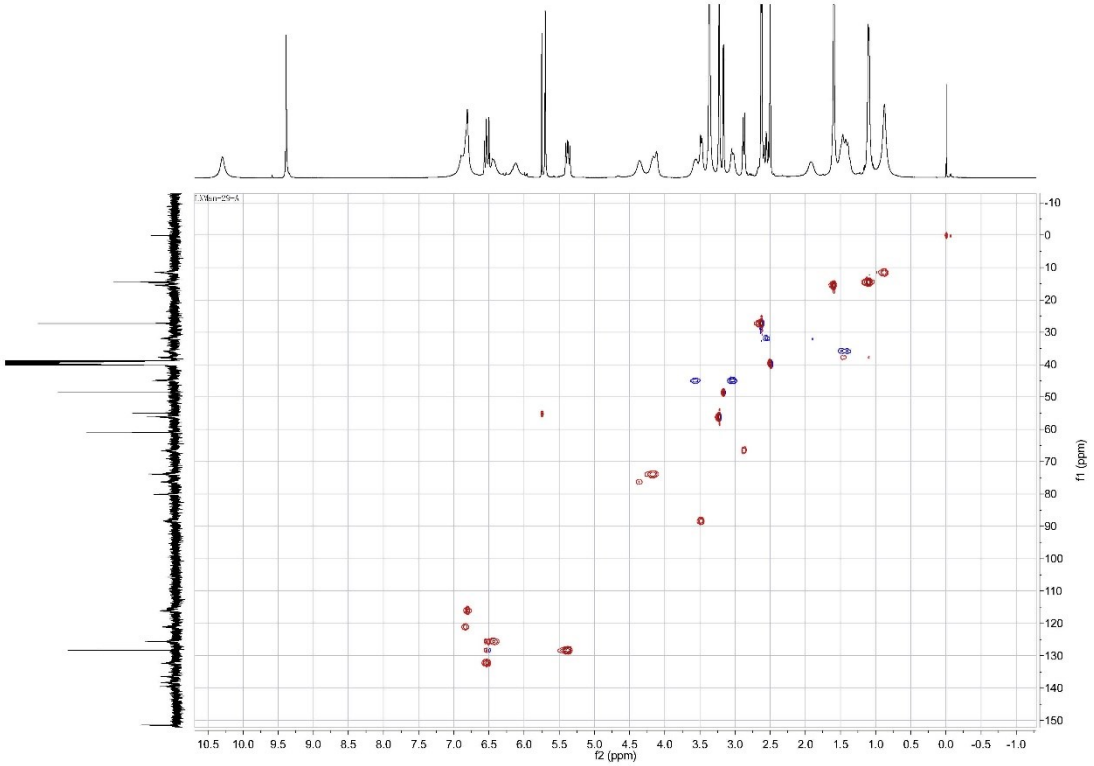

Figure S25. The HMQC spectrum of **6** in $(CD_3)_2SO$.

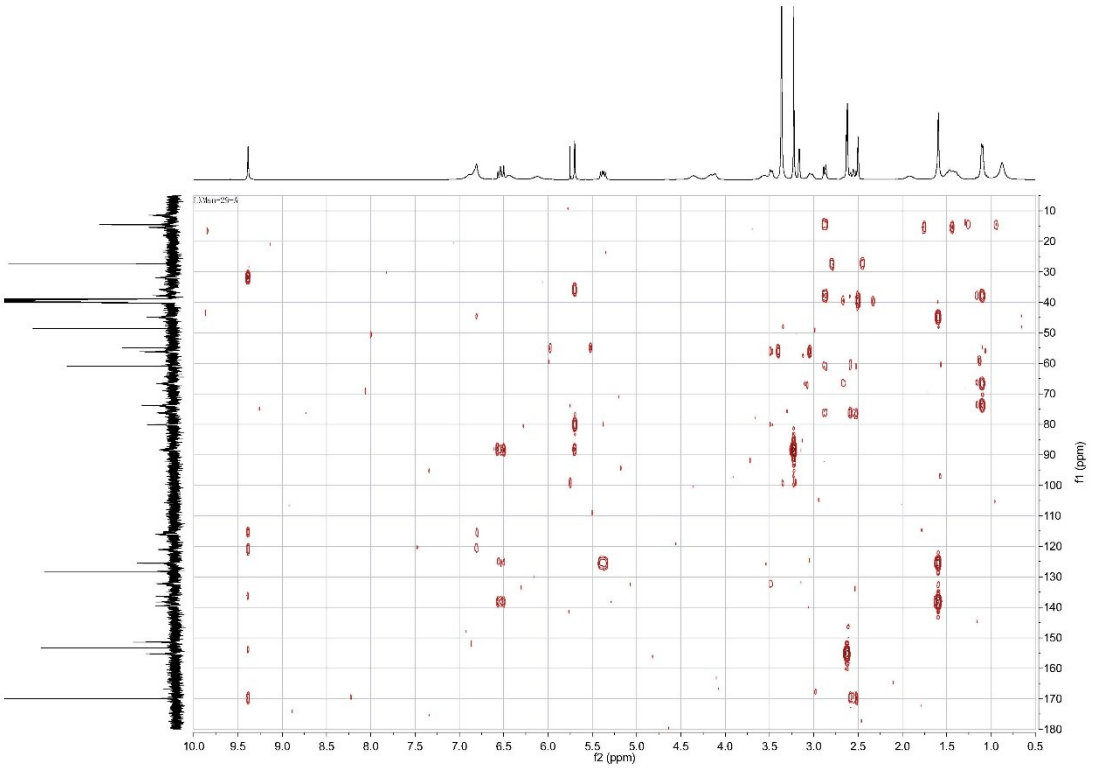

Figure S26. The HMBC NMR spectrum of **6** in $(CD_3)_2SO$.

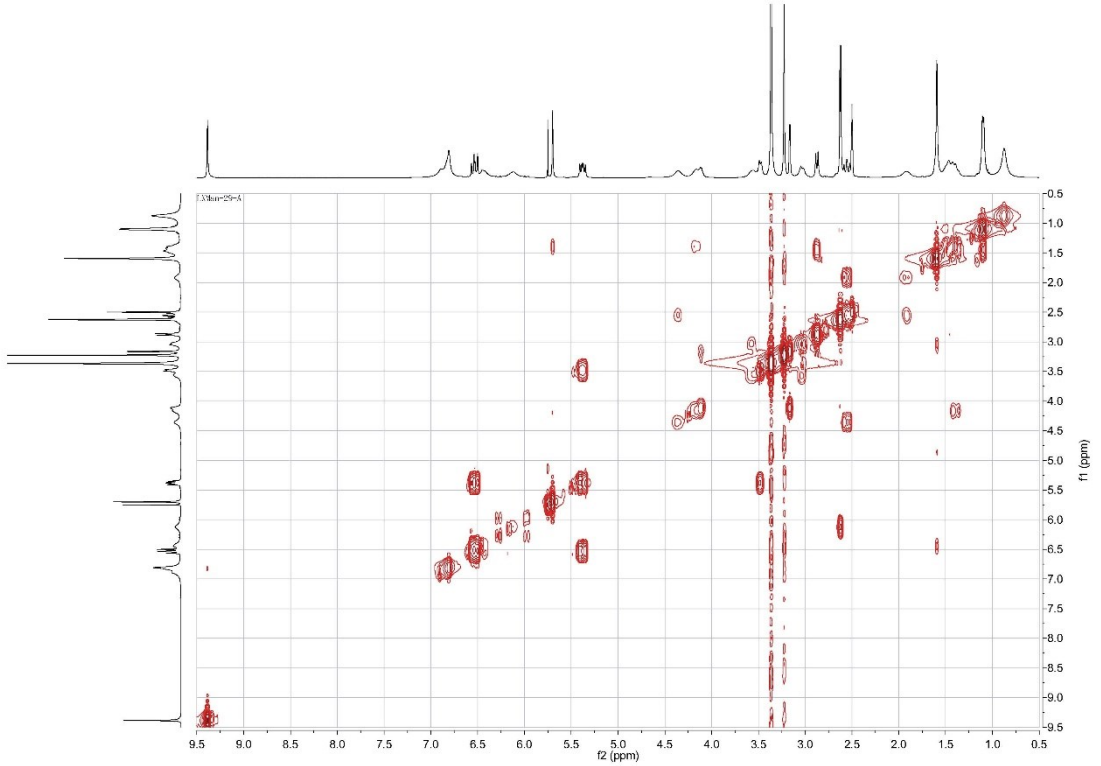

Figure S27. The ^{1}H-^{1}H COSY spectrum of **6** in $(CD_3)_2SO$.

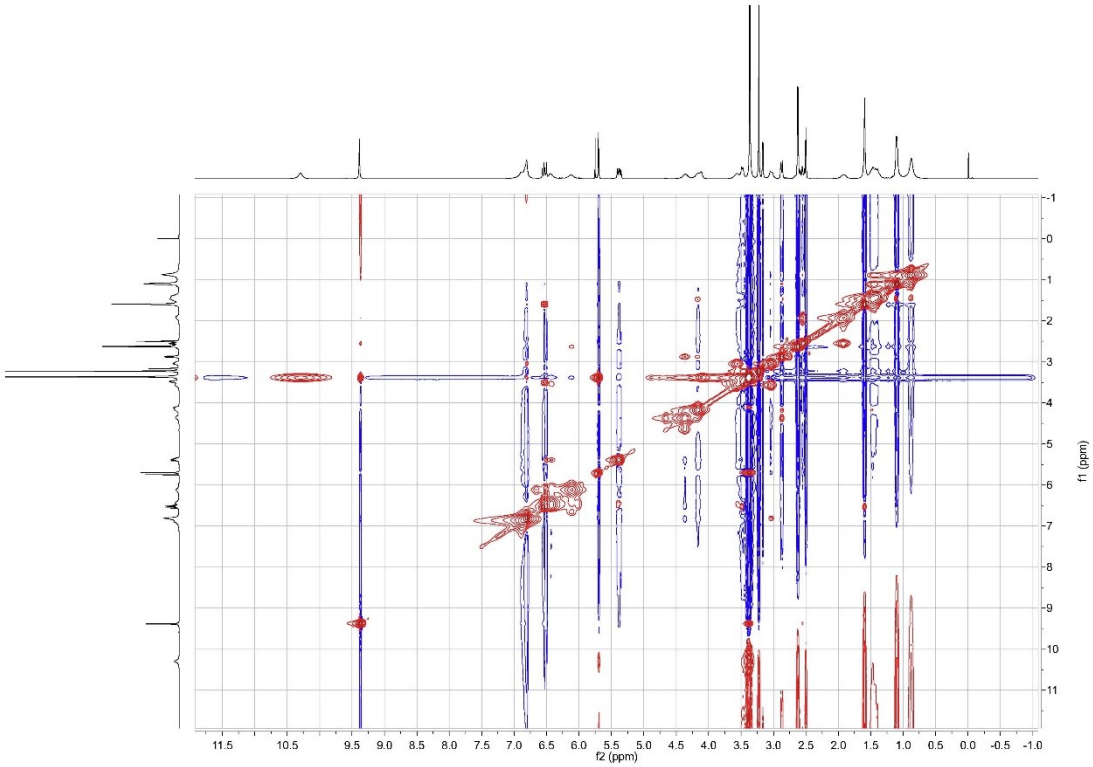

Figure S28. The NOESY spectrum of **6** in $(CD_3)_2SO$.

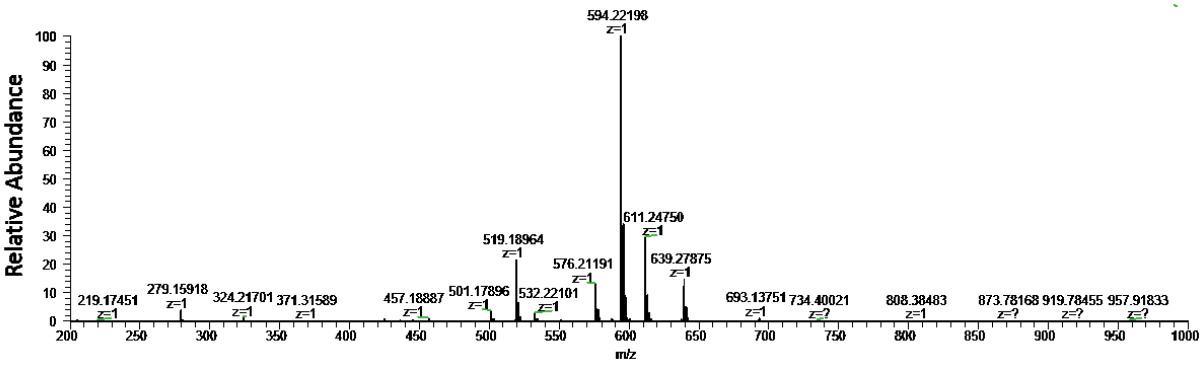

Figure S29. The HRESI mass spectrum of **6**.

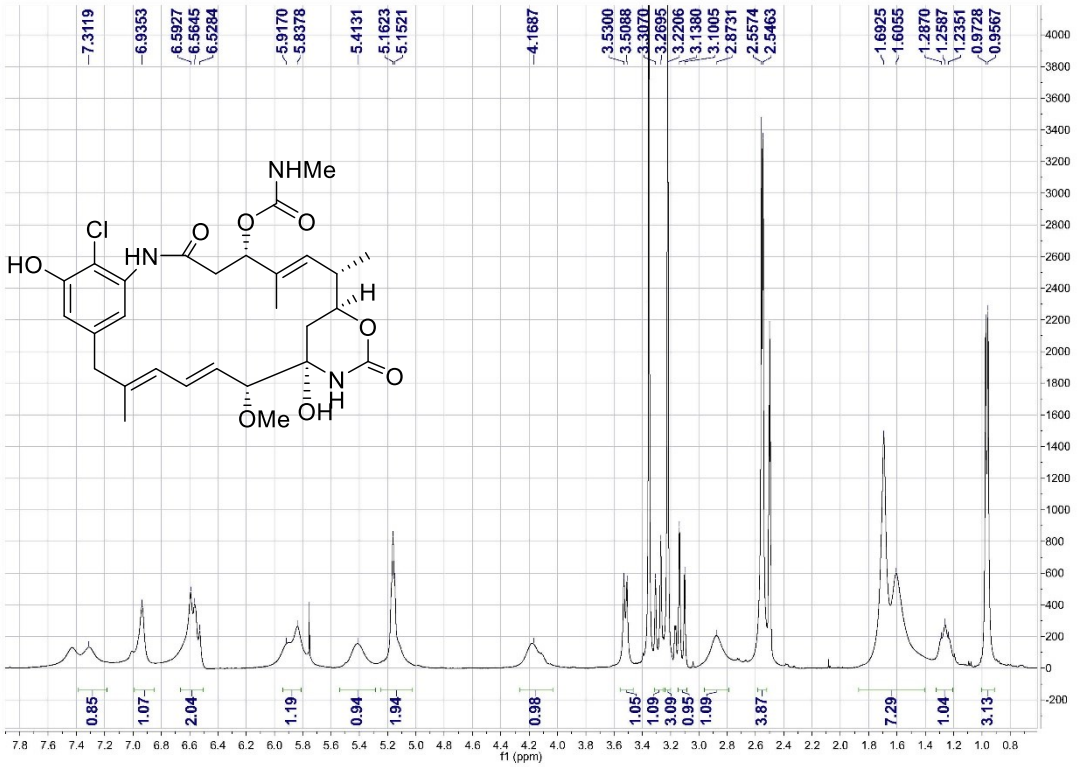

Figure S30. The ^{1}H NMR spectrum of **7** in $(CD_3)_2SO$.

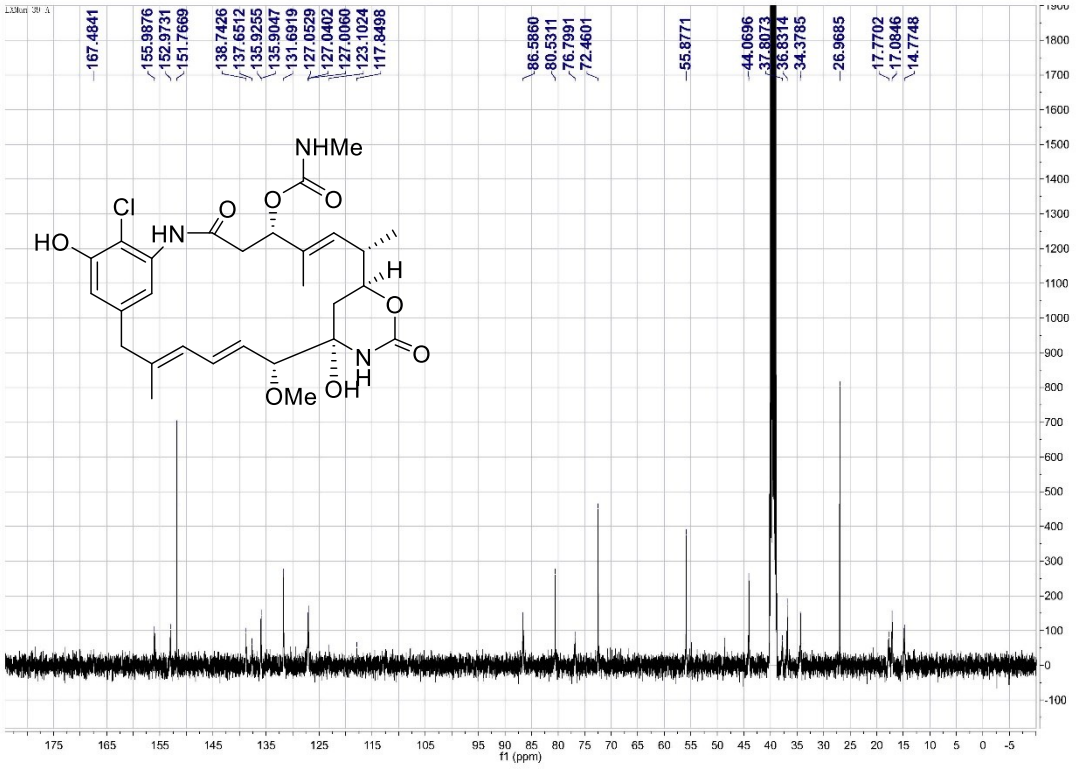

Figure S31. The ^{13}C NMR spectrum of **7** in $(CD_3)_2SO$.

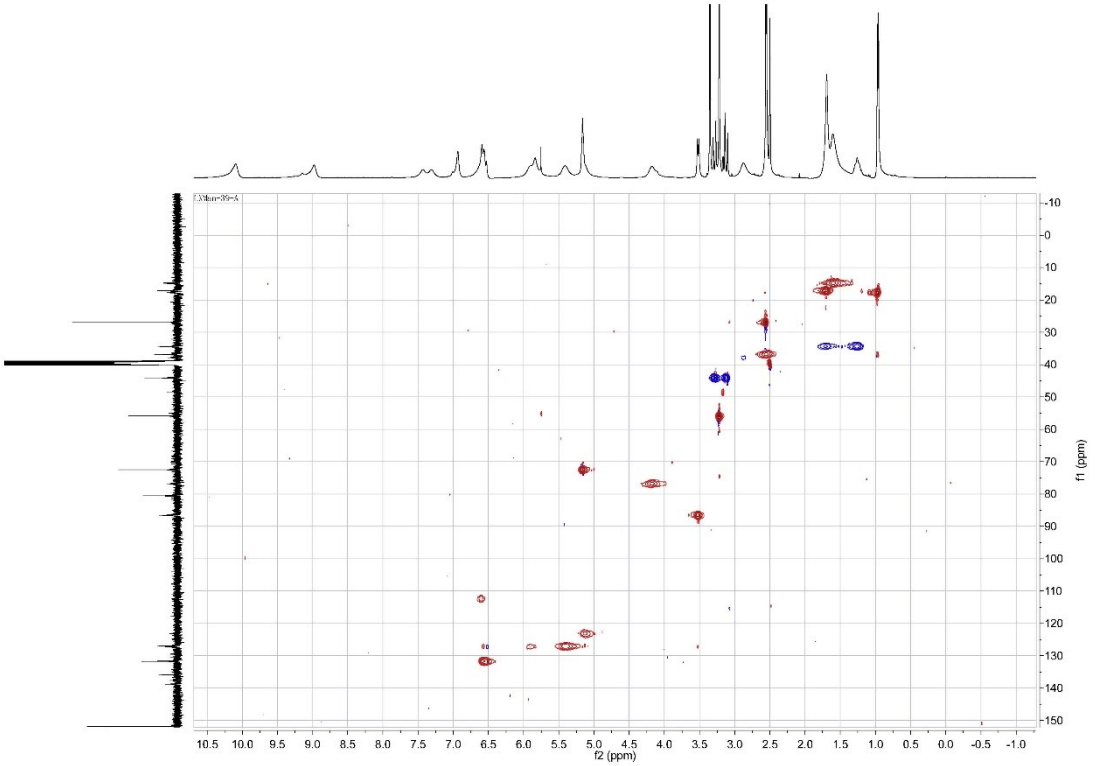

Figure S32. The HMQC spectrum of **7** in $(CD_3)_2SO$.

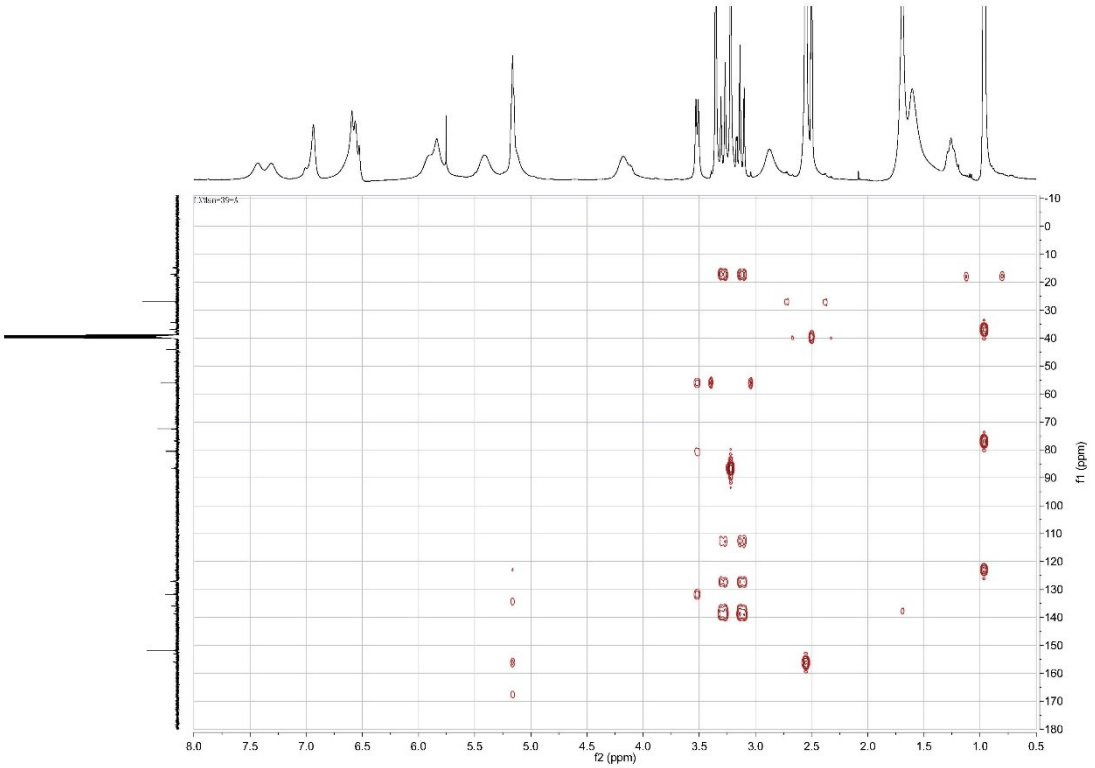

Figure S33. The HMBC NMR spectrum of **7** in $(CD_3)_2SO$.

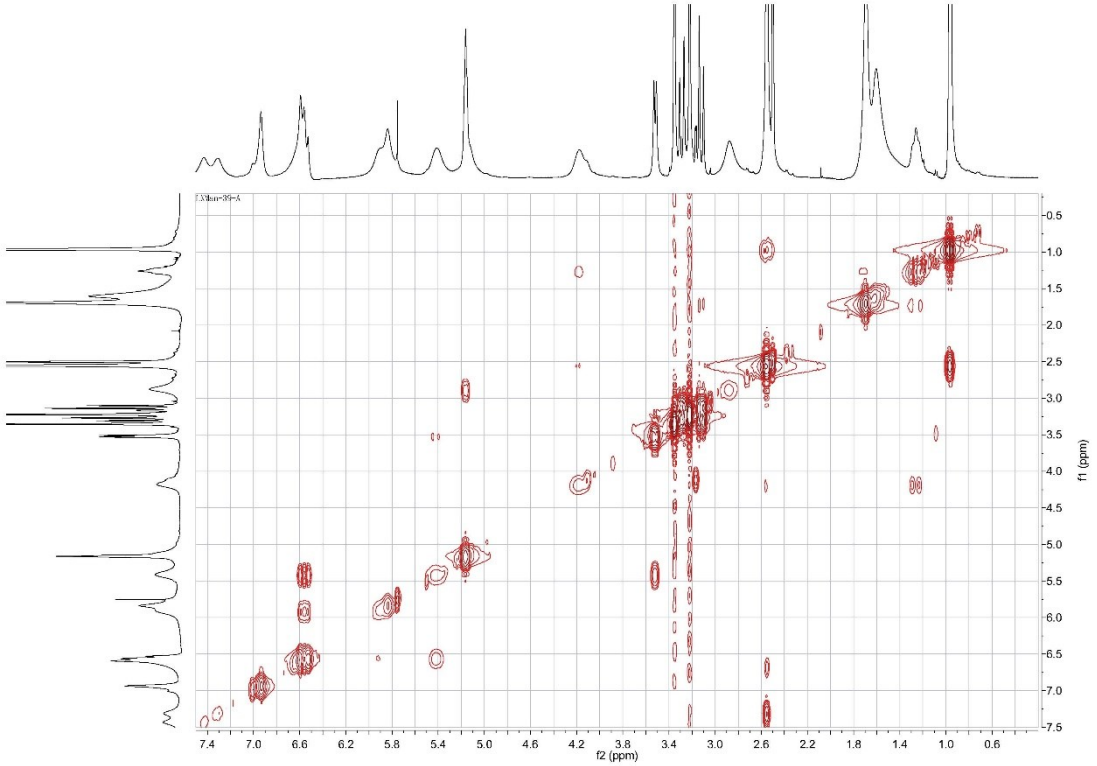

Figure S34. The ^{1}H-^{1}H COSY spectrum of **7** in $(CD_3)_2SO$.

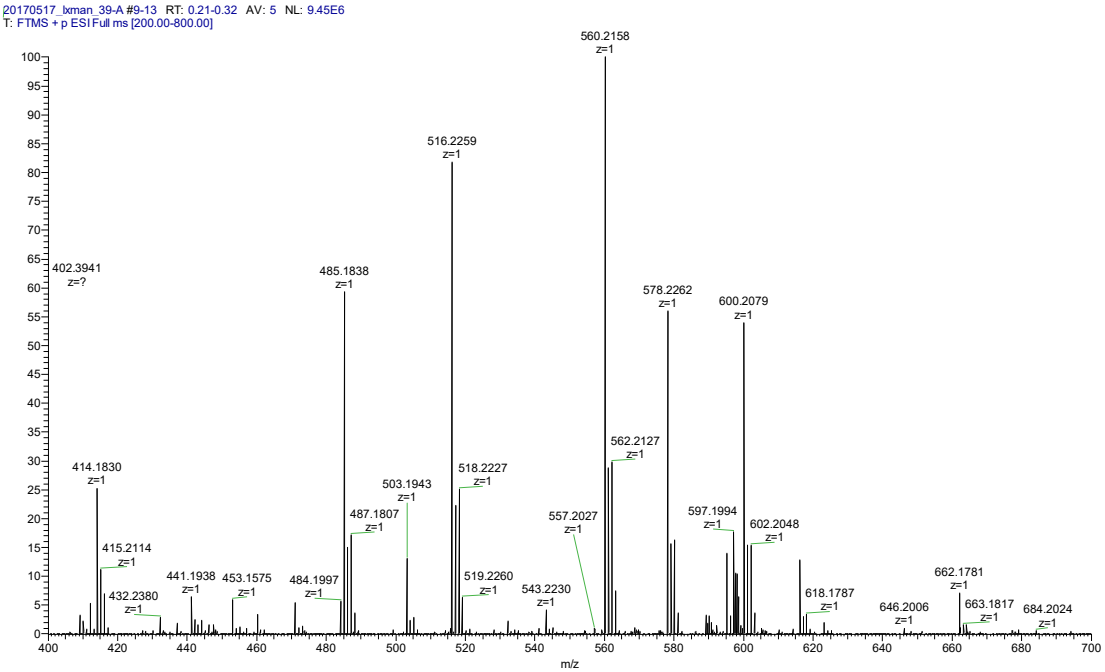

Figure S35. The HRESI mass spectrum of **7**.

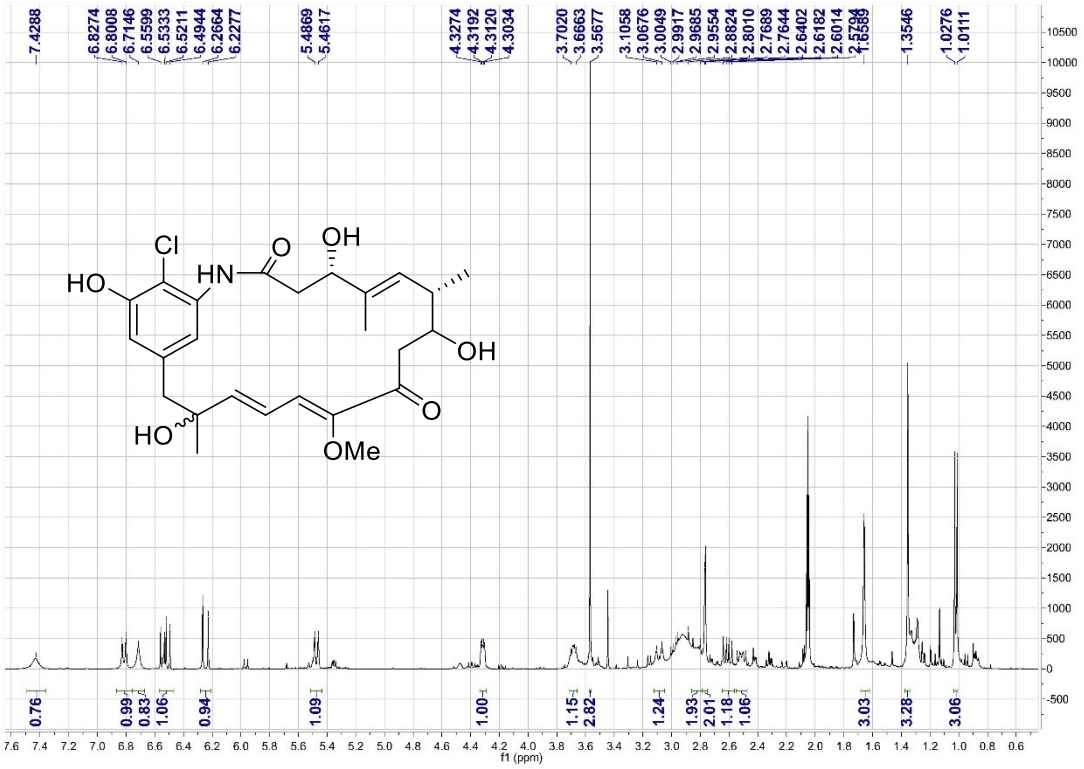

Figure S36. The ^{1}H NMR spectrum of **8** in CD_3COCD_3.

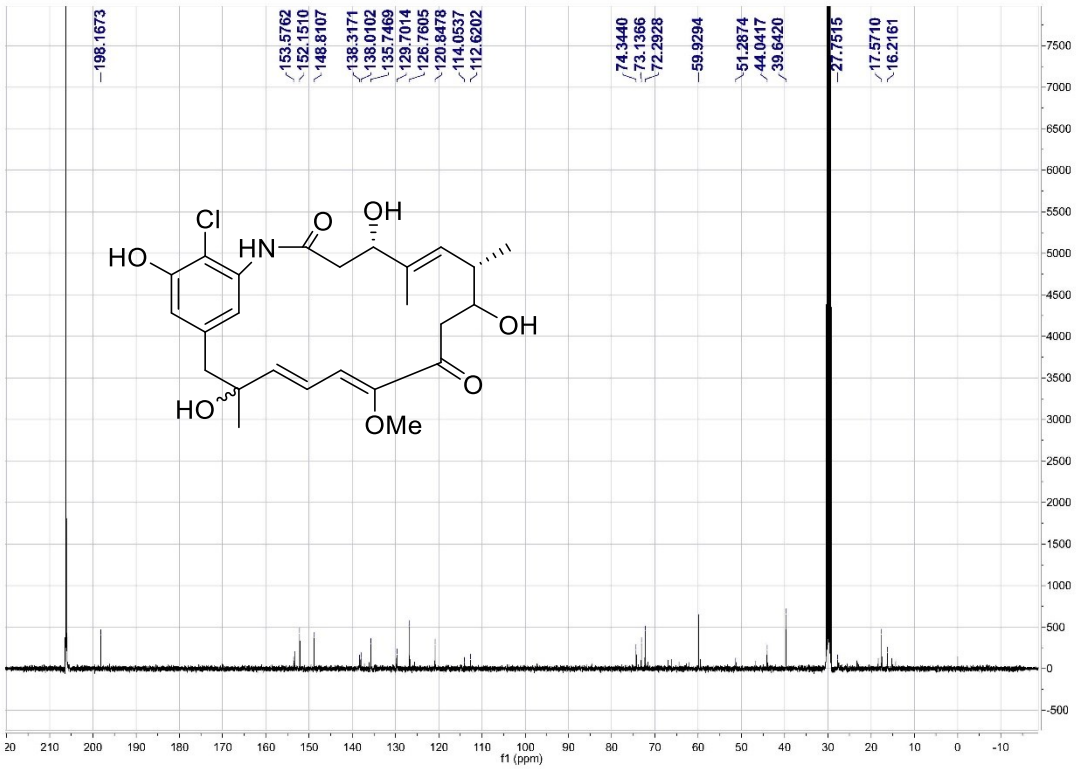

Figure S37. The ^{13}C NMR spectrum of **8** in CD_3COCD_3.

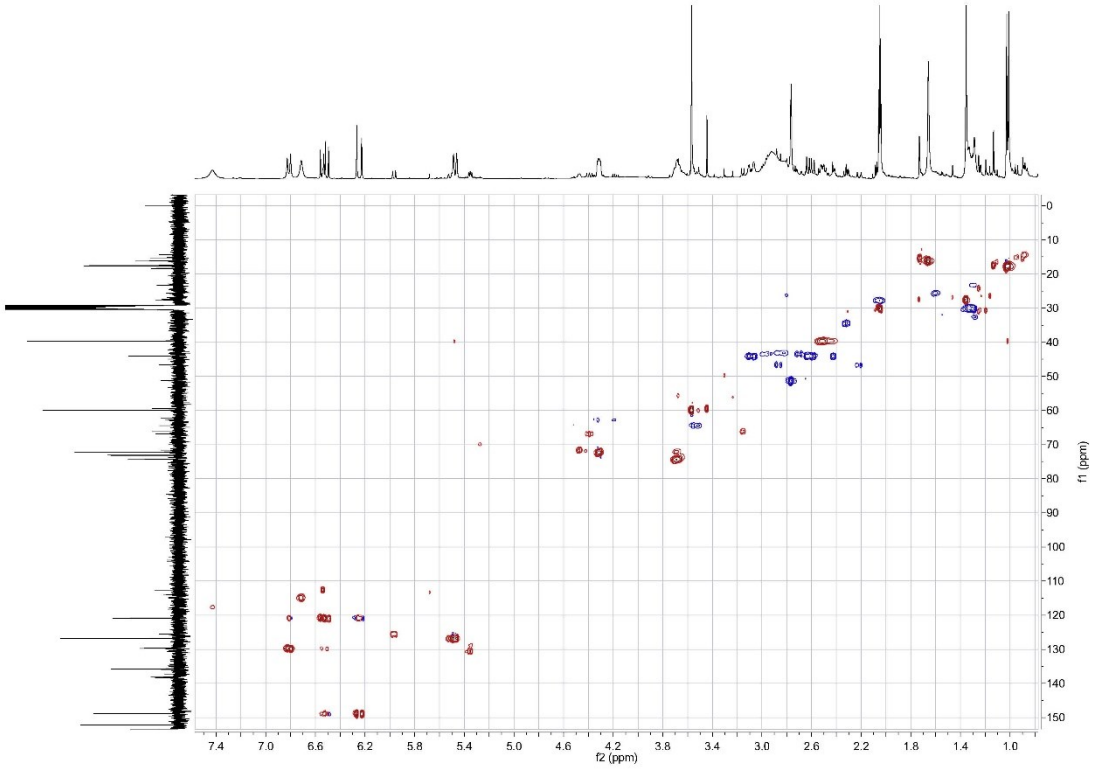

Figure S38. The HMQC spectrum of **8** in CD_3COCD_3.

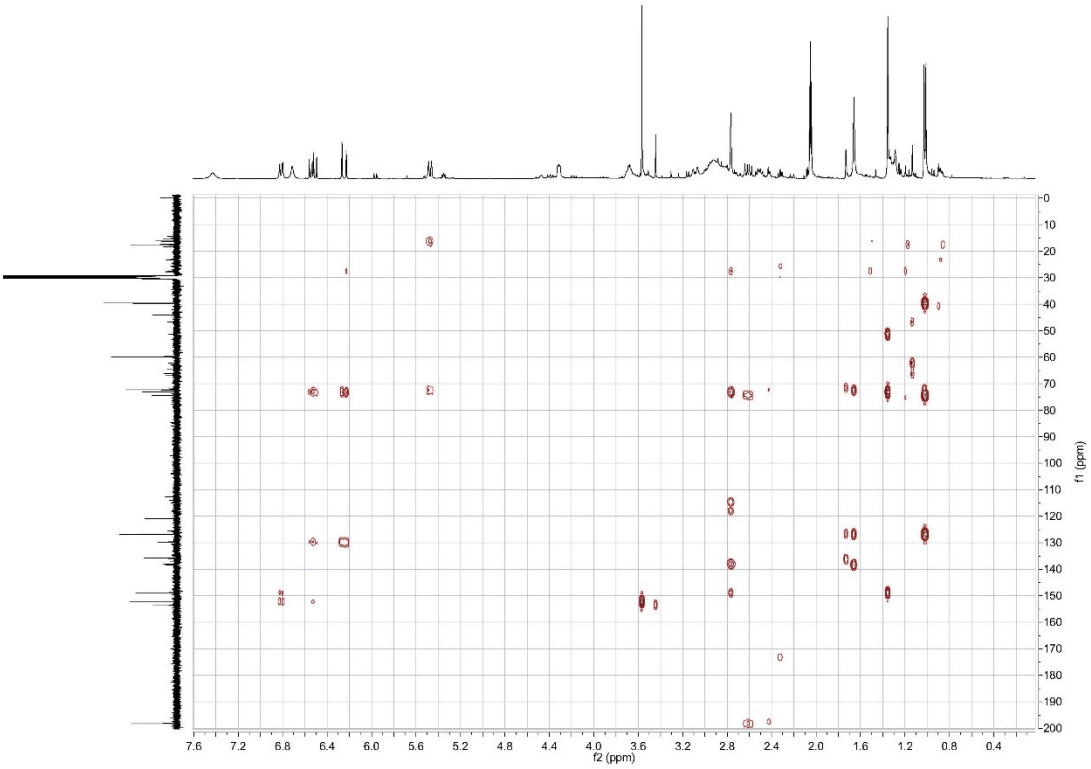

Figure S39. The HMBC NMR spectrum of **8** in CD_3COCD_3.

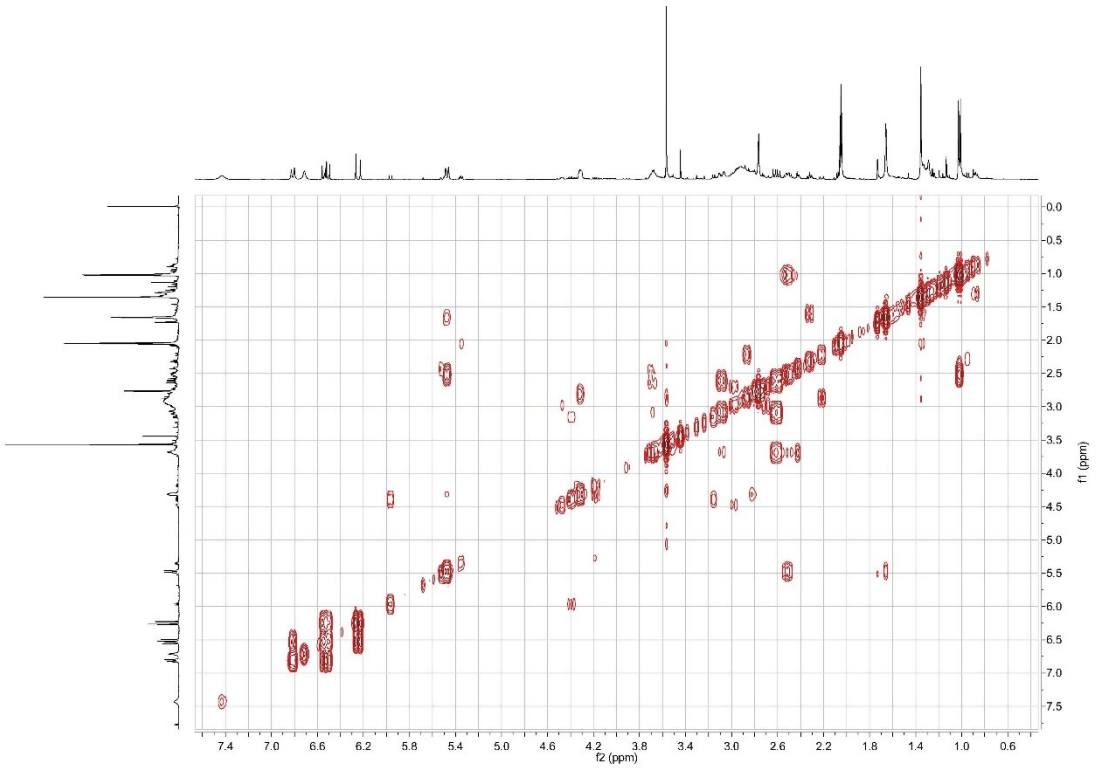

Figure S40. The ^{1}H-^{1}H COSY spectrum of **8** in CD_3COCD_3.

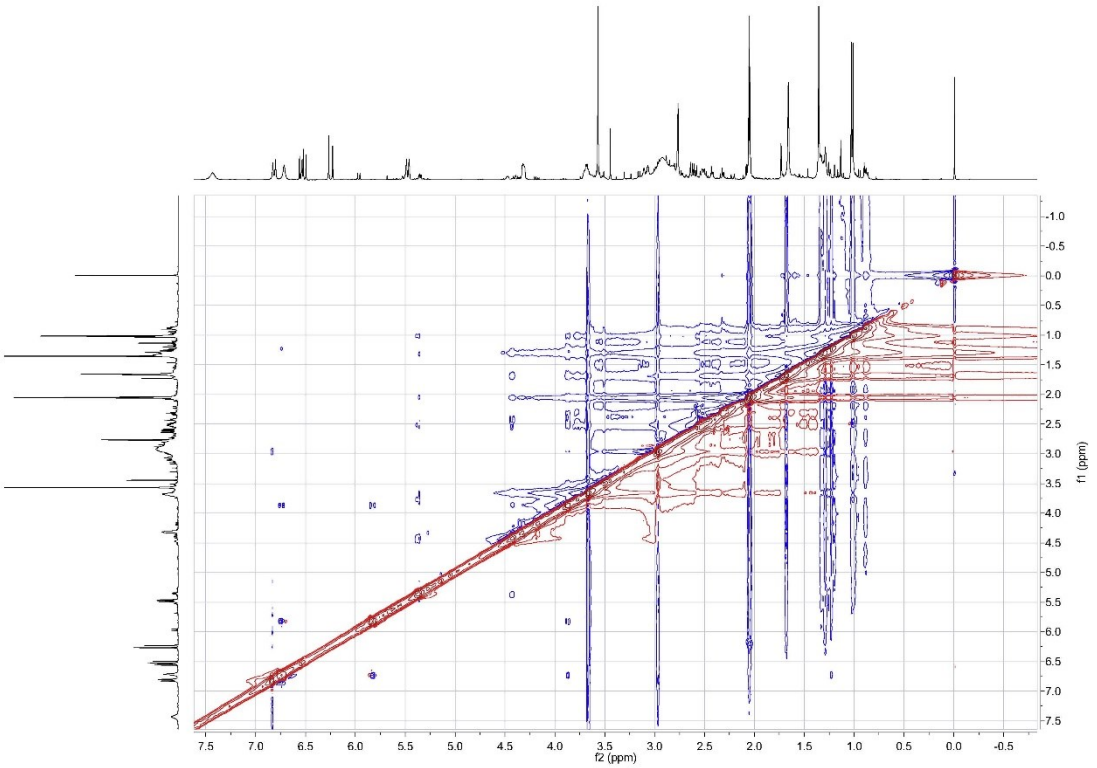

Figure S41. The NOESY spectrum of **8** in CD_3COCD_3.

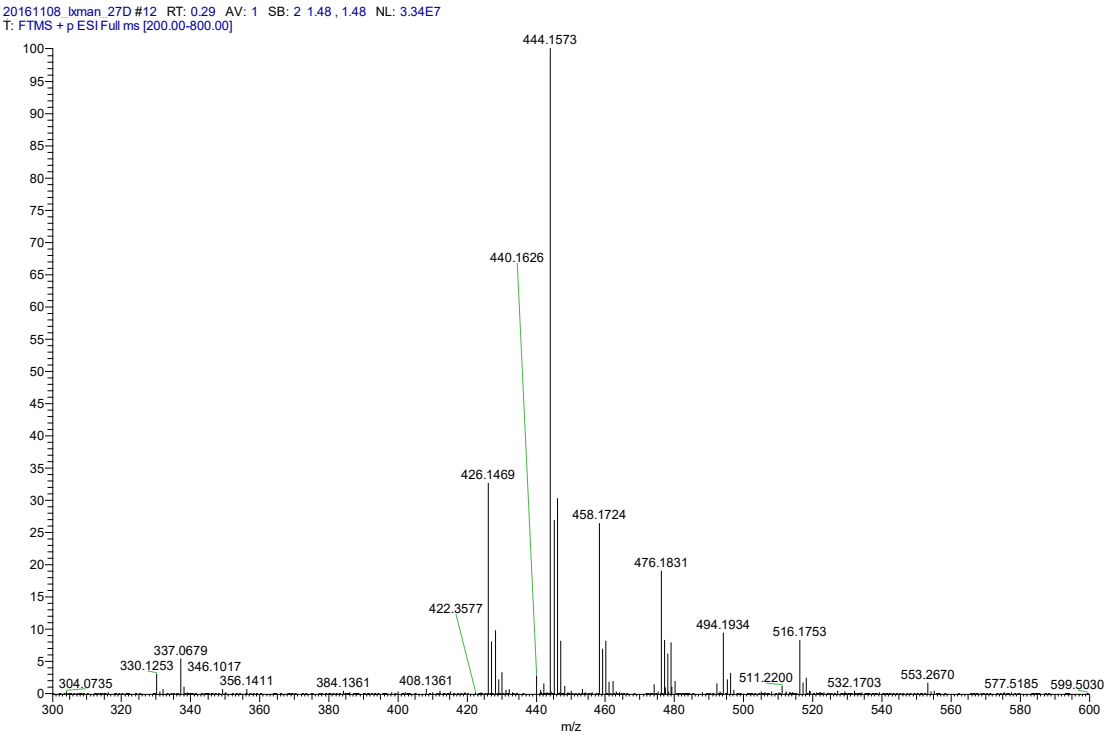

Figure S42. The HRESI mass spectrum of **8**.

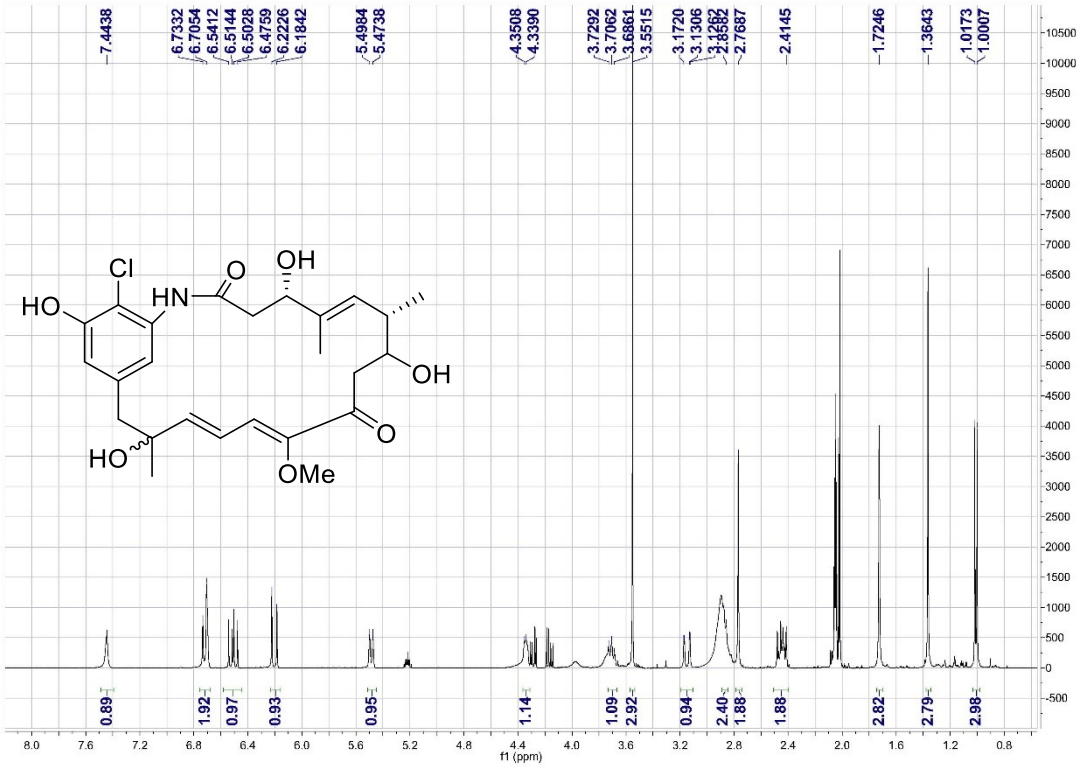

Figure S43. The ^{1}H NMR spectrum of **9** in CD_3COCD_3.

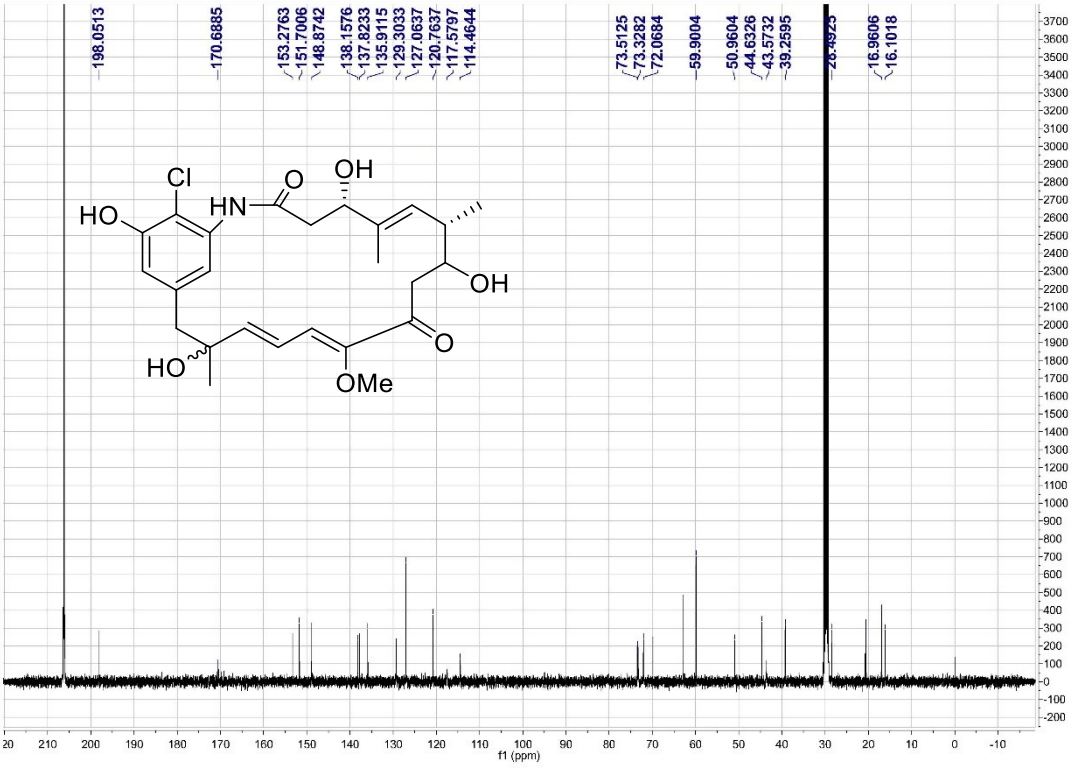

Figure S44. The ^{13}C NMR spectrum of **9** in CD_3COCD_3.

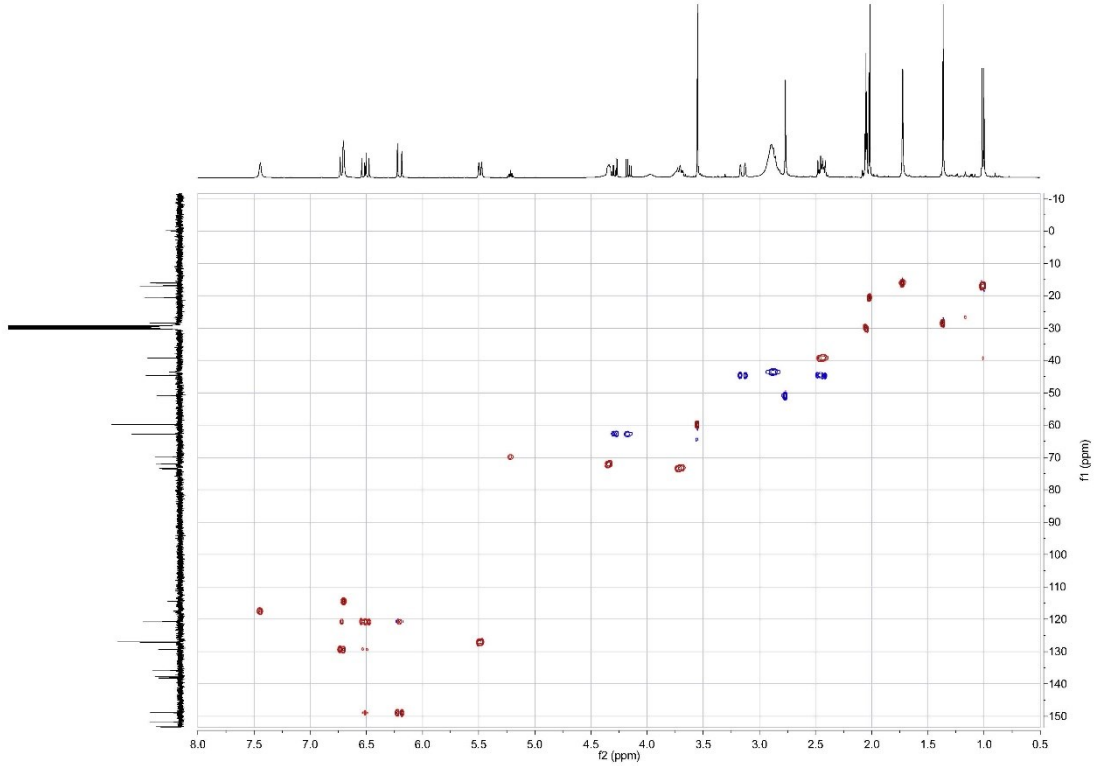

Figure S45. The HMQC spectrum of **9** in CD_3COCD_3.

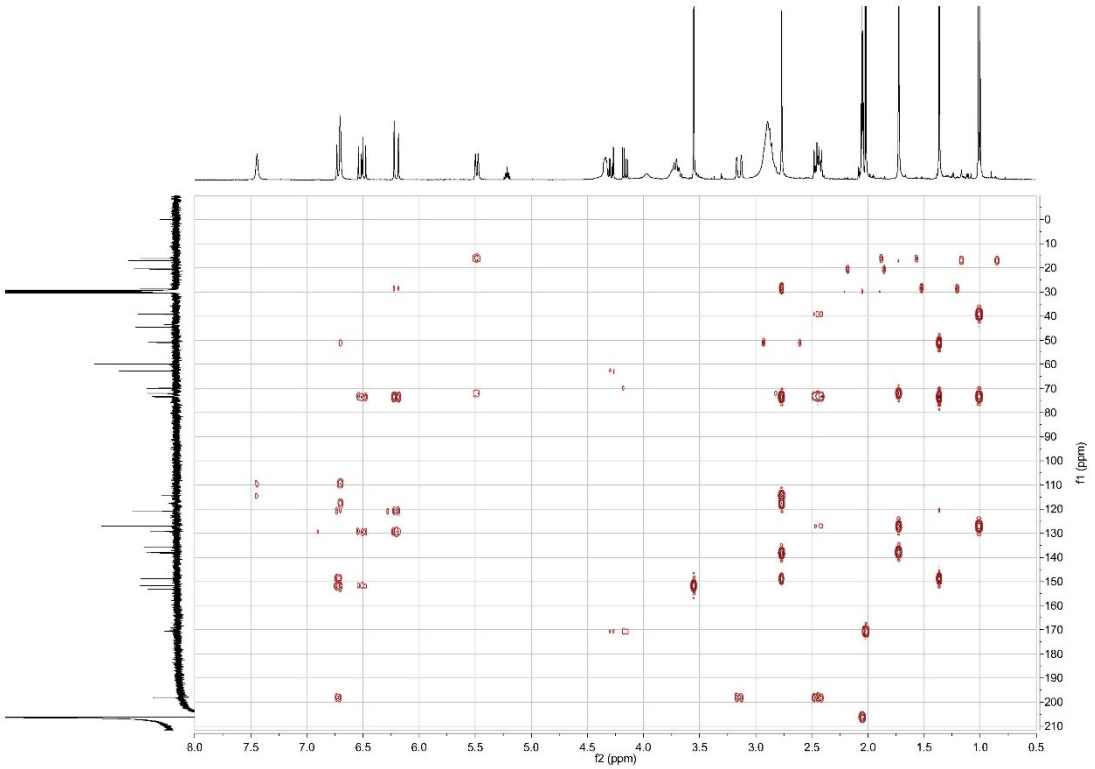

Figure S46. The HMBC NMR spectrum of **9** in CD_3COCD_3.

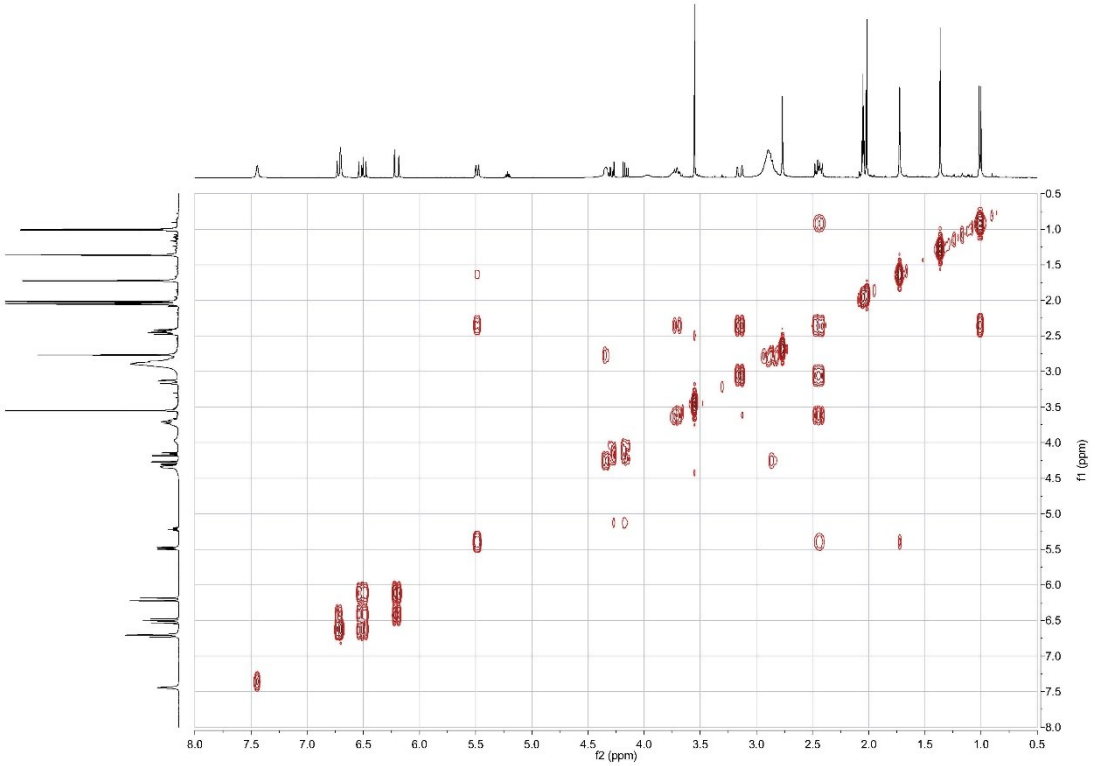

Figure S47. The ^{1}H-^{1}H COSY spectrum of **9** in CD_3COCD_3.

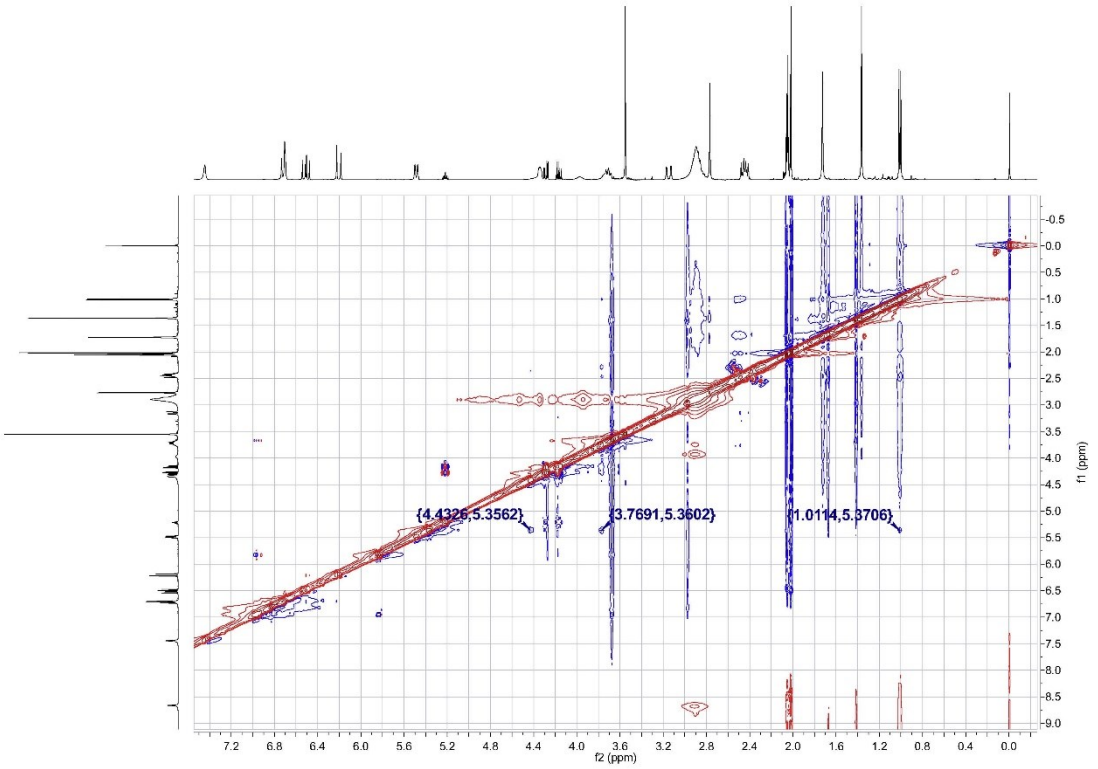

Figure S48. The NOESY spectrum of **9** in CD_3COCD_3.

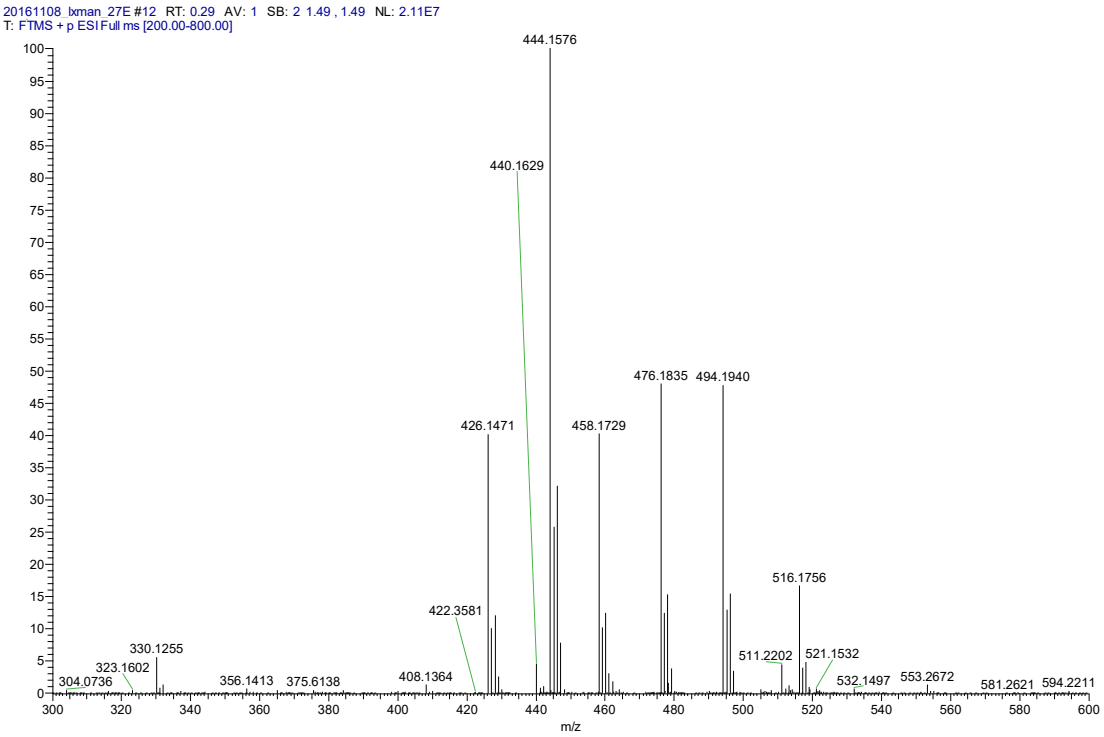

Figure S49. The HRESI mass spectrum of **9**.

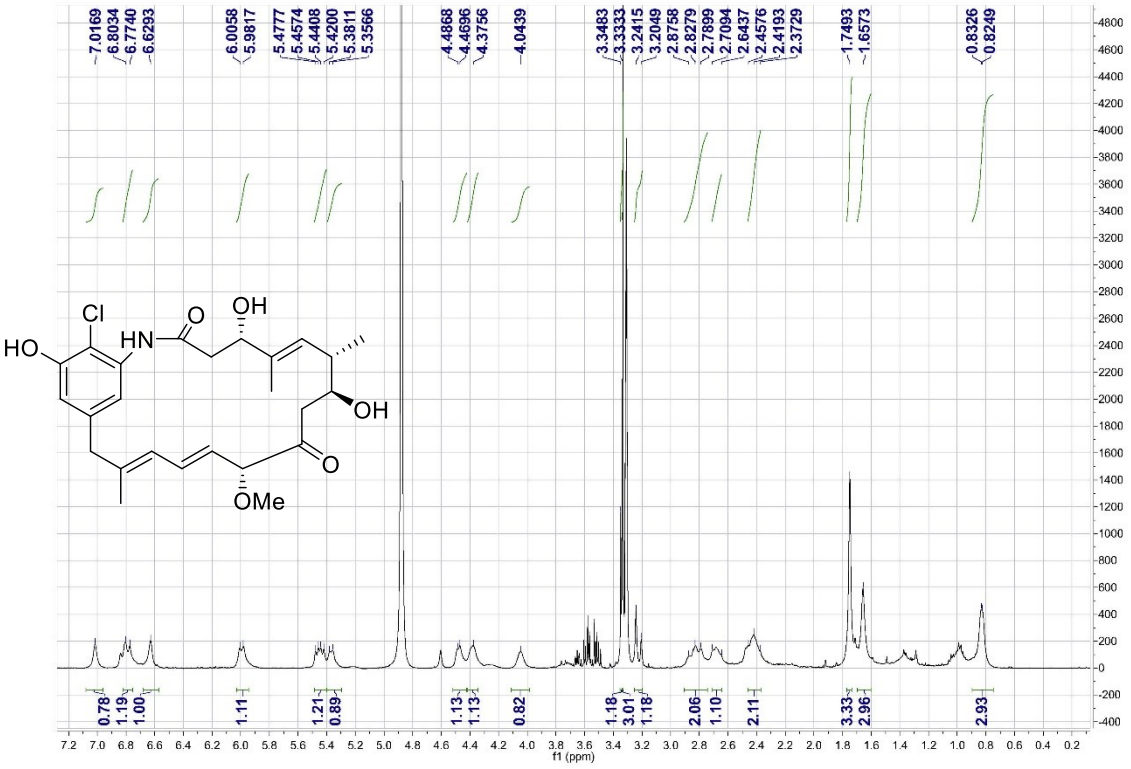

Figure S50. The ^{1}H NMR spectrum of **10** in CD_3OD.

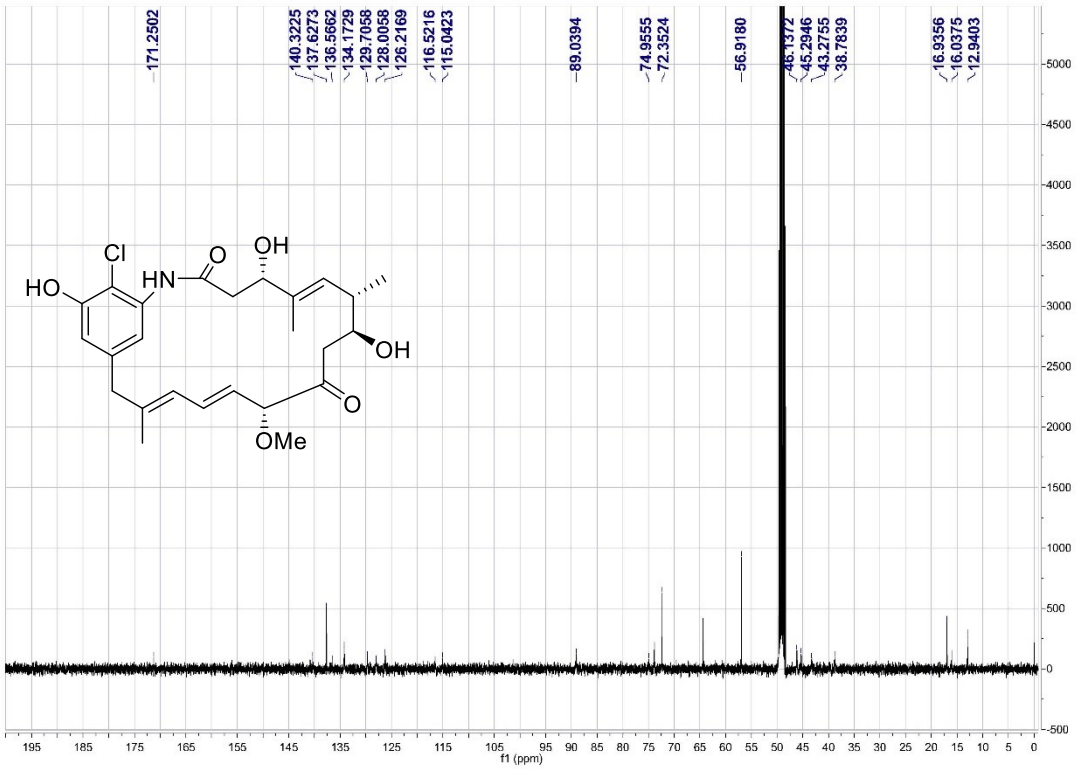

Figure S51. The ^{13}C NMR spectrum of **10** in CD_3OD.

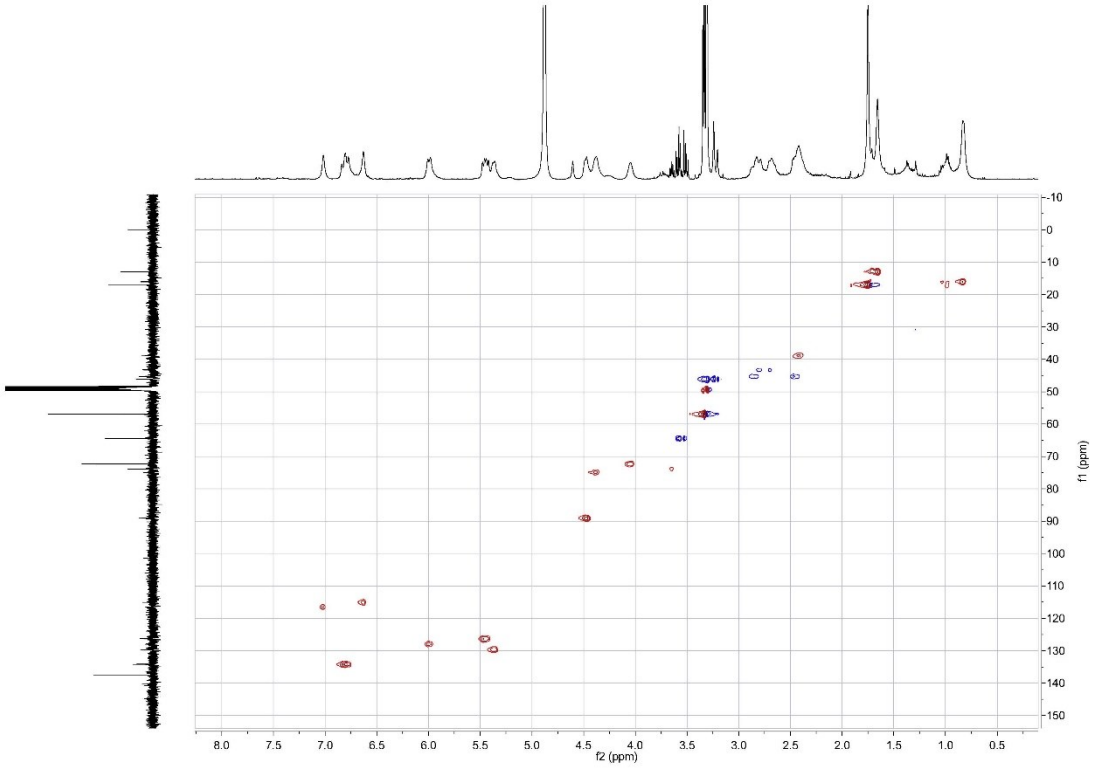

Figure S52. The HMQC spectrum of **10** in CD_3OD.

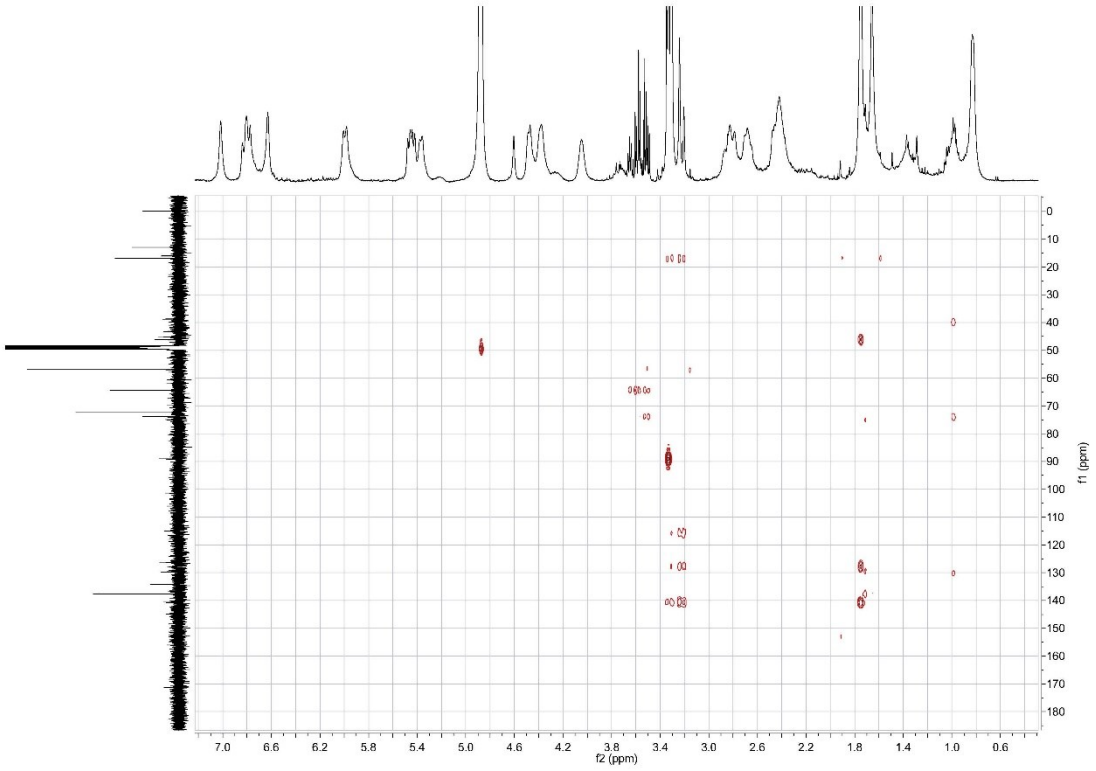

Figure S53. The HMBC NMR spectrum of **10** in CD_3OD.

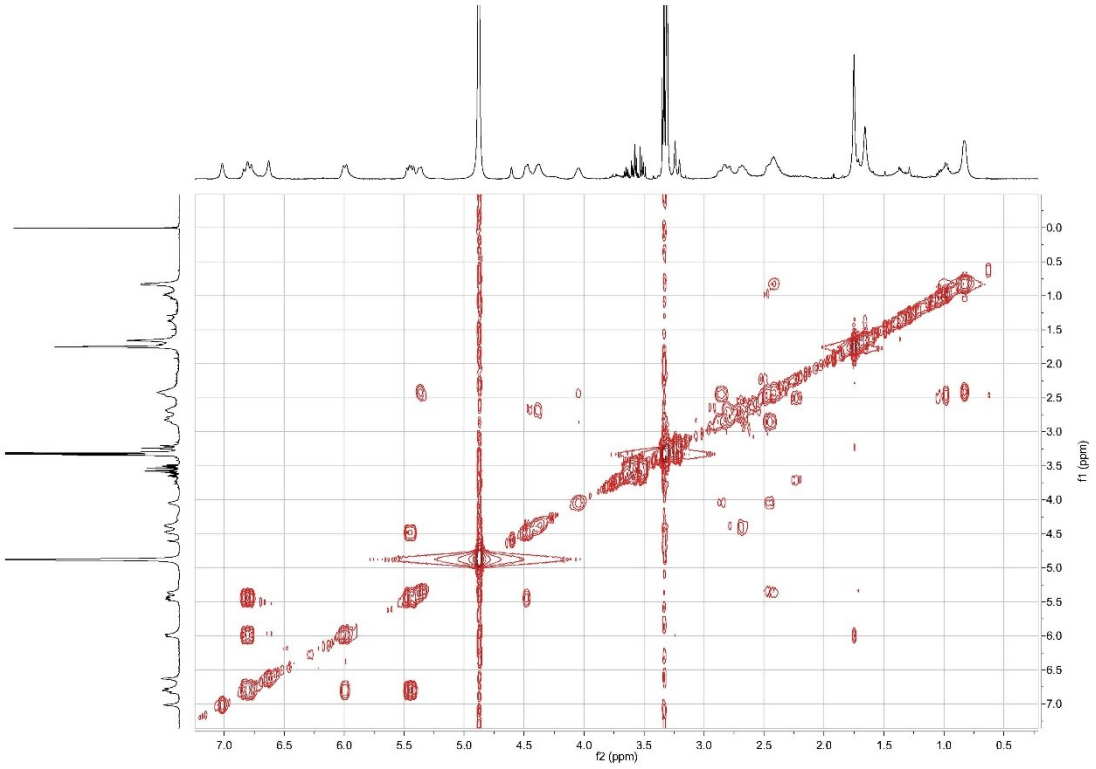

Figure S54. The ^{1}H-^{1}H COSY spectrum of **10** in CD_3OD.

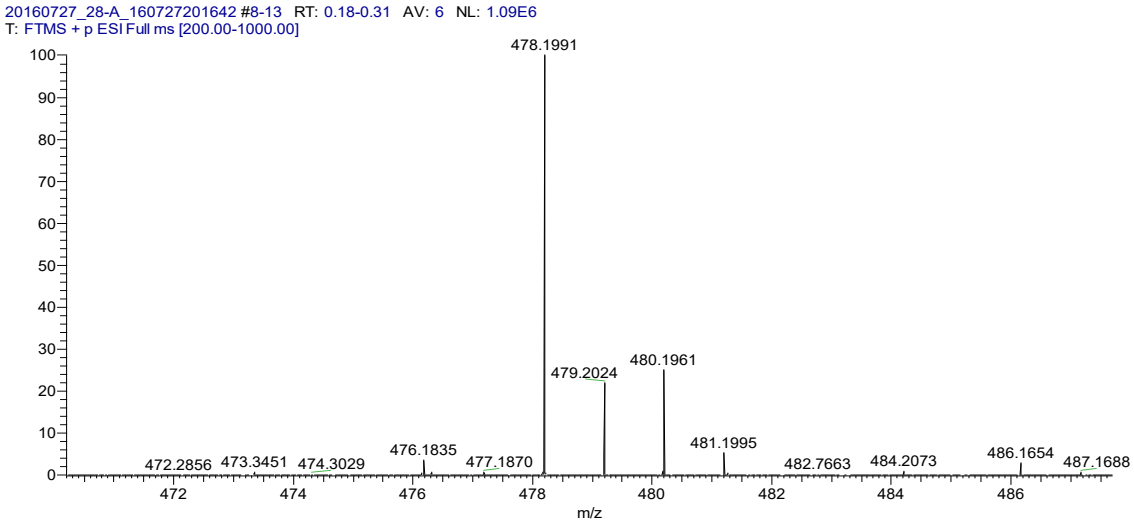

Figure S55. The HRESI mass spectrum of **10**.

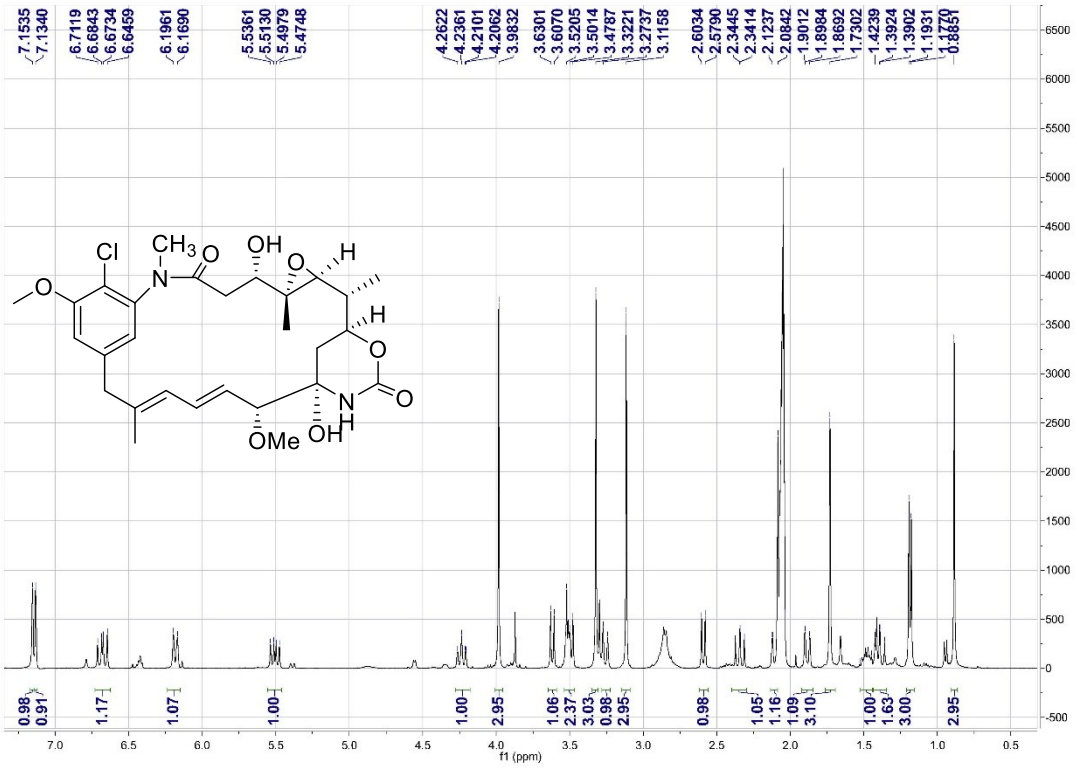

Figure S56. The ^{1}H NMR spectrum of **11** in CD_3COCD_3.

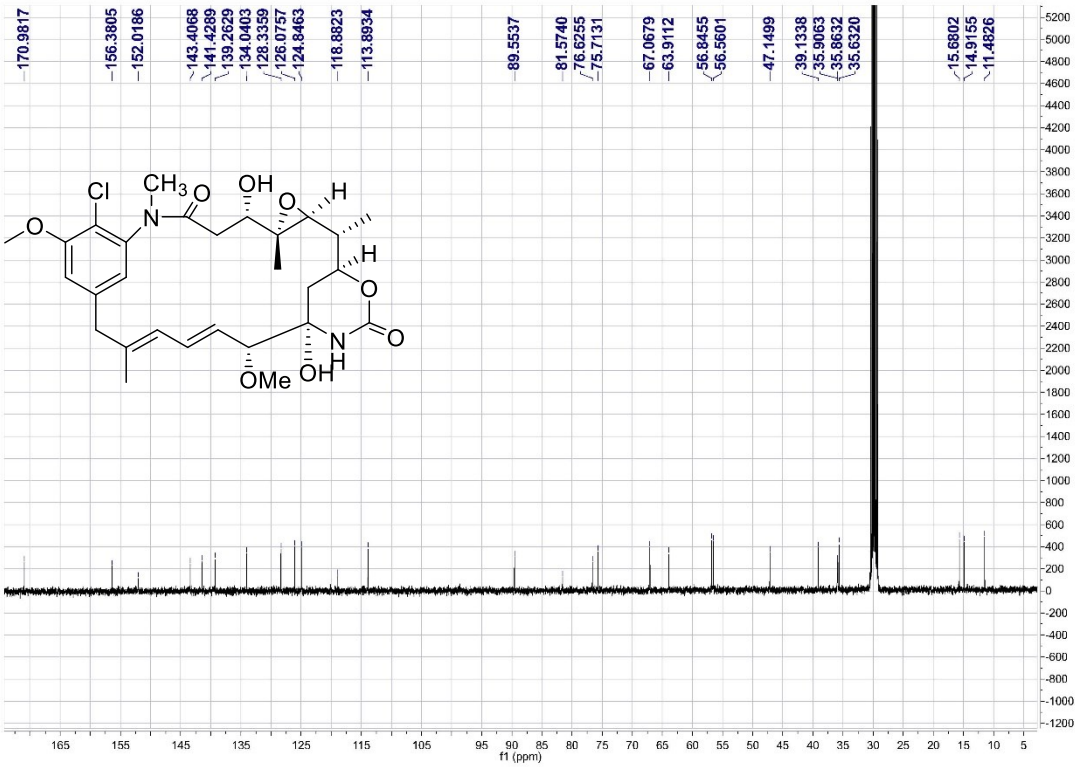

Figure S57. The ^{13}C NMR spectrum of **11** in CD_3COCD_3.

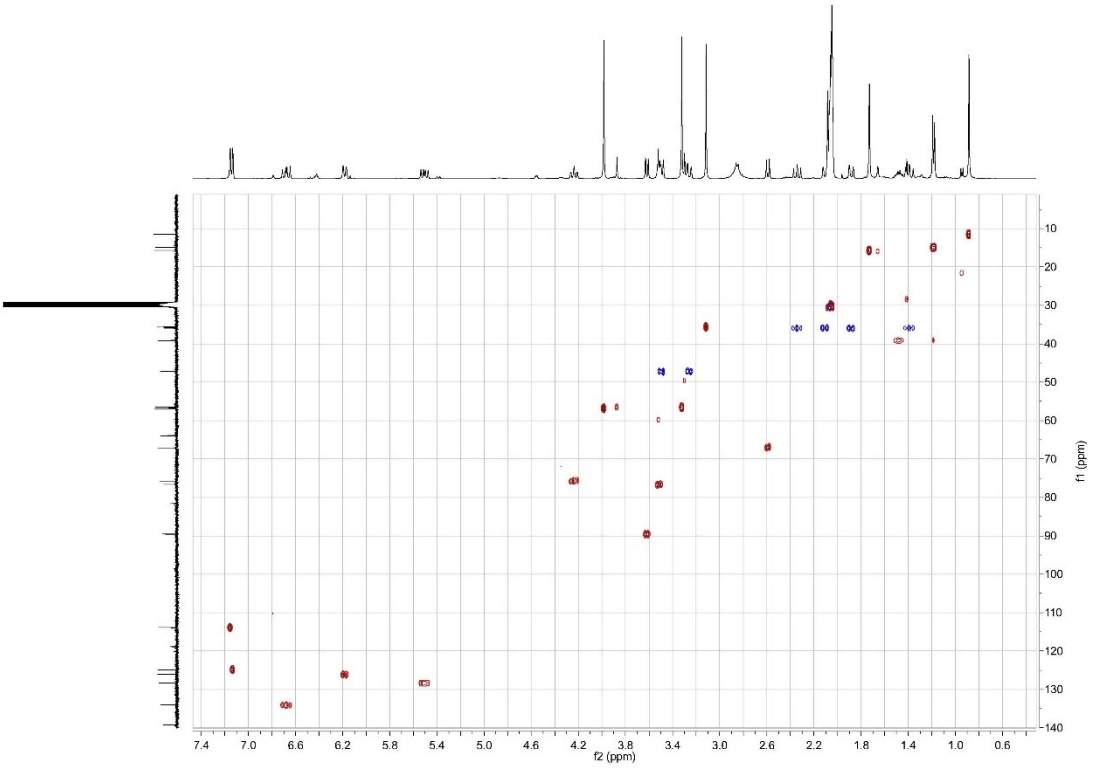

Figure S58. The HMQC spectrum of **11** in CD_3COCD_3.

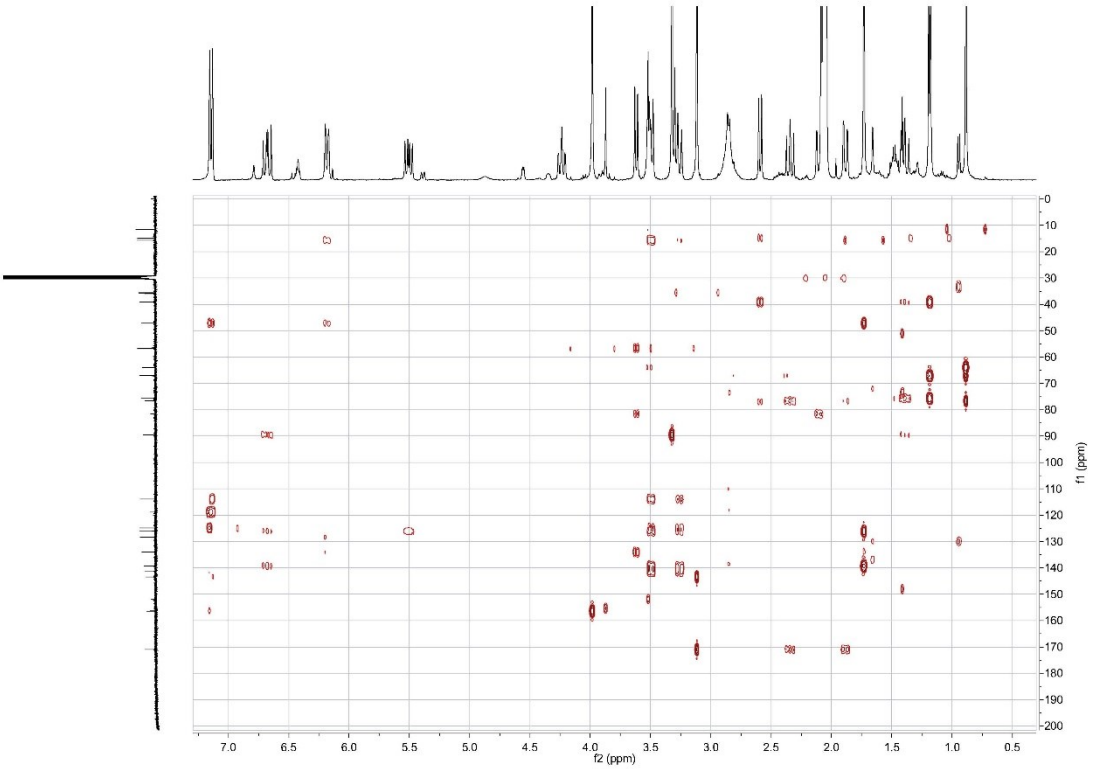

Figure S59. The HMBC NMR spectrum of **11** in CD_3COCD_3.

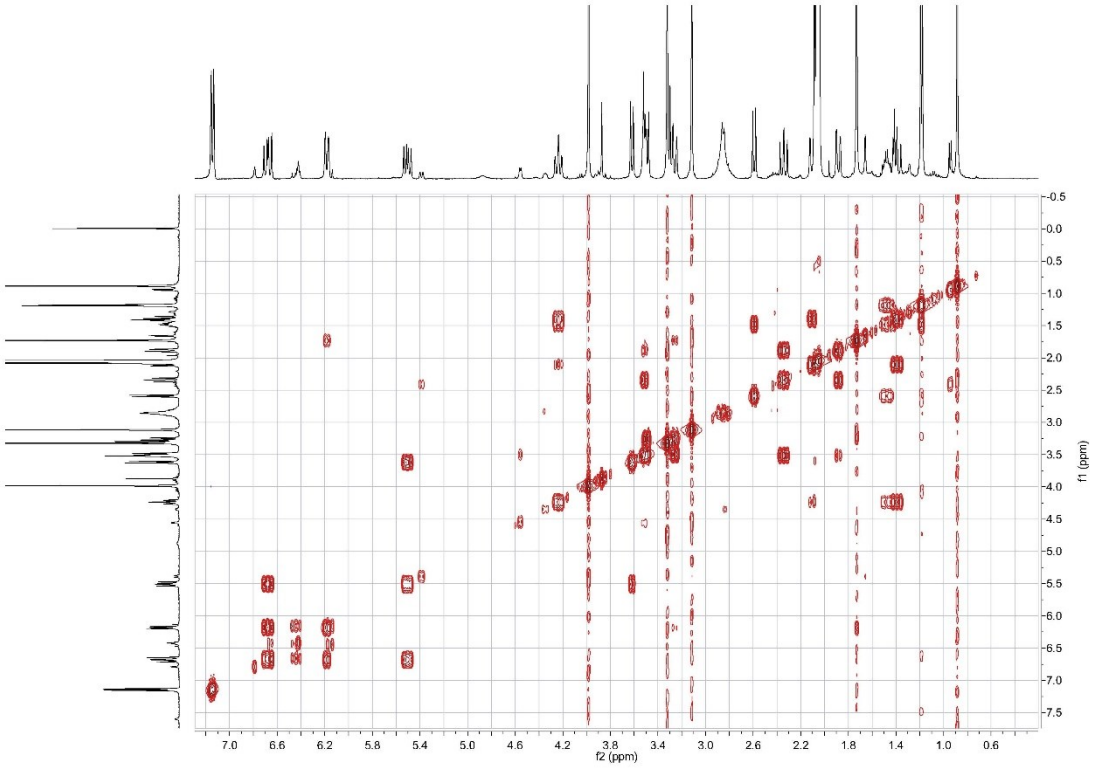

Figure S60. The ^{1}H-^{1}H COSY spectrum of **11** in CD_3COCD_3.

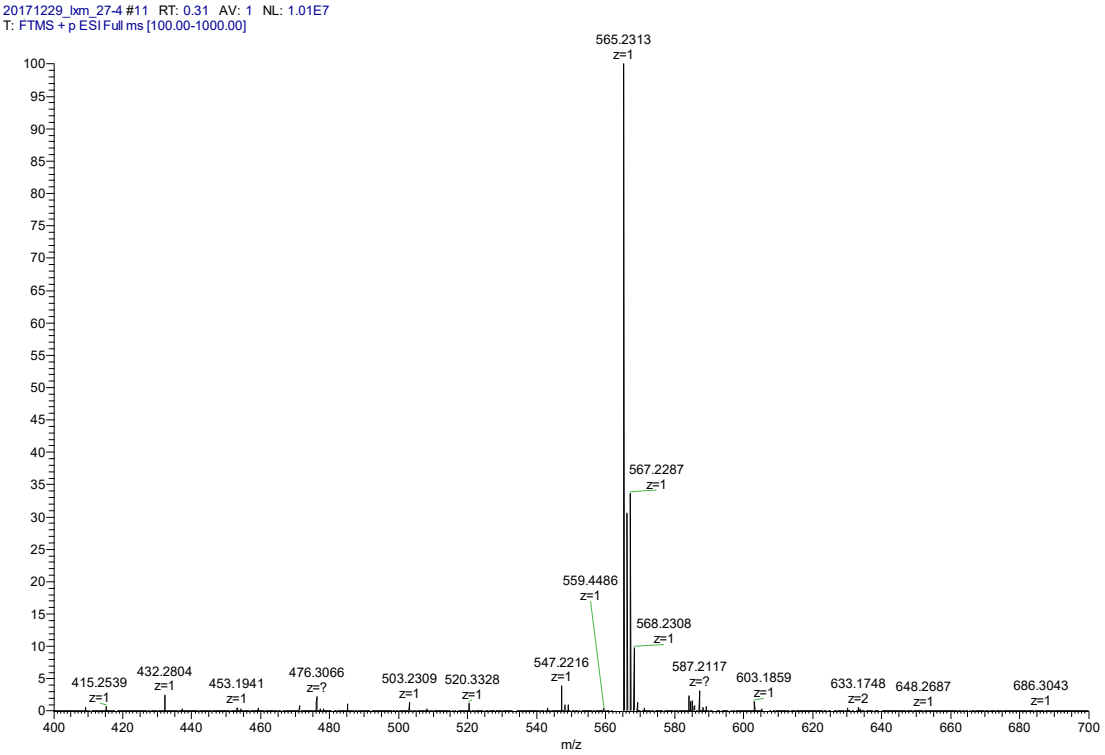

Figure S61. The HRESI mass spectrum of **11**.

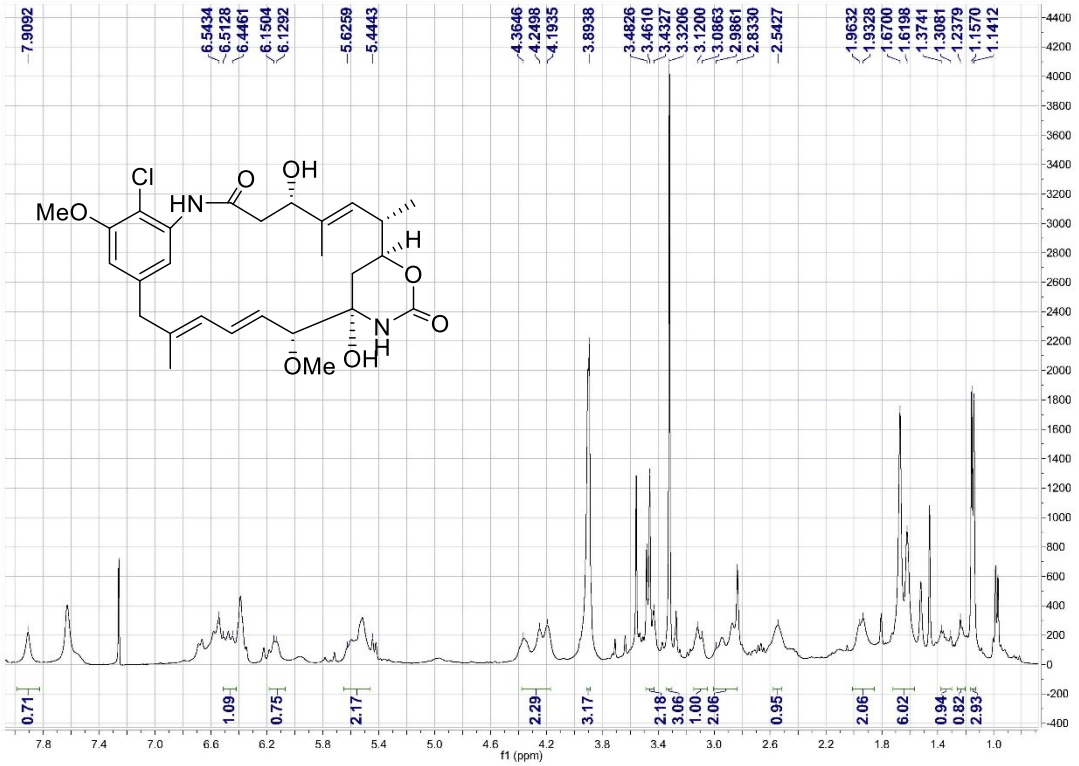

Figure S62. The ^{1}H NMR spectrum of **12** in $CDCl_3$.

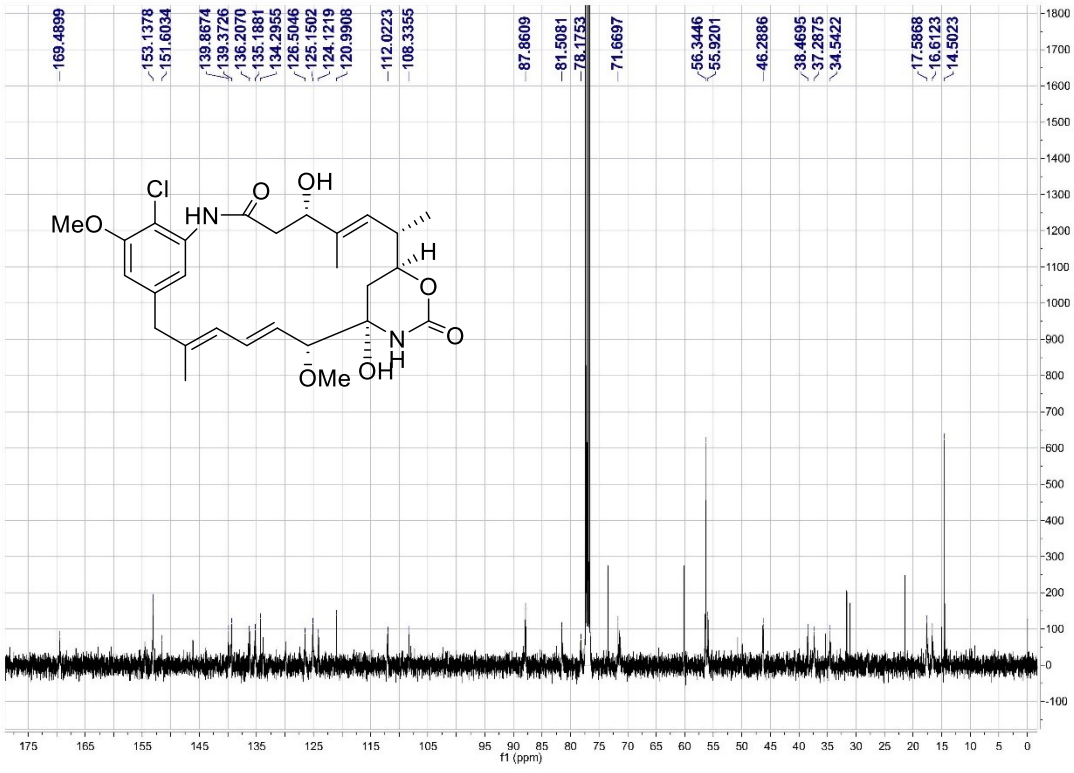

Figure S63. The ^{13}C NMR spectrum of **12** in $CDCl_3$.

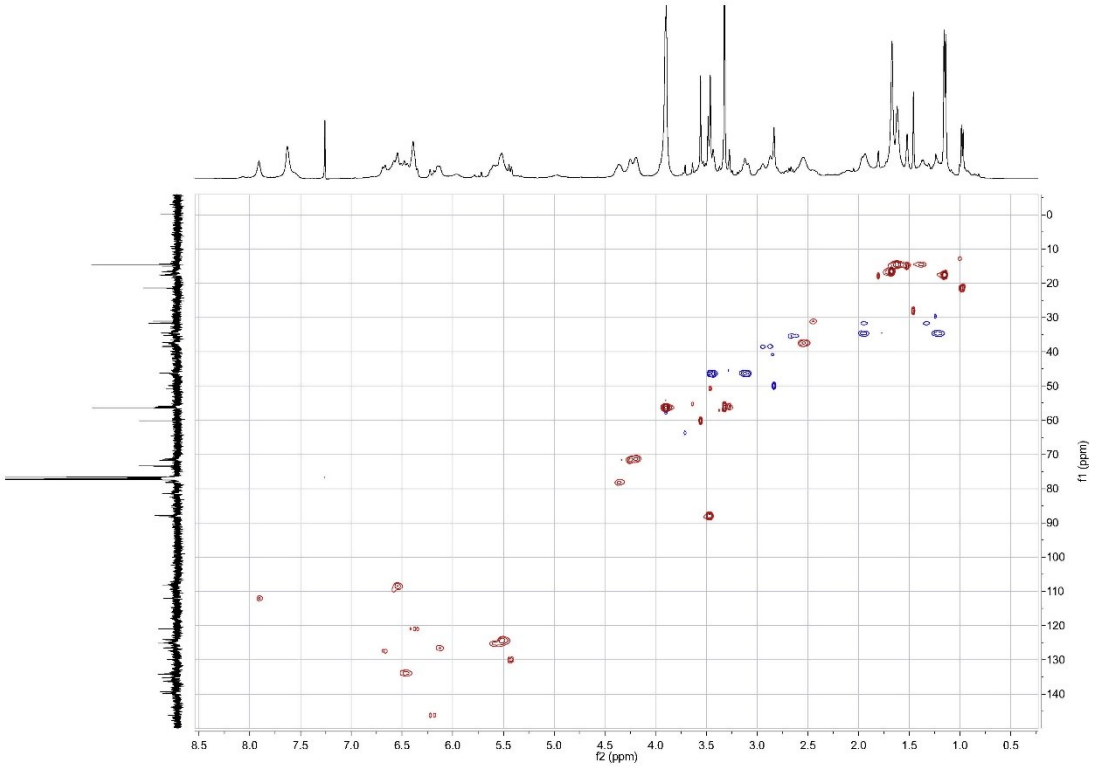

Figure S64. The HMQC spectrum of **12** in $CDCl_3$.

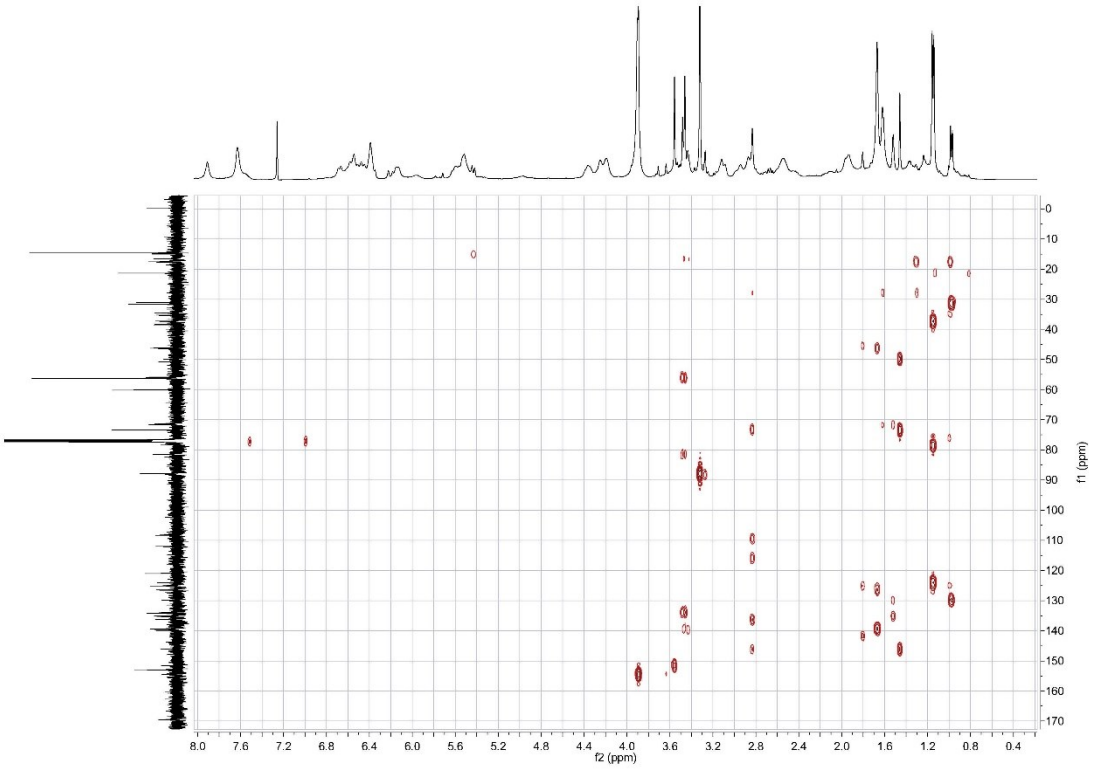

Figure S65. The HMBC NMR spectrum of **12** in $CDCl_3$.

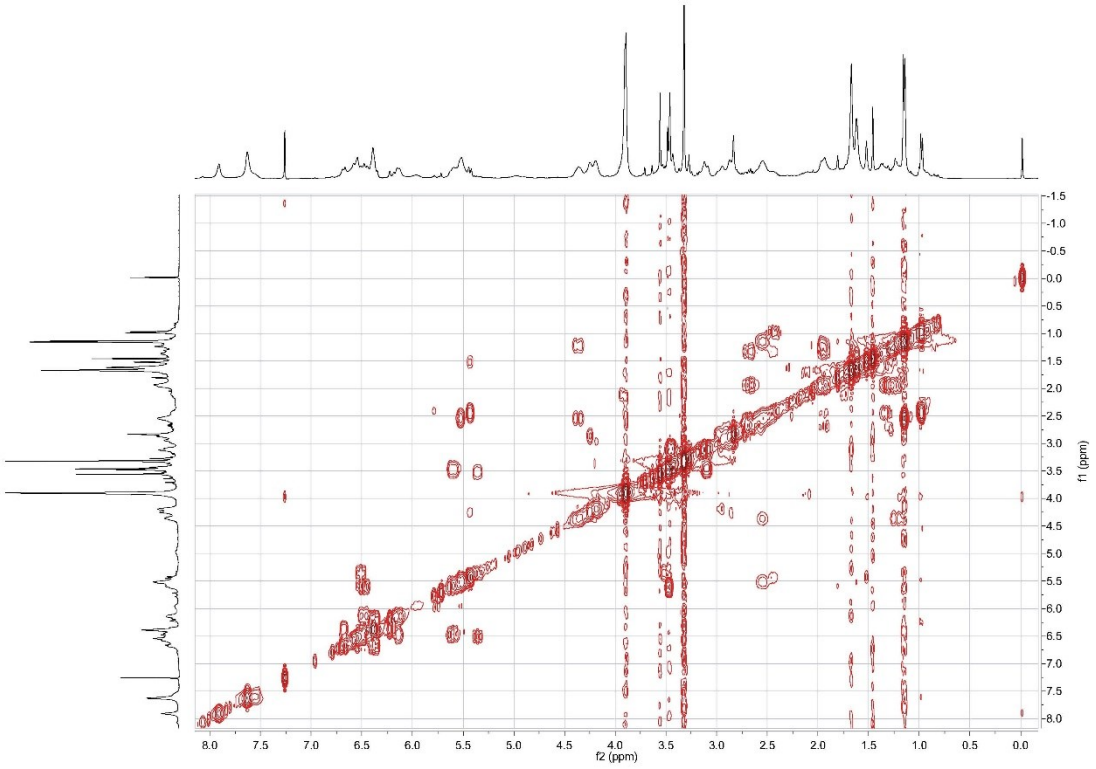

Figure S66. The ^{1}H-^{1}H COSY spectrum of **12** in $CDCl_3$.

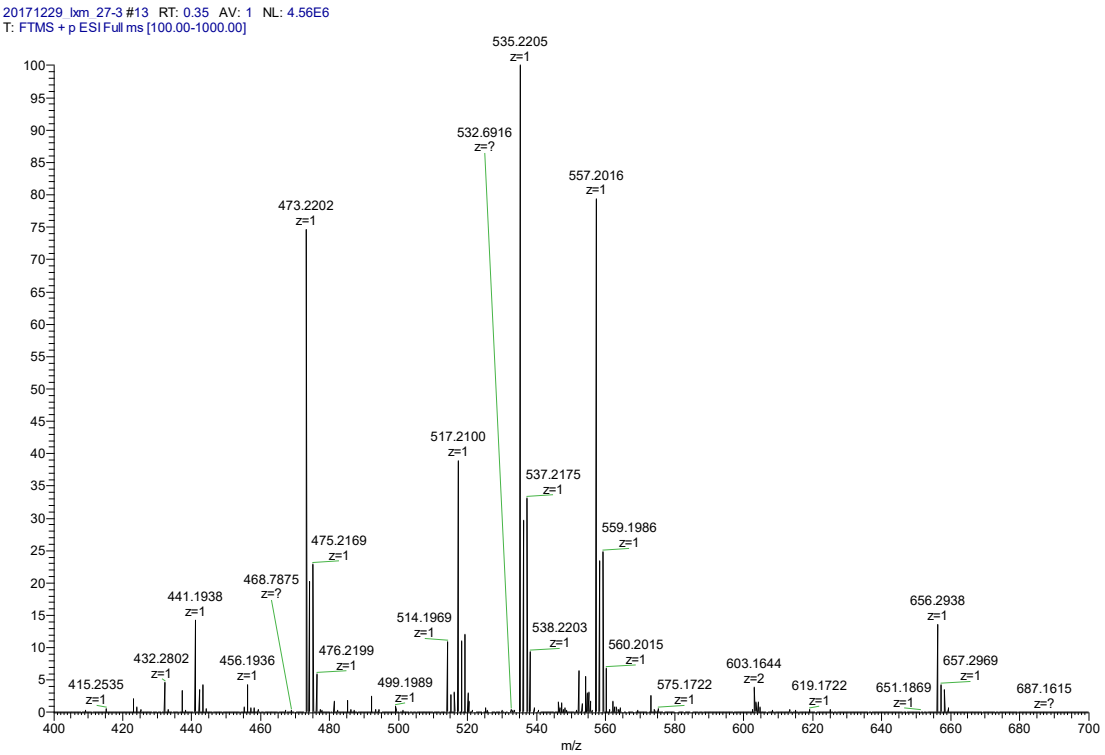

Figure S67. The HRESI mass spectrum of **12**.

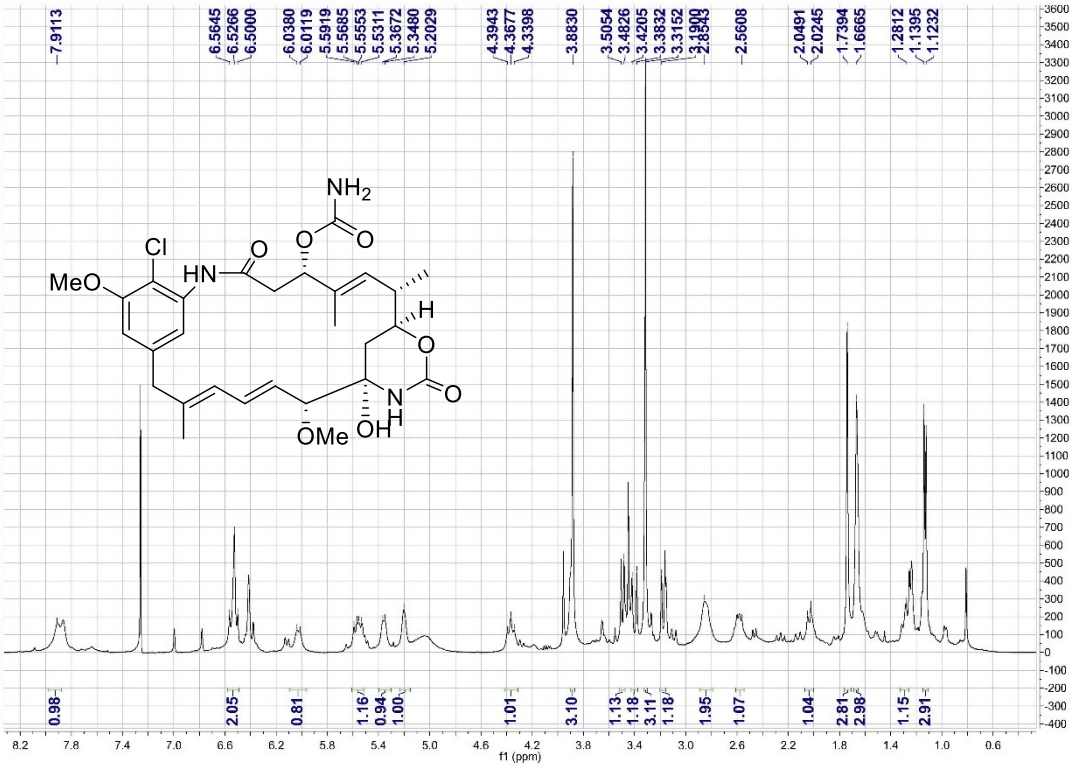

Figure S68. The ^{1}H NMR spectrum of **13** in $CDCl_3$.

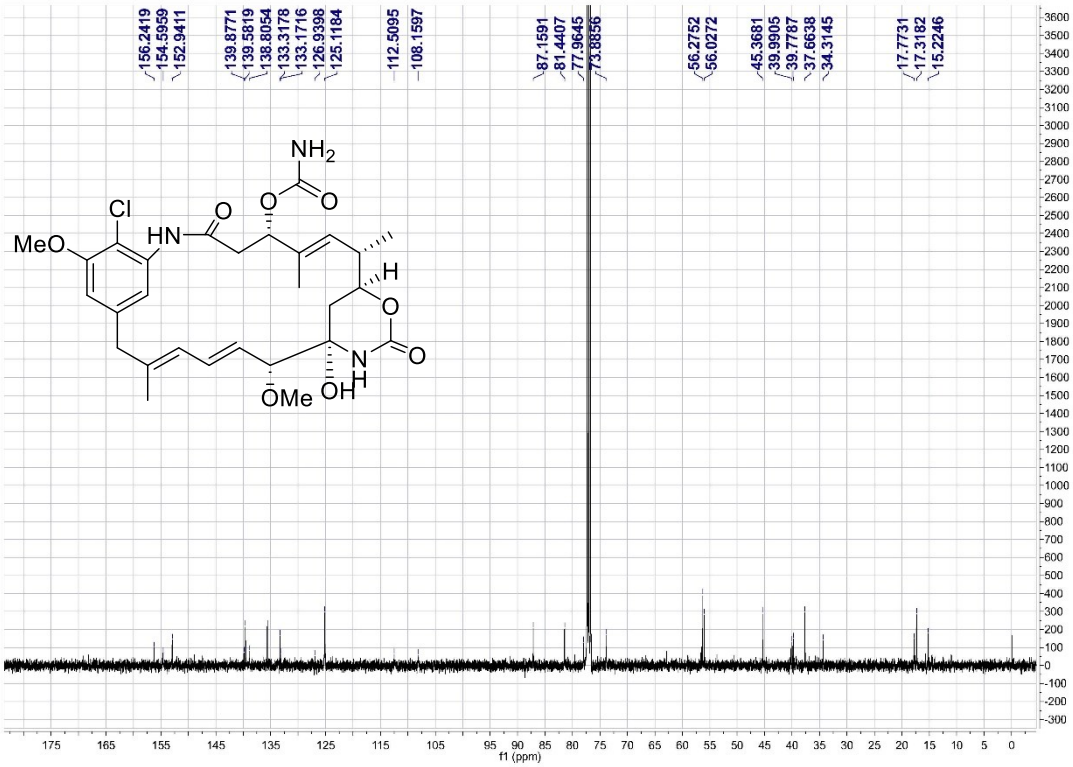

Figure S69. The ^{13}C NMR spectrum of **13** in $CDCl_3$.

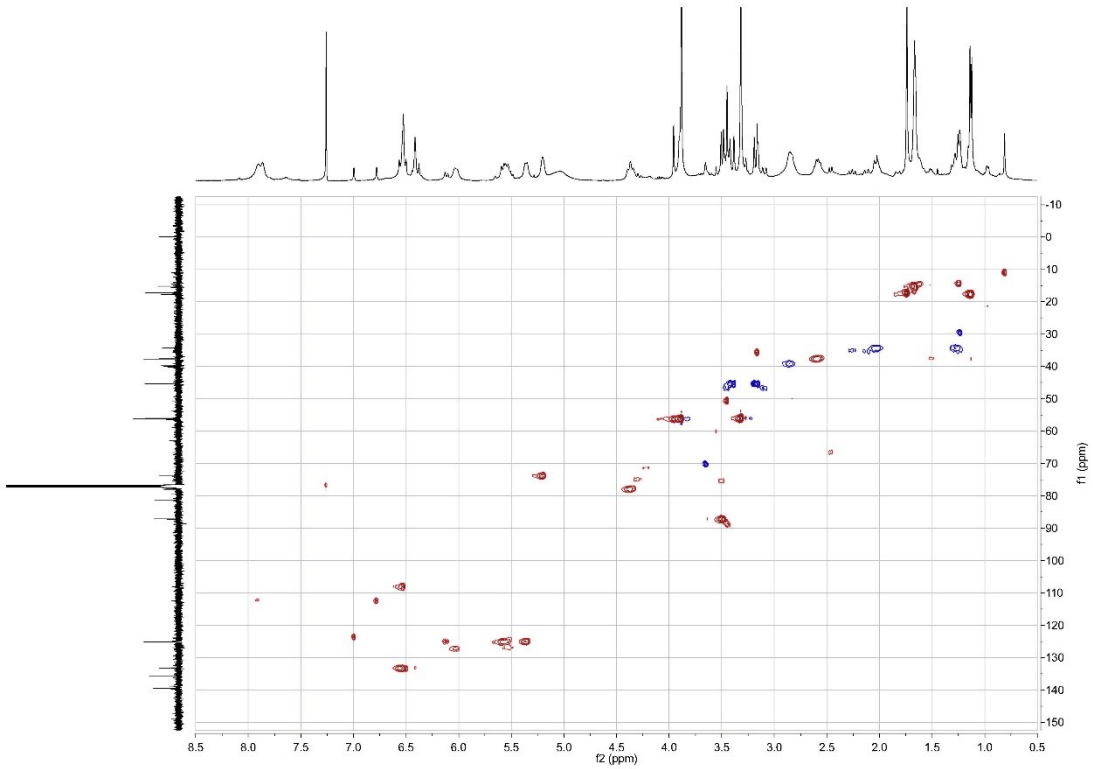

Figure S70. The HMQC spectrum of **13** in $CDCl_3$.

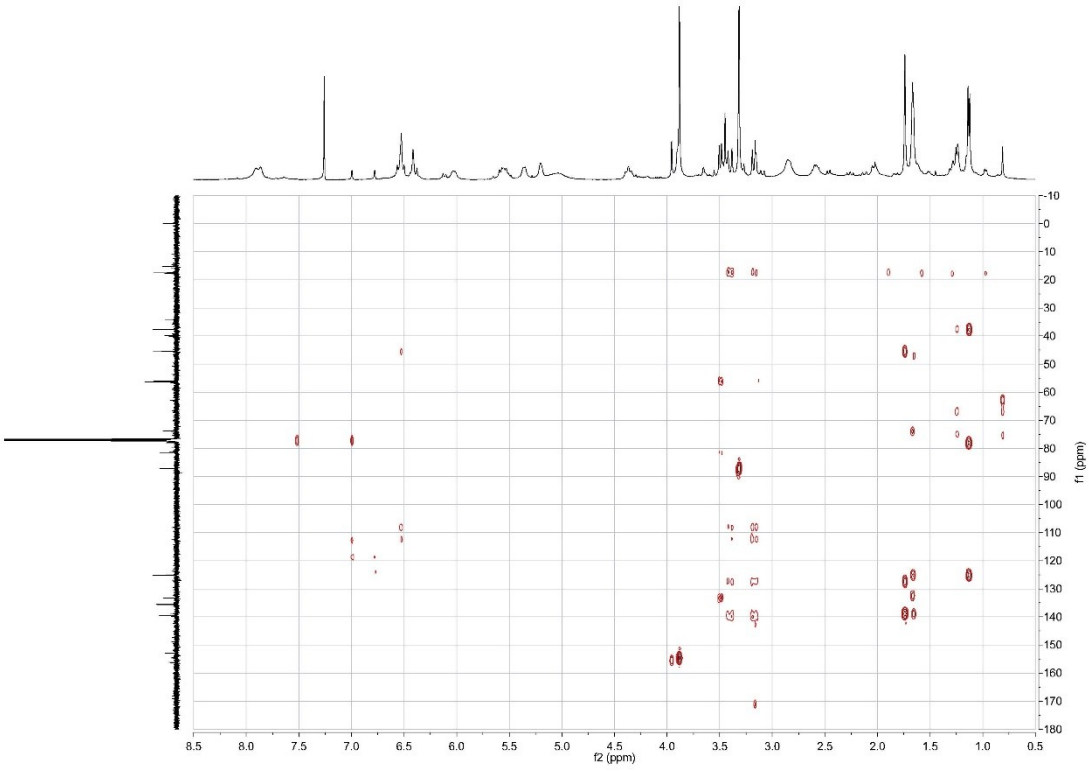

Figure S71. The HMBC NMR spectrum of **13** in $CDCl_3$.

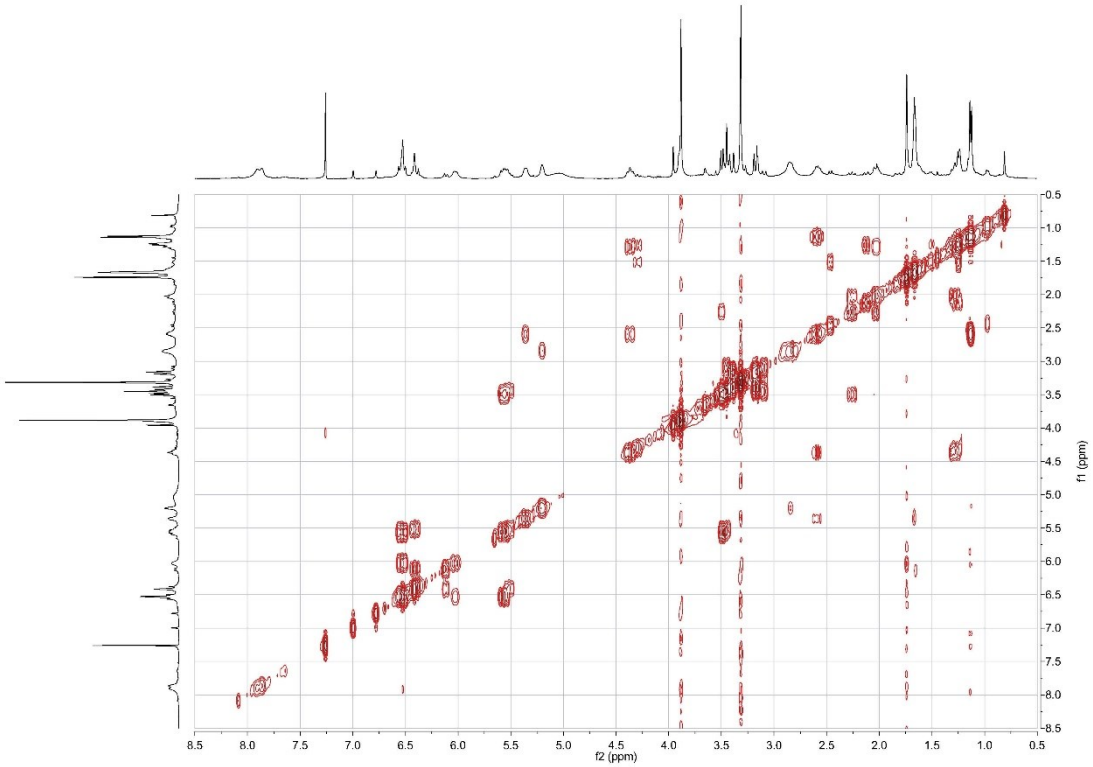

Figure S72. The ^{1}H-^{1}H COSY spectrum of **13** in $CDCl_3$.

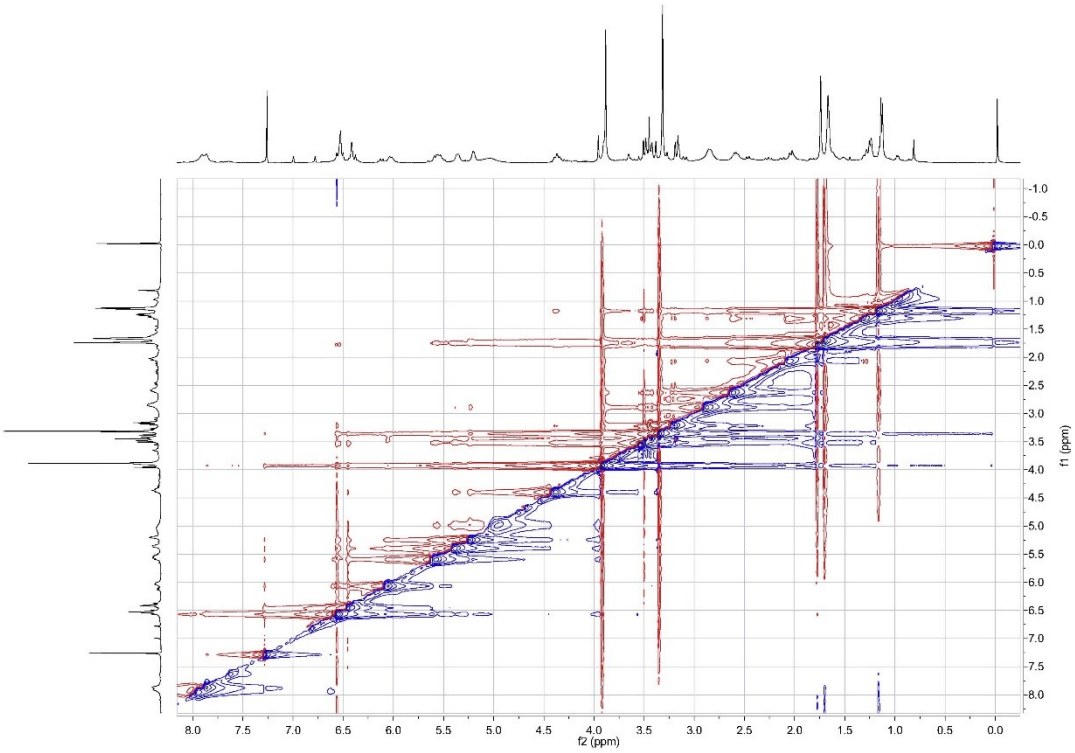

Figure S73. The NOESY spectrum of **13** in $CDCl_3$.

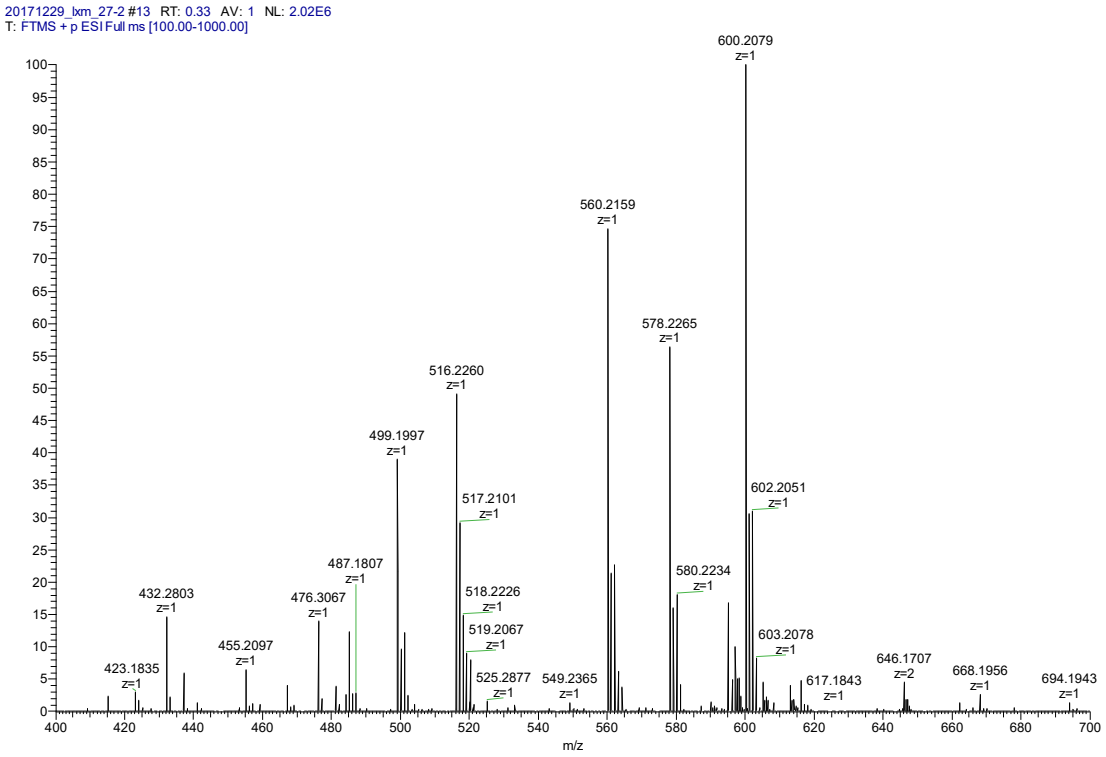

Figure S74. The HRESI mass spectrum of **13**.

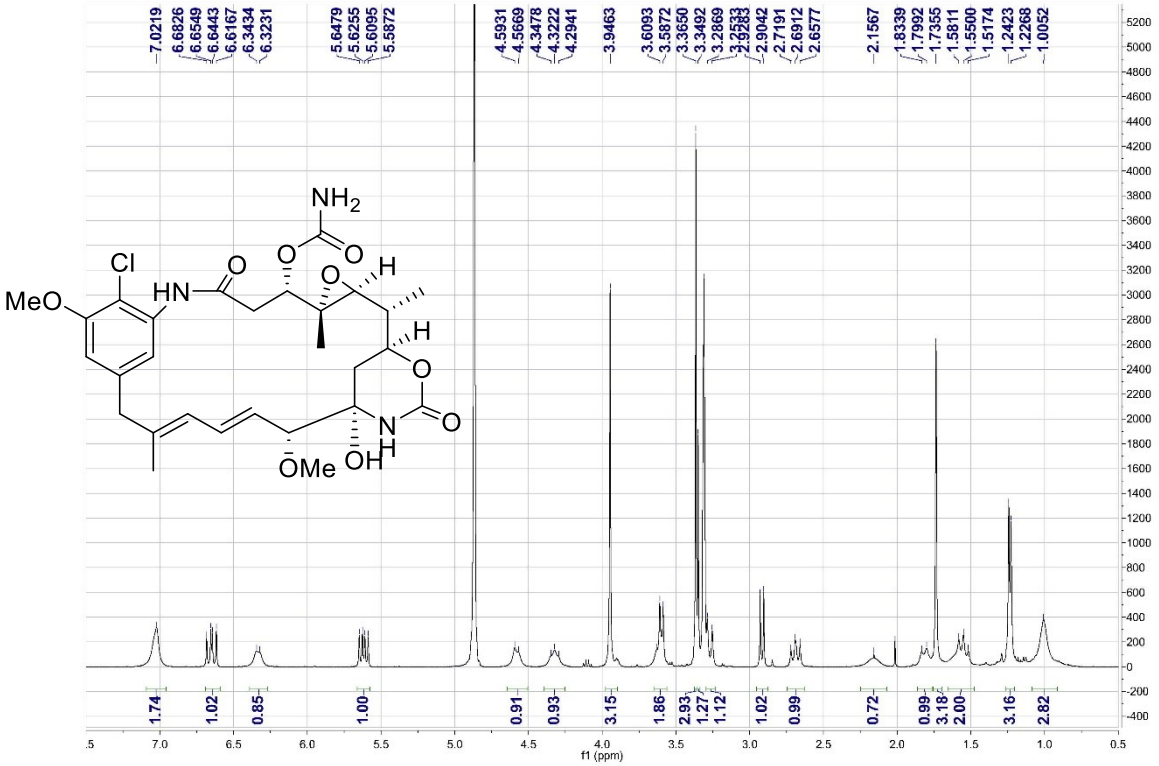

Figure S75. The ^{1}H NMR spectrum of **14** in CD_3OD.

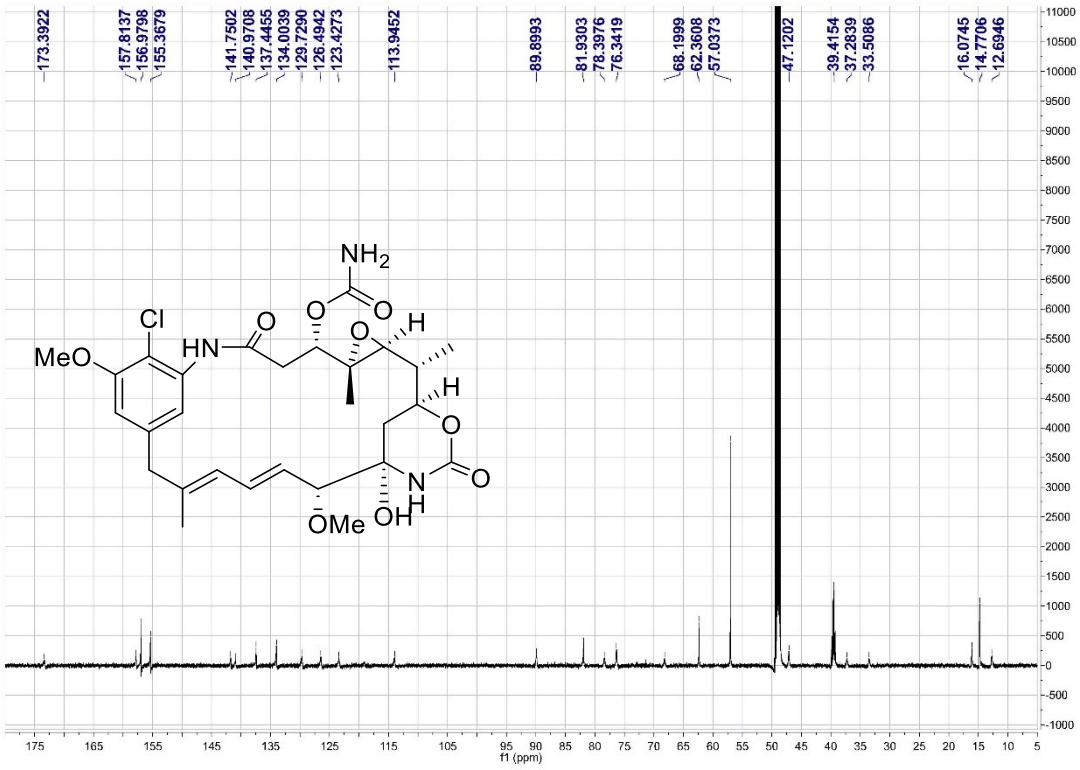

Figure S76. The ^{13}C NMR spectrum of **14** in CD_3OD.

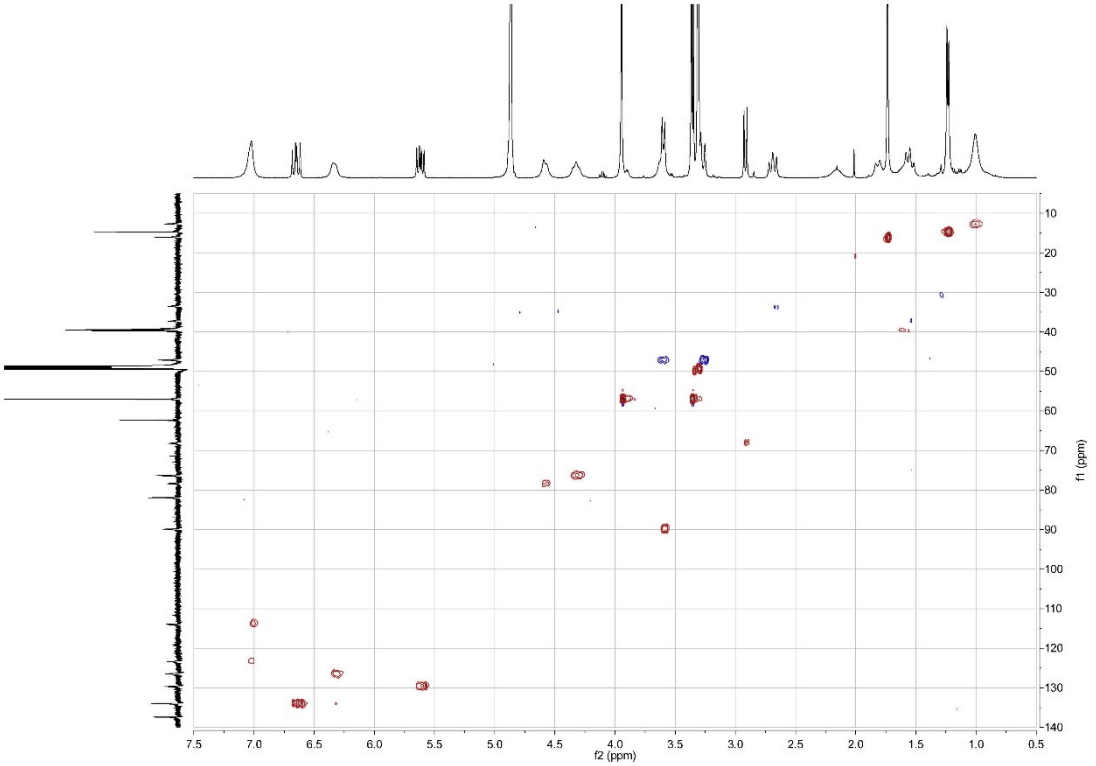

Figure S77. The HMQC spectrum of **14** in CD_3OD

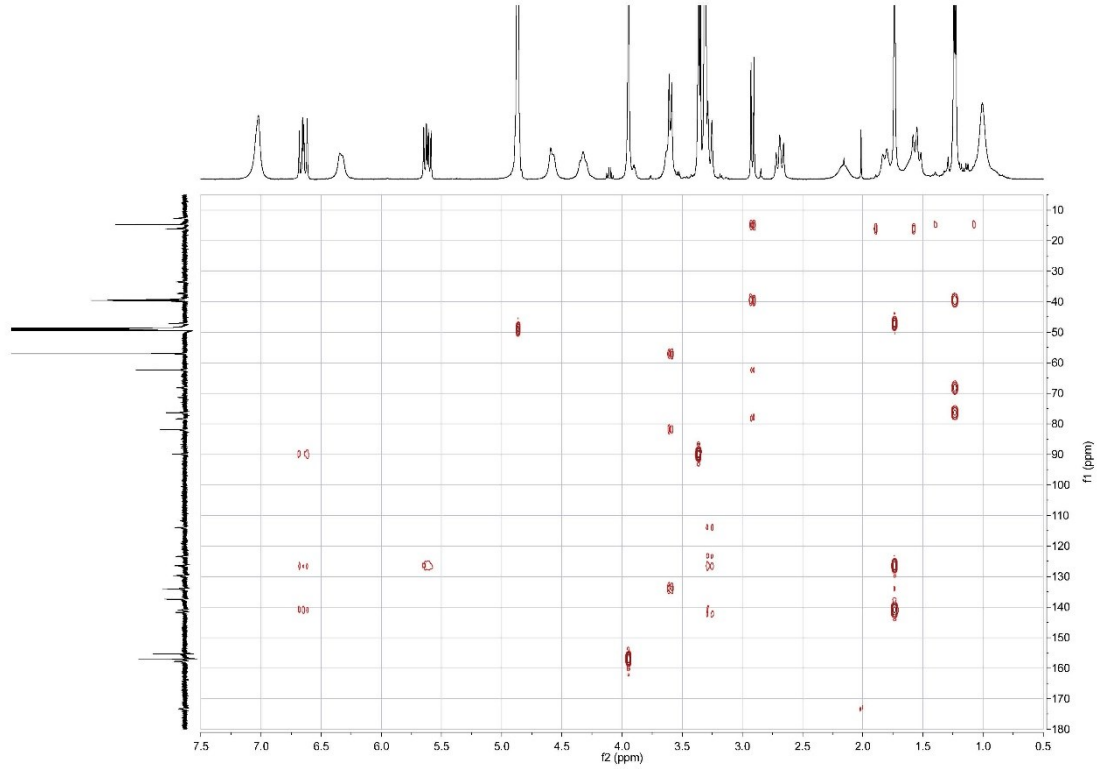

Figure S78. The HMBC NMR spectrum of **14** in CD_3OD.

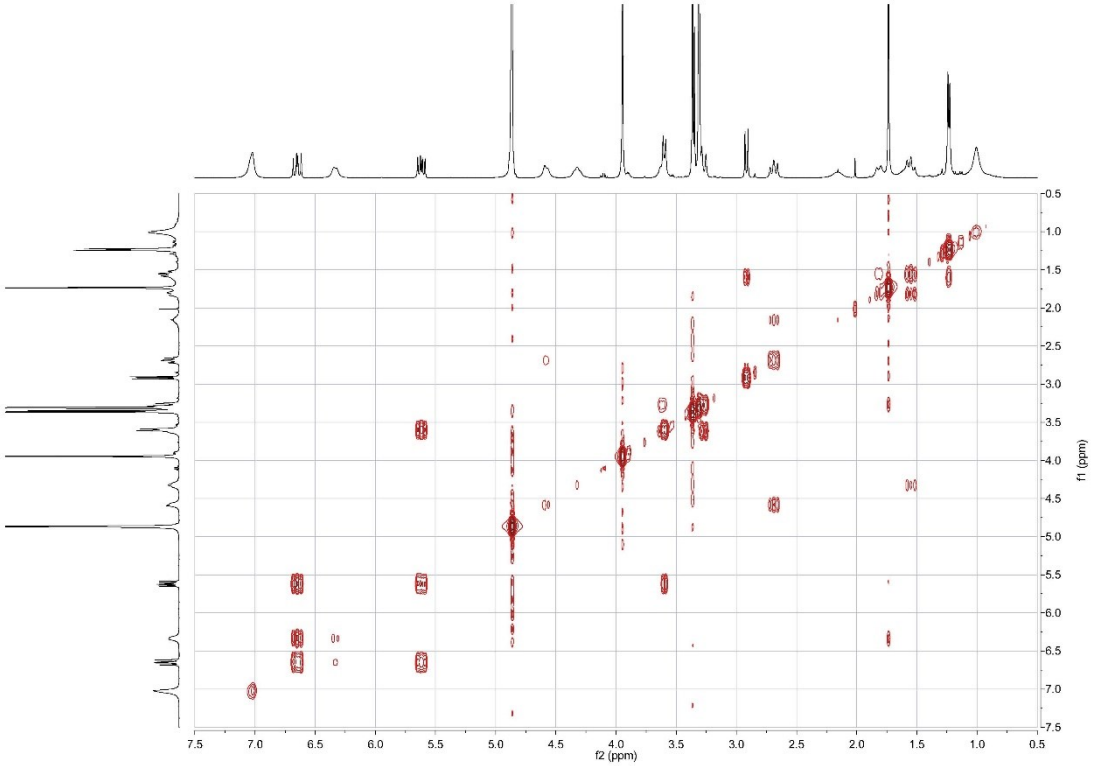

Figure S79. The ^{1}H-^{1}H COSY spectrum of **14** in CD_3OD.

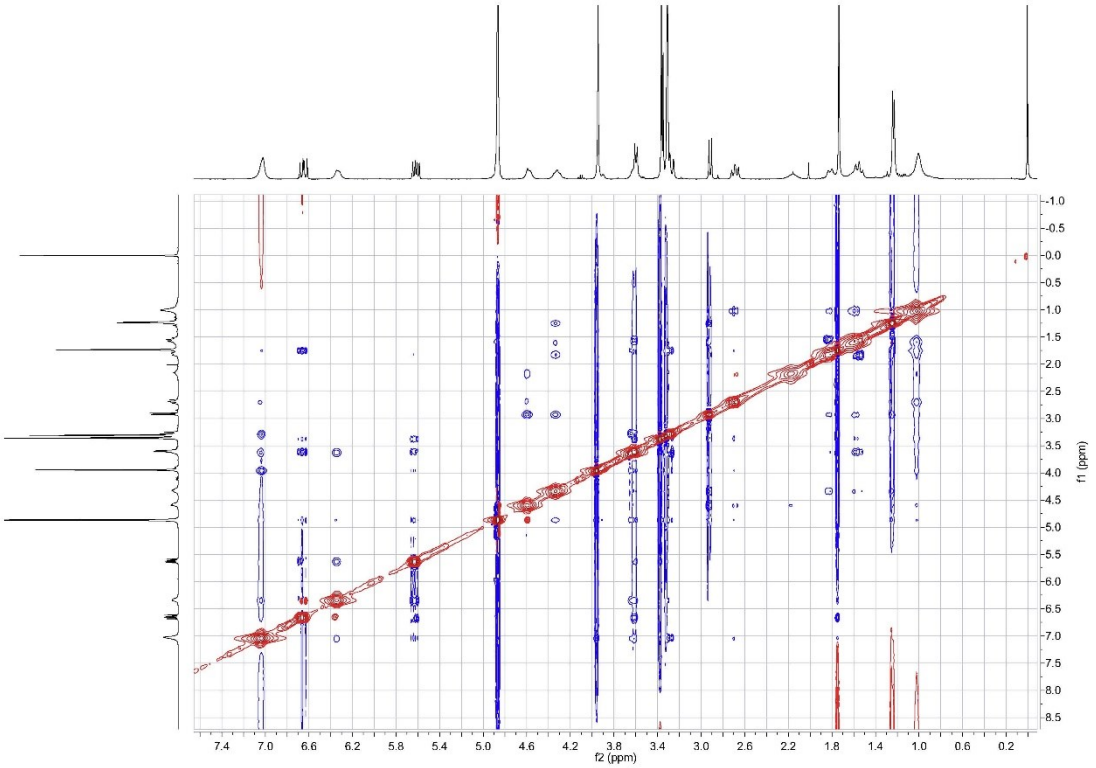

Figure S80. The NOESY spectrum of **14** in CD_3OD.

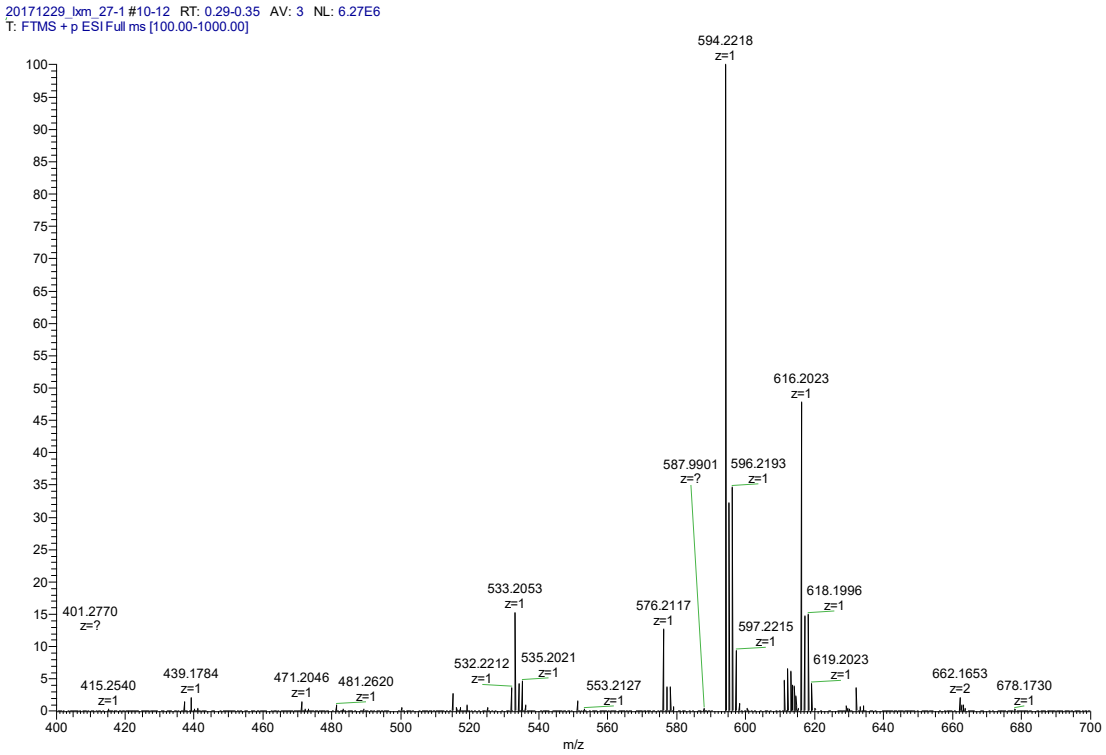

Figure S81. The HRESI mass spectrum of **14**.

4, References

1. Bierman M, Logan R, O'Brien K, Seno ET, Rao RN, Schoner BE (1992) Plasmid cloning vectors for the conjugal transfer of DNA from *Escherichia coli* to *Streptomyces spp*. *Gene* 116:43-49.
2. Paget MS, Chamberlin L, Atrih A, Foster SJ, Buttner MJ (1999) Evidence that the extracytoplasmic function sigma factor sigmaE is required for normal cell wall structure in *Streptomyces coelicolor* A3(2). *J Bacteriol* 181:204-211.
3. Wang F, He Q, Su K, Gao F, Huang Y, Lin Z, Zhu D, Gu L (2016) The PilZ domain of MrkH represents a novel DNA binding motif. *Protein Cell* 7:766-772.
4. He Q, Wang F, Liu S, Zhu D, Cong H, Gao F, Li B, Wang H, Lin Z, Liao J, Gu L (2016) Structural and biochemical insight into the mechanism of Rv2837c from *Mycobacterium tuberculosis* as a c-di-NMP phosphodiesterase. *J Biol Chem* 291:3668-3681.
5. Gibson DG, Young L, Chuang RY, Venter JC, Hutchison CA, 3rd, Smith HO (2009) Enzymatic assembly of DNA molecules up to several hundred kilobases. *Nat Methods* 6:343-345.
6. Ding XM, Tian YQ, Chiao JS, Zhao GP, Jiang WH (2003) Stability of plasmid pA387 derivatives in *Amylcolatopsis mediterranei* producing rifamycin. *Biotechnol Lett* 25:1647-1652.
7. Wilkinson CJ, Hughes-Thomas ZA, Martin CJ, Bohm I, Mironenko T, Deacon M, Wheatcroft M, Wirtz G, Staunton J, Leadlay PF (2002) Increasing the efficiency of heterologous promoters in actinomycetes. *J Mol Microbiol Biotechnol* 4:417-426.
8. Gregory MA, Till R, Smith MC (2003) Integration site for *Streptomyces* phage phiBT1 and development of site-specific integrating vectors. *J Bacteriol* 185:5320-5323.
9. Orellana EA,Kasinski AL (2016) Sulforhodamine B (SRB) assay in cell culture to investigate cell proliferation. *Bio Protoc* 6.